Electric Micro Propulsion

Development of a LaB_6 Cathode for Micro Electric Thrusters.

T.G.E. van 't Klooster 4163397

MSc Thesis Report

Airbus

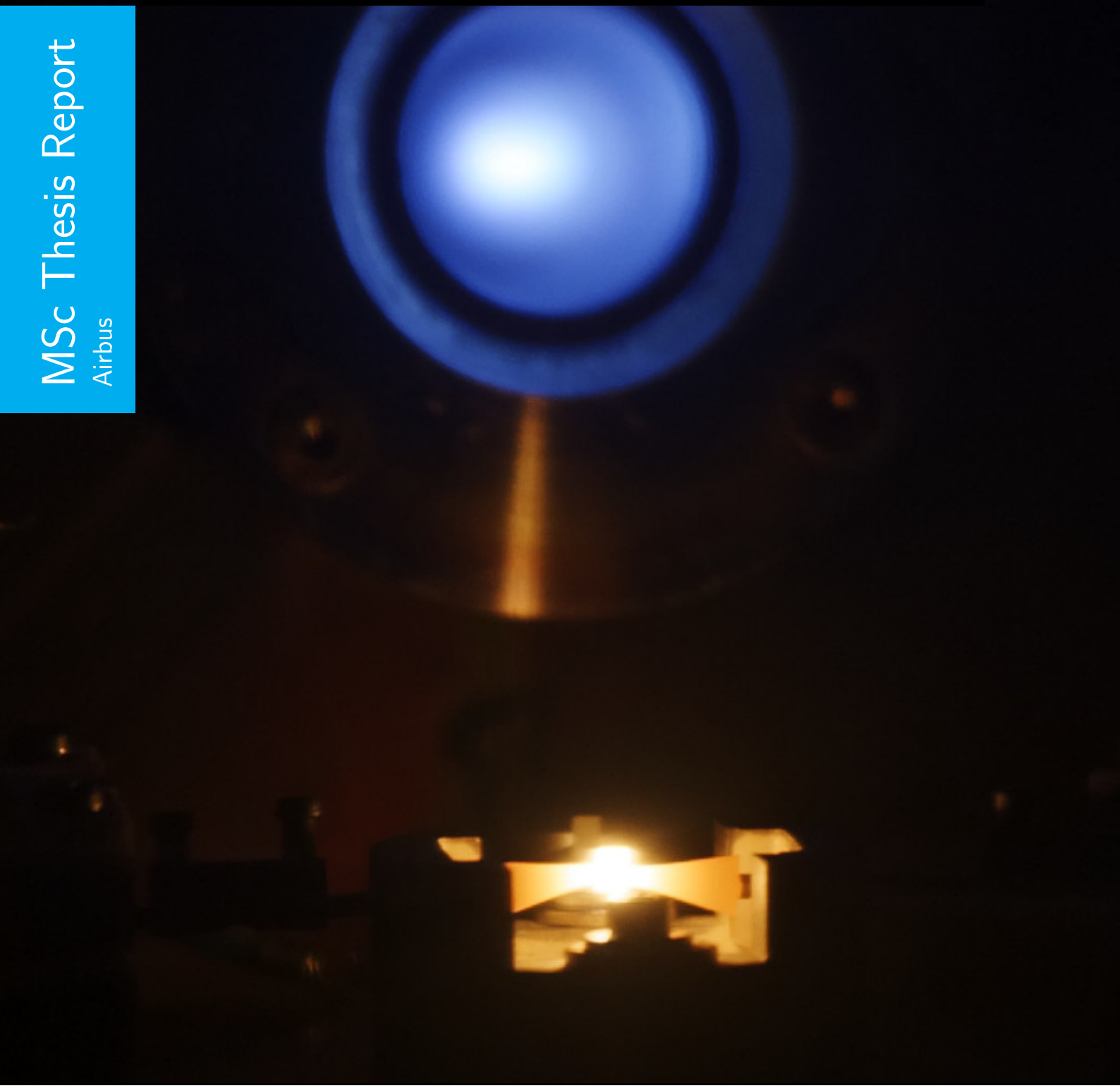

TU Delft Delft University of Technology

Aerospace Engineering

June 21, 2018

MICRO PROPULSION

DEVELOPMENT OF A LaB_6 CATHODE

by

T.G.E. van 't Klooster

as part of the

AE5810 Thesis

in MSc. Aerospace Engineering

at Delft University of Technology

Author:	Thomas van 't Klooster	tgevantklooster@gmail.com
Supervisors:	Dr. Franz Georg Hey	franz.hey@airbus.com
	Max Vaupel	max.vaupel@airbus.com
Professor:	Dr. Angelo Cervone	a.cervone@tudelft.nl

TU Delft Delft University of Technology

AIRBUS

VERSION CONTROL

Version	Date	Changes
1.0	01-12-2017	Creation of draft version
1.1	09-01-2018	Updated: Structure of report Added: Literature Study, Market Survey
1.2	10-04-2018	Updated: Layout style of report Added: Fundamentals, Experimental Setup
1.3	04-05-2018	Updated: Structure of report Added: Vacuum Test Campaign, Cathode Storage
1.4	14-05-2018	Updated: Vacuum Test Campaign, Market Survey Added: Commercial Feasibility Analysis
1.5	29-05-2018	Updated: Initial check and comments
1.6	21-06-2018	Updated: Feedback and finalisation

PREFACE

This is the MSc Thesis report written by Thomas van 't Klooster for the AE5810 Thesis programme of the Master of Science of Aerospace Engineering at Delft University of Technology. The MSc Thesis consists out of a sixth months period of full time research that is conducted after the literature study period of two months. Afterwards, the Master Thesis Graduation will take place.

I would like to express my gratitude to my supervisors Franz Georg Hey and Max Vaupel, Professor Angelo Cervone and my electric propulsion engineering colleague Jonathan Bach for their assistance and tutoring. Next to that, I would like to thank the whole team at Airbus for having a very interesting and educative MSc Thesis period. Finally, I would like to thank the Delft University of Technology, particularly the faculty of Aerospace Engineering, for putting available their facilities and resources.

Thomas van 't Klooster, Airbus, Advanced Projects, Immenstaad am Bodensee, Germany

June 21, 2018

SUMMARY

There is a trend in the miniaturisation of satellites. They not only become smaller, but lighter and more powerful as well. A large growth in the nano-satellite sector is present in the form of CubeSats. These milk carton size satellites use commercial of the shelf components in order to keep the costs low and to allow for technology demonstrations for future larger space missions. In order to increase their current mission lifetime from 1 - 2 years, electric micro propulsion systems are being developed. These systems are able to provide sufficient velocity increments in order to maintain the CubeSat within the required orbit.

Electric micro propulsion systems make use of Coulomb forces to accelerate charged particles. The method is to inject a propellant gas such as xenon into a cylindrical discharge chamber. The propellant is ionised by means of electron bombardment. The electrons that are required in order to do so are pulled from the cathode into the thruster system. Inside the discharge chamber they experience an electromagnetic field, where the resulting Lorentz force makes them gyrate in the projection plane that is perpendicular to the magnetic field lines. As the propellant is inserted in the discharge chamber, a neutral gas pressure builds up. Next, the electrons that are emitted from the cathode are colliding with the neutral gas particles, which causes them to be ionised. These charged particles get accelerated out of the discharge chamber by the electrostatic field in order to create the required thrust. The goal is to develop an affordable, low complexity and efficient cathode for a high performance micro propulsion system that can be used on small satellites. In the future, the whole system can be miniaturised in order to realise an electric thruster system that can be implemented on CubeSats in order to expand their mission lifetime.

The current graphite needle tip cathode can be successfully used as an electron source for propellant ionisation and plasma plume neutralisation in combination with the xenon fed engineering model electric thruster. The thermionic LaB_6 cathode is capable of achieving an emission current up to 64 mA with 56 Watts of input power. This is realised by using graphite needle tips on the end of molybdenum posts that heat the LaB_6 emitter pellet. The micro High Efficiency Multistage Plasma Thruster is operated with a mass flow of 2.0 sccm. It uses an anode voltage and anode current of 700 V and 63 mA respectively. The cathode current is equal to 5 mA. Furthermore, the nominal power to thrust ratio is equal to 25.5 W/mN and the specific impulse that is achieved equals 930 s, dependent on the applied settings. The divergence efficiency ranges from 80 - 90 % and the total system efficiency is currently equal to 80 %. This total efficiency needs to be improved in the subsequent iterations of the design.

NOMENCLATURE

Abbreviation	Description
AIAA	American Institute of Aeronautics and Astronautics
AOCS	Attitude Orbit and Control System
ARCS	Austrian Research Centres Seibersdorf
ARTES	Advanced Research in Telecommunications Systems
AWG	All Wire Gauge
CO2	Carbon dioxide
COTS	Commercial-Off-The-Shelf
CNES	Centre national d'études spatiales
CTE	Coefficient of Thermal Expansion
DLR	Deutsches Zentrum für Luft- und Raumfahrt
EGSE	Electrical Ground Support Equipment
EOL	End of Life
EPIC	Electric Propulsion Innovation & Competitiveness
ESA	European Space Agency
ESD	Electrostatic Discharge
GN2	Gaseous Nitrogen
GTO	Geostationary Transfer Orbit
HET	Hall Effect Thruster
HV	High Voltage
IPR	Intellectual Property Right
IR	Infrared
LN2	Liquid Nitrogen
LEO	Low Earth Orbit
LOX	Liquid Oxygen
LT	Local Time
MAI	Manufacturing, Assembly & Integration
MGSE	Mechanical Ground Support Equipment
MiXI	Miniature Xenon Ion Thruster
MLI	Multi Layer Insulation
MRIT	Miniature Radio Frequency Thruster
NASA	National Aeronautics and Space Administration
NGGM	Next Generation Gravity Mission
PAN	Polyacrylonitrile
PCB	Printed Circuit Board
PEEK	Polyether ether ketone
POM	Polyoxymethylene
PPE	Polyphenylene ether
PPU	Power Processing Unit
PTFE	Polytetrafluorethylene
PVC	Polyvinylchloride
RF	Radio Frequency
RIT	Radio frequency Ion Thruster
RPA	Retarding Potential Analyser
SSD	Sample Standard Deviation
USA	United States of America
TED	Thales Electron Device
TPF	Terrestrial Planet Finder
TRL	Technology Readiness Level
WBS	Work Breakdown Structure
WFD	Work Flow Diagram

LIST OF SYMBOLS

Symbol	Description	Unit
A	Area	[m^2]
B	Magnetic flux density	[T]
C_{ij}	Thermal conductance	[W/K]
eV	Electronvolt	[J]
E	Young's modulus	[GPa]
F	Force	[N]
f	Frequency	[Hz]
g_0	Sea-level gravity	[m/s^2]
h	Height	[m]
I	Moment of Inertia/Second Moment of Inertia	[m^4]
I_{xx}	Mass moment of Inertia around x-axis	[kg·m^2]
I_{yy}	Mass moment of Inertia around y-axis	[kg·m^2]
J	Emitted current	[A/m^2]
j	Safety factor	[-]
k	Boltzmann constant	[J/K]
k	Thermal conductivity	[W/(mK)]
L	Length	[m]
M_w	Molecular weight	[u]
m	Mass	[kg]
n	Number of mols	[-]
P	Pressure	[Pa]
P	Power	[W]
P_a	Ambient pressure	[Pa]
$PTTR$	Power to thrust ratio	[W/mN]
q	Particle charge	[C]
R	Resistance	[Ω]
R_L	Lamor radius	[m]
R_m	Mirror ratio	[-]
r	Radius	[m]
$sccm$	Standard cubic centimetre per minute	[cm^3/min]
T	Temperature	[K]
T_F	Fahrenheit	[^{o}F]
T	Torque	[Nm]
t	Thickness	[m]
t	Time	[s]
U	Voltage	[V]
V	Volume	[m^3]
v	Velocity	[m/s]
w	Width	[m]
δ	Displacement	[mm]
θ	Deflection angle	[deg]
Θ_m	Pitch angle	[deg]
μ	Mean	[-]
μ_E	Gravitational parameter Earth	[m^3/s^2]
ρ	Density	[kg/m^3]
ρ	Electrical resistivity	[Ωm]
σ	Sample standard deviation	[-]

CONTENTS

LIST OF TABLES

LIST OF FIGURES

1

INTRODUCTION

The market for small satellites is growing and it is growing fast [7]. One of the largest contributors to this growth is due to the fact that more and more CubeSats are being launched. These satellites are becoming more powerful and capable of replacing larger satellites. Moreover, there is more space available for these CubeSats to be launched by piggybacking on various larger satellite launchers, that do not have bigger satellites to place in their launch bays. In this manner, many CubeSats can be put into orbit a relatively short time. A recent example of this is the successful launch[1] of the Indian Polar Satellite Launch Vehicle (PSLV) in February 2017, which carried 101 CubeSats.

CubeSats are not only getting more powerful instruments, sensors and electronics, but they are also being equipped with electric / micro propulsion systems in order to allow for orbit keeping. These systems require and dissipate a lot of power, which needs to be evacuated to space in the form of heat. This is possible, for both small satellites as well as CubeSats, using foldable and flexible radiator panels that are connected using flexible thermal straps. Electric propulsion systems are not only used for orbit keeping, but also for orbit raising manoeuvres and future interplanetary missions. The main goal of the electric micro propulsion system (μN thrust range) that is currently being developed is to realise a low complexity, affordable and efficient successfully operating cathode. In this way the system can be miniaturised in the future and in that way implemented in CubeSats. It is common practice for space (sub)systems and components to be organised base on a Technology Readiness Level in order to quantify the readiness of all new developments for flight in space. It consists out of nine levels that can be seen in Figure 1.1 [1]. The current Technology Readiness Level (TRL) of the to be developed micro propulsion system that uses a thermionic cathode is level 4. This means that it has been tested on a component level in a laboratory environment (i.e. vacuum chamber).

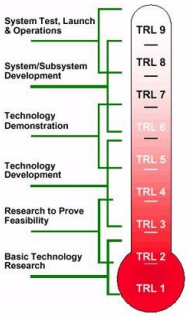

Figure 1.1: Technology Readiness Levels [1]

One of the developments at Airbus lies within electric propulsion. The site in Friedrichshafen is developing micro electric propulsion systems that are used for highly precise attitude and position control systems for spacecrafts. Since solar panels are becoming more and more efficient, electric power consuming systems such as electric thruster systems have developed as well. With the high specific impulses of more than 3000 s [8, 9] that can be achieved with electric propulsion systems, large savings can be made in terms of propellant mass if electric propulsion systems are used instead of chemical propulsion ones. This also means that satellites can extend their mission lifetime with the same amount of propellant. Furthermore, this makes small and cost efficient design of satellites possible, and in addition to that, gives the possibility for a larger payload mass. Moreover, possibilities for orbit changes, orbit corrections, drag compensation, deorbiting, formation flight, constellation deployment and interplanetary missions become realisable for future satellite designs that utilise electric thruster systems. The goal of the current research is to develop the electron source for a micro electric thruster system in order to enhance the overall system efficiency. Because of the wide range of possible applications for these systems the market is very open to it which makes development interesting.

[1] https://www.isispace.nl/dutch-nanosatellite-company-gets-101-cubesats-launched-recordbreaking-pslv-launch/ | Visited on 09 November 2017

The purpose of this MSc Thesis report is to analyse and continue the research that has been performed on electric micro propulsion systems. This involves a focus on the cathode system in particular, with the used materials and their characteristics. In addition to that, compatibility with the alternative propellant iodine is investigated. In this manner the development of a LaB_6 thermionic cathode can be realised. The approach that is followed includes performing research on experimental models, tests, analyses, their discussions and conclusions. In the end the target is to realise a functioning LaB_6 thermionic cathode that can be used in thruster mode while operating with a high efficiency multistage plasma thruster.

First, the research questions, aim and objectives for the MSc Thesis are discussed in Chapter 2. Next to that, Chapter 3 summarises the most important outcomes of the literature study phase, concerning the fundamentals, cathode type trade off and market review. Furthermore, requirements and design options are evaluated in Chapter 4. In addition to that, the experimental setup and the performed vacuum chamber tests are treated in Chapter 5. The storage of cathodes is discussed in Chapter 6. Subsequently, Chapter 7 deals with the commercial feasibility analysis. Finally, conclusions and interesting recommendations are given in Chapter 8.

2

RESEARCH QUESTIONS, AIMS AND OBJECTIVES

In order to elaborate on the research questions, aim and objectives, this chapter is divided in four parts. First, Section 2.1 will elaborate on the research questions. Afterwards, Section 2.2 will deal with the research aim. Subsequently, the research objectives are discussed in Section 2.3. Finally, Section 2.4 gives an illustration of the research framework and the project planning including a Gantt chart is discussed in Section 2.5.

2.1. RESEARCH QUESTIONS

The research questions concern the main topics of the research to be solved and focus on the sources the researcher needs in order to establish the research perspective. The research questions consist out of central questions (that are combined with the research framework in Section 2.4) and different level sub-questions that follow from these central research questions. The goal of the research questions is to provide an adequate steering function, so that more sub-questions can follow from them. Then, lower level questions can be solved and provide answers to the higher level research questions. In addition to that, they need to be useful, realistic, feasible, clear and informative. The thesis research questions are defined below [10].

1. What criteria are relevant in order to asses the performance of various types of cathodes for micro electric propulsion systems?
2. What is the value and quality of the different types of cathodes in view of the assessment criteria?
3. What do we learn from comparing results from the analyses and results of the different types of cathodes in order to establish recommendations on how to develop an efficient cathode for micro propulsion systems?

Combining the first research question with the research framework discussed in Section 2.4, an adequate steering function for the research is established. It makes clear what theories need to be studied in order to establish the assessment criteria. These criteria will in turn give a research perspective. The second central research question cannot be answered before the first one is. The answer of the second research question will provide sufficient information in order to be able to answer the third research question. From the third question it is clear that it cannot be answered before having answered the second question. The answer of the third central research question is able to ascertain whether the objective of the thesis project has been achieved and if so, to what extent.

2.2. RESEARCH AIM

This section discusses the general research aim of the research. The goal of the thesis project is contribute to scientific research by evaluating the adequacy of multiple thermionic cathode solutions for micro electric propulsion systems for space systems. Eventually, the objective of the thesis research is to design, manufacture and test a light weight and high performance (both propulsive as well as mechanical) thermionic cathode for a micro electric thruster.

2.3. RESEARCH OBJECTIVES

This section will discuss the research objectives. The goal is to define the research area which is done by reviewing the work that has already been carried out by other academics in the area of micro propulsion. Simultaneously, the industry best practice in this field of propulsion engineering are benchmarked. In this manner, the areas that are relevant for the research can be identified. Furthermore, the current understanding alongside with any opposing views are addressed. These items will be shortly discussed below.

- **Review the academic research performed on micro propulsion -** One of the first actions to be performed involves reviewing the academic research that has been performed on the topic. In this manner, it can be made sure what fields of the topic remain interested to perform research on and what field are not (i.e. have been studied and concluded for a large part already).

- **Benchmark the current industry developments -** In addition to the academic research, there exist certain industry developments which need to be investigated as well. This involves both the European as well as the non-European companies that are developing electric propulsion systems.

- **Address current understanding alongside opposing views -** This part has been up for discussion at the start of the MSc Thesis at Airbus in Germany. The goal is to discuss the topic with supervisors Franz Georg Hey, Max Vaupel and other colleagues in order to gather different opinions and views on the field of micro propulsion engineering.

In the next part, the MSc thesis project context will be shortly described. Afterwards, the research objective that contains the research goals which follow from the project context is discussed.

Project Context
The development of technologies in electric micro propulsion systems will not only allow for orbit keeping and interplanetary missions, but also for cost efficient orbit raising manoeuvres. The second generation of ESA's Galileo satellite system is planning to use this technology in order to performed required orbit insertion. In this manner the costs of a launch to a GTO[1] can be strongly diminished by performing orbit raising from LEO[2] to GTO or other high elliptic orbits using electric propulsion [11].

Research Objective
The research objective of the MSc Thesis is to further develop a cathode for electric micro propulsion systems, by comparing the thermal and electrical performance of different thermionic cathodes made from different materials. The research will consist out of a practical oriented approach. The current aim is that the thermionic cathode shall be made from LaB_6 (i.e. Lanthanum Hexaboride) and this needs to be tested for. This material has a low work function and has one of the highest electron emissivities, which will be discussed later in more detail. Based on the exploration of the project context, the practice oriented research will be of the engineering design type. The following five steps describe the practice oriented research [10].

1. **Problem Analysis -** In the first phase, the *problem analysis*, the problem is brought to the attention of the stakeholders. The goal of this is to bring the problem into the open such that it becomes transparent and can be discussed by all stakeholders. This involves the discussion of the to be developed technology and for what reasons this development is necessary. It is made clear what the problem involves, why it is a problem and whose task it is to solve it and to which extent.

2. **Diagnosis -** Next, as the problem has been identified and acknowledged by all stakeholders, the *diagnostic phase* follows. In this phase, the background and the causes of the identified problem will be examined. In addition to that, the goal is to find a solution that contains certain courses of action that need to be taken in order to solve the posed problem.

3. **Design -** Subsequently, as the problem analysis an the diagnosis are made, an intervention plan needs to developed in order to find a solution for the posed problem. Considering the micro propulsion topic, this involves the design of a cathode that will be able to let the micro propulsion system realise the required thrust of up to 200 μN [12]. The requirements are further discussed in Section 4.1.

4. **Intervention/change -** In this phase a course of intervention or change will be set in motion in order to solve the problem. This involves carrying out the set plan or design for the problem statement. As with many engineering problems, new problems will arise during the design and analysis. These need to be reported and documented consistently.

5. **Evaluation -** The last phase of the practice oriented research consists out of the evaluation part. In this phase, it will be verified whether the implemented changes to the problem actually solve the posed problem. As mentioned in the previous steps, often new problems occur during the analysis which cause the posed problem to be only partially solved in many cases. If this holds, then the five steps described in this section need to be repeated from step one. Therefore, this whole process is described as an intervention cycle [10].

[1] Geostationary Transfer Orbit
[2] Low Earth Orbit

2.4. RESEARCH FRAMEWORK

In this part a schematic presentation of the research framework is given. It can be seen in Figure 2.1. The research framework gives an overview of the subsequent steps that need to be taken during the research. As an initial step, four implementations of the conceptual model that will be analysed (A, B, C and D) are established. The actual design implementations will be further described in the LaB_6 thermionic cathodes design option tree in Figure 4.3 in Section 4.2.

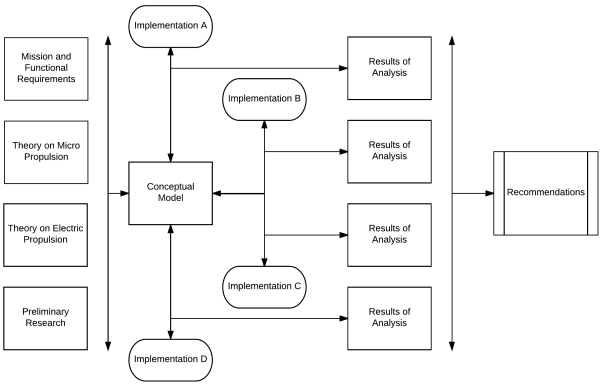

Figure 2.1: Thesis Project Research Framework

2.5. PROJECT PLANNING AND GANTT CHART

This section focuses on the logistics of carrying out the thesis work. In order to generate a clear structure of the work, it is divided into work packages. These packages and the structure will be discussed in Section 2.5.1. Next to that, a Gantt chart is constructed in order to schedule the work in Section 2.5.2.

2.5.1. WORK BREAKDOWN STRUCTURE

This section describes the Work Breakdown Structure (WBS) which is related to the thesis work carried out by the author. The research is divided into several work packages that are divided into different phases in the project. For example, WP2000 and WP3000 have been carried out during the two month literature study period, whereas the other ones are performed during the thesis. The work packages are identified and described, after which the work breakdown structure is given in Figure 2.2.

- **WP1000 - Management, Quality and Product Assurance -** This work package is dealt with continuously during all phases of the project. It is important to keep quality and product assurance aspects into account at all phases. Furthermore, management will play an important role as well and is performed throughout the entire project.
- **WP2000 - Technical Survey and Benchmarking -** This work package initiates Phase A of the project and takes the market survey and literature study into account. Next to that, an analysis will be made on the suppliers and manufacturers that are involved in the project.
- **WP3000 - Project Definition -** In the project definition the research objective and the problem statement will be established. This includes establishing the research questions and sub-questions. Next to that, the requirements are identified and the mission scope will be defined. In addition to that, the functional flow and functional breakdown diagram are established. Finally, Phase A of the project is concluded with a feasibility study and risk analysis of the design concept.
- **WP4000 - Preliminary Prototypes Design and Manufacturing -** The next phase of the project, Phase B, starts with the preliminary mechanical and thermal design of the thermionic cathode that will be used for electric micro propulsion systems. In order to assemble the test prototypes, procurement will be an important item in this phase of the project as well.
- **WP5000 - Preliminary Prototypes Testing Phase -** This work package concludes all the items that are required in order to successfully test the prototypes. This will be done by creating a test campaign that includes the test setup, the test instrumentation and the test plan. The tests will include thermal, electrical as well as mechanical aspects in order to characterise the performance of the prototypes. With this work package, Phase B of the project will be concluded.

- **WP6000 - Final Prototypes Design Manufacturing and Testing -** Phase C of the project commences with the final mechanical and thermal design of the thermionic cathode. In this phase of the project, procurement will play an important role in order to realise the final assembly of the product. At the instant that this step has been concluded, the final prototype can be tested for propulsion, thermal and mechanical aspects. Finally, the development of the technology will be finalised and validated in order to conclude the last phase of the project (Phase C).
- **WP7000 - Commercial Assessment -** The goal of this work package is to document a commercial feasibility analysis according to the standards posed by the European Space Agency (ESA). The purpose is to analyse the strategic context and commercial potential of the proposed activity and to demonstrate that the initiative is capable of conceiving commercial exploitation. It includes information about the target customers, the competition, the strengths, weaknesses, opportunities and threats. In addition to that it provides information about the financial and market objectives, the cost and pricing, the migration plan and finally, the partnerships that are used in order to realise the product.

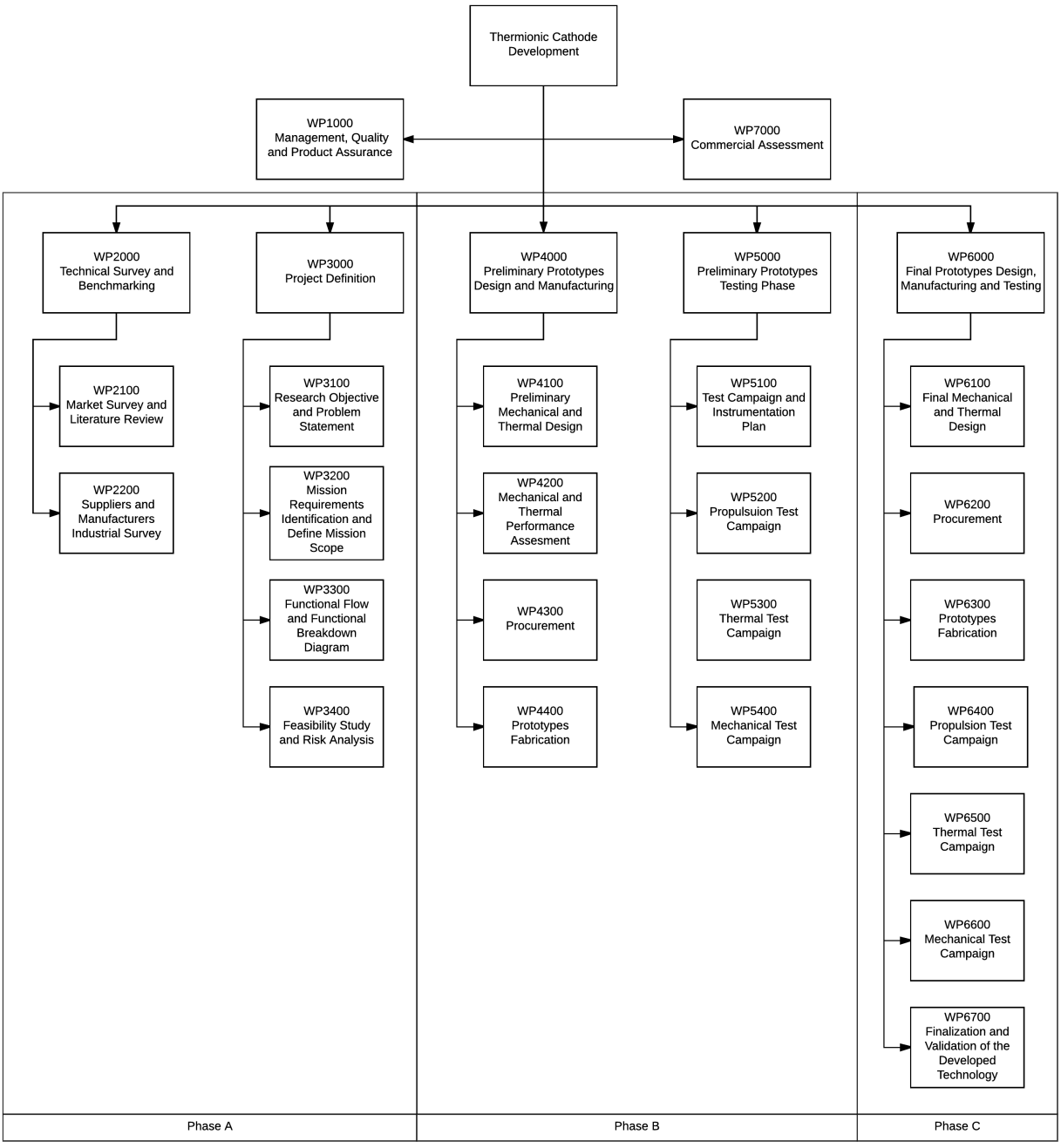

Figure 2.2: Thesis project Work Breakdown Structure

2.5.2. GANTT CHART

This section combines the MSc Thesis main elements into a comprehensive schedule in the form a Gantt chart (Figure 2.3). This gives an overview of the tasks that are to be performed and allows for easy tracking of the entire project. Furthermore, the key review points are indicated. Next to that, additional important milestones such as points of specific achievements relative to the end goal and deliverables such as reports, presentations and manuals are indicated. Main activities are indicated with a blue overhead bar. Meetings are indicated in green and deliverables are indicated in red. Furthermore, project freezes are indicated in orange.

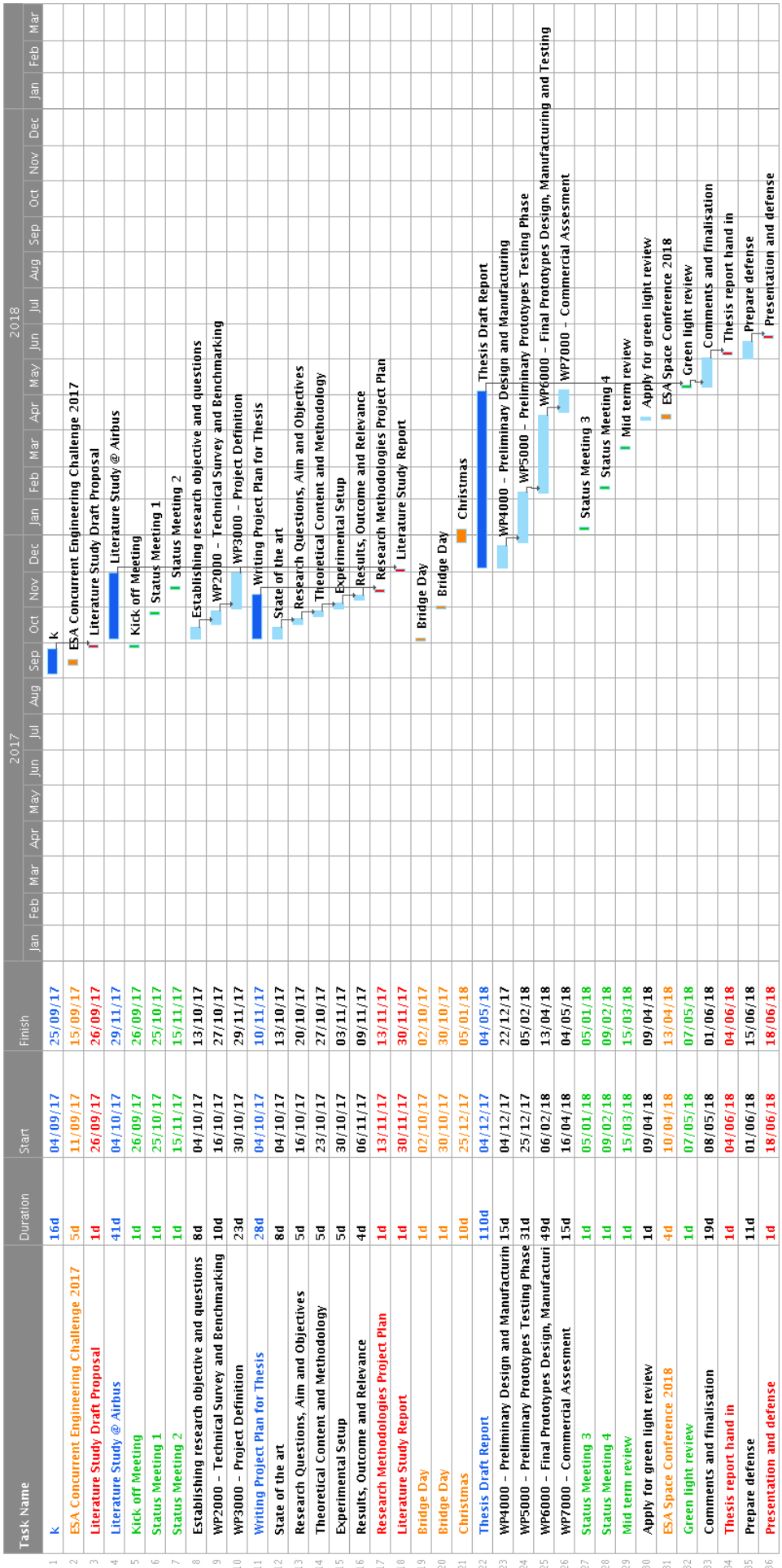

Figure 2.3: Gantt chart MSc Thesis project

3

LITERATURE STUDY OUTCOMES

This chapter will summarise the most important outcomes that are found during the literature study phase. These main aspects have been researched during that period and are therefore are already included in the literature study report and have been graded as well. First, a short summary about the fundamentals will be given in Section 3.1. Next, the main aspects of the literature review in terms of cathode type selection are given in Section 3.2. Finally, the most important points considering the market review are given in Section 3.3.

3.1. FUNDAMENTALS

There a two aspects which are of most importance for electron emission in cathode systems for electric thruster applications. These are the possible amount of electron emission in terms of a physical point of view which is related by the Richardson relation. Next to that, the Child-Langmuir relation describes the total amount of possible charge within a certain control volume. These are shortly addressed in this section.

Richardson Relation
In order to remove an electron from the lowest energy level and to emit it into vacuum, an energy of E_0 is required. Next to that, in order to emit an electron from the Fermi level E_f, it needs to be given an energy that is equal to $E_0 - E_f$, which is also called the work function W_0. This work function describes the *minimum* energy that is required in order to remove and electron from an uncharged specimen. This process is illustrated by Figure 3.1. It is shown how electrons are distributed amongst various energy levels within the material. Hence, the work function is an important parameter as materials with lower work functions require less energy (in the form of heat) in order to emit electrons. The work functions of common used emitter materials for cathodes are listed in Table 3.1 [2, 9, 13].

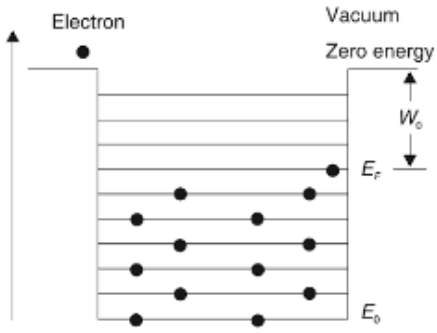

Figure 3.1: Electron distribution among energy levels [2]

Table 3.1: Work function emitter materials

Material	W_0 [eV]
Tungsten	4.87
LaB_6	2.69
CeB_6	2.5
Lithium	2.5
C12A7	2.4
BaO-W	2.1
Caesium	1.81
BaO	1.55

The cathode material needs to have a work function that is as low as possible. In this way, the minimum amount of energy is needed for an electron in the highest occupied electron state of a material at 0 K to emit sufficiently far into vacuum in such a way that it is no longer affected by the electric fields from the material. The goal for the electron is to overcome the attractive forces of the surface atoms and the loss in kinetic energy due to the inter material collisions. If the material is heated until the electron has a sufficient amount of kinetic energy to escape its electron shell, then thermionic emission occurs. As thermionic emission is an important aspect for electron bombardment in electric propulsion systems, it will be explained below. It is described by Equations (3.1) and (3.2) [9, 14, 15].

$$J = AT^2 \exp\left(\frac{-e\phi}{kT}\right) \tag{3.1}$$

$$A = \frac{4\pi \cdot m_e \cdot k^2 \cdot e}{h^3} = \frac{4\pi \cdot 9.109 \cdot 10^{-31} \cdot \left(1.38 \cdot 10^{-23}\right)^2 \cdot 1.602 \cdot 10^{-19}}{\left(6.626 \cdot 10^{-34}\right)^3} = 1200641 \ \text{A m}^{-2} \text{K}^{-2} \tag{3.2}$$

In these equations, J is equal to the emitted thermionic current density, A is a constant (with a value of 120 A/cm^2/K^2, evaluated by Equation (3.2) [16]), T is the material temperature, k is the Boltzmann's constant, e is the charge of an electron, m_e is the mass of an electron, h is Planck's constant and ϕ is the work function. From this equation it can be concluded that a material that has a low work function will emit a larger amount of current at a given temperature compared to a material that has a higher work function. Therefore, a cathode made from a material with a low work function does not need to be heated as strongly as another cathode made from another material with a higher work function in order to emit the same amount of electrons. The emitted electrons are used to bombard the propellant that is used in the propulsion system in order to create charged ions. These ions are then accelerated through the discharge chamber by means of an electrostatic field in order to generate the required thrust. Figure 3.2 gives an illustration of the possible emission current for common emitter materials [17, 18].

Child-Langmuir Relation

In the space applications where micro electric thruster systems play a role, there is a vacuum environment. Therefore the emitted electrons cannot be directly neutralised after emission as they would be in an environment such as Earth's atmosphere where the free path of the electrons is limited because of other particles. Hence, they form a volume of charge that is also called *space charge*. In conducted experiments and operating micro electric propulsion systems, these "clouds" of charged particles are attracted by the positive anode. Hence, a flow of electrons occurs between the closed electrical circuit from the cathode (emitter) to to the anode. However, the current flow that is possible between these stations is limited. This is described by the Child- Langmuir Law in Equation (3.3). It states that the space charge limited current I_A in a plane parallel vacuum diode varies by the three halves power of the anode voltage U_A and inversely as the square of the distance d that separates the cathode and the anode. Furthermore, ϵ_0 equals the vacuum permittivity, e the charge of a single electron, m_e the mass of an electron and A the cross sectional area over which the electrons are distributed [19, 20].

$$I_A = \frac{4\epsilon_0}{9}\sqrt{\frac{2e}{m_e}} \cdot \frac{A}{d^2} \cdot U_A^{\frac{3}{2}} \tag{3.3}$$

Thus, even if an unlimited amount of electrons would be able to be emitted from a cathode emitter, then the amount of electrons in a volume, or more specific, the current flow between the cathode and the anode, would be limited as described by the Child-Langmuir law in Equation (3.3). This is due to the fact that Coulomb repulsion of equally charged particles such as ions (and electrons) occurs in a volume which causes a saturation effect so that the amount of charged particles per volume is limited. Therefore, the current that can be realised between the cathode (emitter) and the anode depends on both the Child-Langmuir relation and the physical amount of possible electron emission of the emitter material as described by the Richardson law. The current flow that can be realised between the cathode and the anode is plotted in Figure 3.3. Results can be seen for cathode to anode distances d from 1 mm to 4 mm. The anode surface area equals $A = \pi R^2 = \pi \cdot 0.01^2$ m^2. It can be seen that for smaller distances between the cathode and the anode, a larger current flow can exist for an equal anode potential.

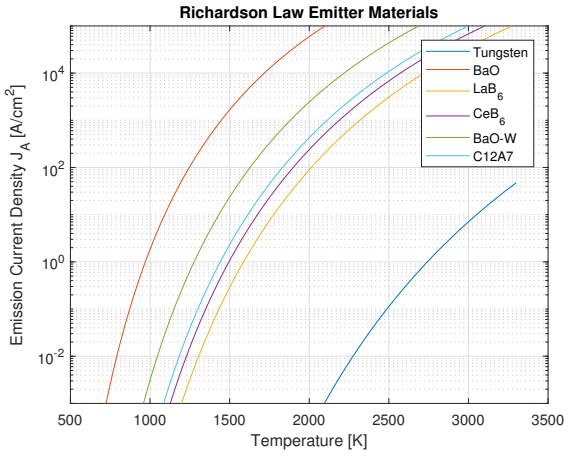

Figure 3.2: Richardson Law emitter materials

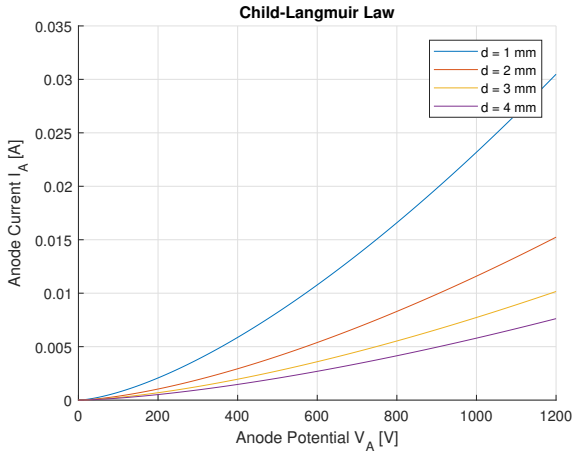

Figure 3.3: Child-Langmuir Law current LaB_6 cathode setup

3.2. CATHODE TYPES

This section evaluates the trade off for the various cathode types that exists and shows with which one the cathode development will be continued. Cathode types that are interesting for micro propulsion applications in particular are a thermionic cathode, a hollow cathode and a radio frequency cathode. In order to perform a trade-off on above mentioned concepts, five trade criteria have been established. These are appropriate in order to define a well-argued trade-off.

1. Performance
2. Affordability
3. Compatibility
4. Lifetime
5. Complexity

Above mentioned trade criteria are now used in order to generate a graphical trade-off for the different cathode types. For the graphical trade off, the grading criteria are defined from best to worst as excellent (green), good (blue), correctable (yellow) and unacceptable (red). These are listed in Table 3.2.

Table 3.2: Ratings Graphical Trade-off

Graded	Colour
Excellent	Green (G)
Good	Blue (B)
Correctable	Yellow (Y)
Unacceptable	Red (R)

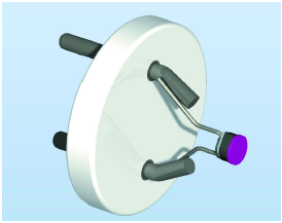

Figure 3.4: Kimball ES-440 LaB_6 single crystal cathode [3]

These ratings will be used for the graphical trade-off, which can be seen in Table 3.3. In this table the trade criteria are listed in the first row and the design options are listed in the first column. A thermionic cathode can be realised using COTS components in a low complexity way. However, the performance in terms of electron emission and heater efficiencies might be lower compared to other systems. Nonetheless, this is a good step forward as an initial design option. Hollow cathodes could perform better in terms of efficiencies and current emission. However, they are more complex and use materials that are susceptible to poisoning. Radio frequency cathodes have a long life time, but are highly complex as they require a high voltage RF coil and a grid system. Therefore, in order to realise a low complexity, affordable and efficient cathode for the miniaturised HEMPT at Airbus, the thermionic cathode will be designed and tested first.

Table 3.3: Graphical trade-off cathode types

Criteria ⇒ Cathode Type ⇓	Performance	Affordability	Compatibility	Lifetime	Complexity
Thermionic cathode	Acceptable (B)	COTS (G)	Good (G)	Acceptable (B)	Low (G)
Hollow cathode	Good (G)	COTS (G)	Suffer from poisoning (Y)	Acceptable (B)	Involved (Y)
Radio Frequency Cathode	Acceptable (B)	Reasonable (Y)	Good (G)	Long (G)	High (R)

3.3. MARKET REVIEW

In terms of the market review it has been found that main competitors exist in the United States of America. These include Kimball Physics, Applied Physics Technologies and Heat Wave Labs [3, 21, 22]. The main aspect which can be found from competitor cathodes is that a direct heating method through the LaB_6 emitter material is applied. As an example, this is shown for the COTS Kimball Physics cathode in Figure 3.4. A large single crystal cylinder is realised in order to create a large planar emitting surface. The goal of this technology is to increase the beam currents. The cathode can be ordered either as a stand alone cathode or on a mounted ceramic base as is illustrated in Figure 3.4. The ceramic base is able to thermally insulate the emitting part of the cathode. The cathode is capable of emitting 500 mA at an operating temperature of 1900 K and a heater current of 11 A. This results in a power to current emission ratio of 0.20 W/mA [3].

4

METHODOLOGY

This chapter elaborates on the base of the cathode vacuum chamber test campaign, which will be described in Chapter 5. First, a requirement analysis is performed in Section 4.1 in order to define the to be used test setups and goals. Next to that, Section 4.2 elaborates on the design options that are made in order to realise a LaB_6 thermionic cathode for micro electric thrusters. Afterwards, in order to give an overview of the materials that are used in these design options, a material discussion is given in Section 4.3. Finally, conclusions are given in Section 4.4.

4.1. REQUIREMENTS

This section will elaborate on the background of the need for micro electric propulsion systems and the requirements that they bring along. One of the main scientific space missions for which a micro propulsion system needs to be developed, is the Laser Interferometer Space Antenna (LISA[1]) mission that will measure gravitational waves. In summary, the goal is measure gravitational waves in order to be able to describe the variation of mass of a cosmic body in relation to fluctuations in time. These gravitational waves are to be measured in a frequency band in between 30 μHz and 1 Hz [4, 23].

The LISA mission consists out of three satellites that are positioned in a triangular configuration in order to realise a triangle interferometer system in space. In this manner the variation in distance between the three satellites can be measured in the picometer range. In order to do so, laser interferometer systems to each other and on proof mass systems inside the satellites are used. This allows measuring the distance of the proof masses to each other, irrespective of the satellites' structure. The triangular constellation follows the Earth's orbit at an angle of 20^o. This is illustrated in Figure 4.1. The equilateral triangle is inclined by 60^o with respect to the ecliptic plane. Next to that, Figure 4.2 shows the propagation of the LISA orbit.

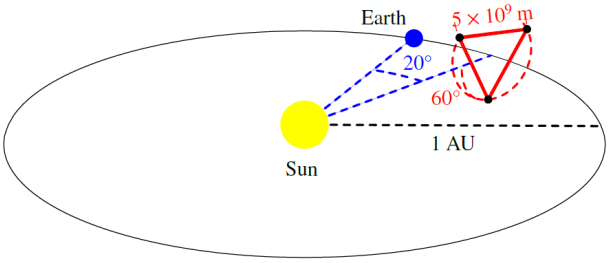

Figure 4.1: Schematic of the LISA science orbit [4]

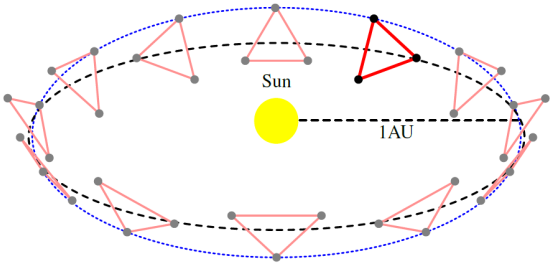

Figure 4.2: LISA orbit propagation [4]

In order to realise those high precise interferometer measurements, the positions of the proof masses need to be protected from perturbations such as solar radiation pressure, solar wind, third body perturbations (e.g. the Moon), atmospheric drag and possible magnetic torque disturbances. Therefore, a precise thruster system is required which has also the capability of operating during the mission life time of 10 years. For example, a thrust of 10 μN is required in order to counteract the solar radiation pressure. Furthermore, a maximum thrust of 100 μN is required [4].

Next to the LISA mission, there are also other and similar scientific space missions which are being researched. These mainly include large constellation formation flying missions such as OneWeb[2] and SpaceX's Starlink[3] that provide global internet access.

[1] `http://sci.esa.int/lisa/` | Visited on 06 September 2017
[2] `http://www.oneweb.world/` | Visited on 29 March 2018
[3] `http://spacenews.com/us-regulators-approve-spacex-constellation-but-deny-waiver-for-easier-deployment-deadline/` | Visited on 29 March 2018

Other missions include space telescopes such as the Darwin[4] space telescope, the Euclid[5] space telescope and the Next Generation Gravity Mission (NGGM[6]). The main characteristic that these satellites have in common is the fact that micro-Newton propulsion systems are required. These are either required to counteract perturbations, maintain highly precise laser links between satellites and/or maintain relative accurate positioning of satellites in constellations. In addition to that, the propulsion systems onboard can not only be used for orbit maintenance, but for orbit raising as well.

In previous similar space scientific missions mainly cold gas thrusters and high power ion thrusters have been used. The development of low power micro electric thrusters for the aforementioned future space mission is highly beneficial in terms of efficiency. Whereas cold gas thrusters have a limited specific impulse of 30 to 90 s, chemical propulsion systems are limited to the range of 200 to 468 s, electric propulsion systems are capable of reaching a specific impulse of more than 3000 s [8, 9]. This results in the fact that large propellant mass savings can be achieved, because of the fact that the energy required to accelerate the propellant is obtained from an external energy source. Nonetheless, it does not mean that the overall mass of the propellant system can be decreased. On the contrary, electric propulsion systems often require substantial power plant and power conversion systems, which will affect the mass budget of the satellite and needs to be taken into account.

Furthermore, electric thrusters typically have a low mass flow rate compared to chemical thrusters and can therefore be operated for a long time period. The high efficiency and low thrust makes them therefore ideal candidates for long term thrusting requirements in e.g. deep space missions or orbit keeping aspects. In addition to that, related to the low thrust and long operating capabilities, throttability of the electric thruster systems can be realised by controlling the propellant mass flow and electric circuit parameters. All these aspects can have beneficial effects in terms of affordability and applicability in the design of future satellites.

Based on these future space missions and mainly the LISA space mission, requirements for both the high efficiency multistage plasma thruster (identifier THR) as well as the cathode (identifier CAT) have been developed. These also lead to requirements for the development of the LaB_6 thermionic cathode. Besides the main general aspects that the cathode shall be an high efficiency, high affordability and simple system, the following requirements in Table 4.1 are defined.

Table 4.1: Thruster and Cathode requirements

Identifier	Requirement
HEMPT-THR-001	A throttable thrust within the range from 50 to 200 μN shall be achieved.
HEMPT-CAT-001	The emission current shall be equal to or greater than 10 mA.
HEMPT-CAT-002	The power consumption shall be in the range from 1 to 15 W.

The requirement *HEMPT-CAT-001* is derived from Equation (4.1). It follows from the fact that the goal has been set for the cathode thruster mode test to achieve a maximum thrust of 200 μN in order to follow up on LISA requirements. In order to be able to so, an emission current by the cathode of at least 10 mA is required. The lower thrust range as stated in *HEMPT-THR-001* can be achieved by tuning the propellant mass flow. The emission current value is given by Equation (4.1). The 10 mA of emission current is based on a xenon thruster, with a xenon molar mass of 126.9 g/mol, an xenon ion charge to mass ratio of $7.14 \cdot 10^5$ C/kg and an ion beam potential of 150 V [5, 24].

$$F_T = I_B \sqrt{\frac{2 m_i \cdot U_B}{q_i}} = 0.010 \cdot \sqrt{\frac{2 \cdot 150}{7.14 \cdot 10^5}} = 205 \ \ \mu\text{N} \tag{4.1}$$

The requirement *HEMPT-CAT-002* comes from the fact that the competitors that are producing LaB_6 thermionic cathodes are using operating powers in the range of 1 - 15 Watts. These products have been discussed in the literature study report [25]. This requirement is also related to the future miniaturisation of the cathodes so that they can be incorporated into micro electric thrusters for CubeSat applications.

[4] `https://www.esa.int/Our_Activities/Space_Science/Darwin_overview` | Visited on 29 March 2018
[5] `http://sci.esa.int/euclid/57039-euclid-dark-universe-mission-ready-to-take-shape/` | Visited on 29 March 2018
[6] `https://www.rheagroup.com/news/next-generation-gravity-mission-will-measure-earths-gravity-field-unprecedented-resolution` | Visited on 29 March 2018

4.2. DESIGN OPTIONS

Now that the requirements are defined, this section will elaborate on the design option tree that is explored in order to realise a high efficient, affordable and low complexity LaB_6 thermionic cathode that can be used for a micro electric thruster. The conceptual and tested applications for LaB_6 thermionic cathodes are shown in the design option tree (DOT) in Figure 4.3. Every option is explained in Table 4.2. They will be addressed in more detail in Chapter 5. As mentioned in Section 3.3, it has been decided to move forward with thermionic cathodes and disregard the hollow and radio frequency cathodes. This is mainly due to the design philosophy based on the three main points: affordability, low complexity and high efficiency.

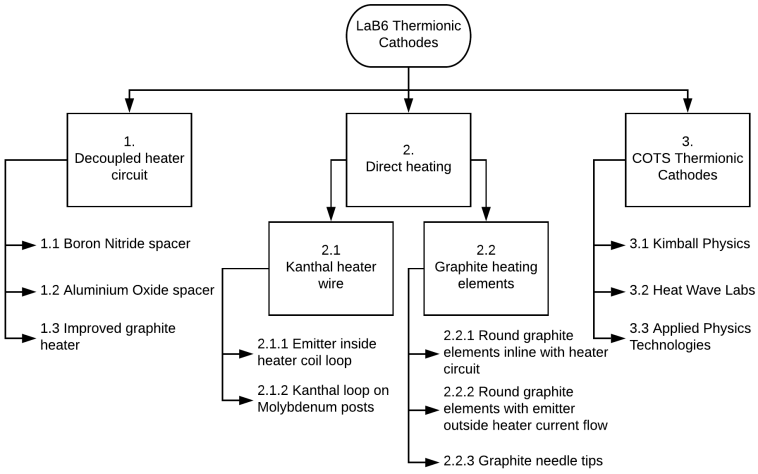

Figure 4.3: LaB_6 Thermionic cathode design option tree

Table 4.2: Cathode design option descriptions

#DOT	Explanation
1.1	The decoupled cathodes make use of a heater that has its own stand alone circuit which is decoupled from the separate cathode - anode circuit. This option uses a graphite heater and an Boron Nitre spacer in order to insert the LaB_6 emitter pellet.
1.2	Another cathode option with a graphite heater makes use of a Aluminium Oxide spacer instead of a BN one.
1.3	A third cathode setup makes use of an improved heater with better thermal performances.
2.1.1	Direct heating means that the cathode emitter pellet shares its cathode - anode circuit with the heater circuit. In this design option a Kanthal heater wire to heat up the LaB_6 emitter pellet.
2.1.2	The second Kanthal wire cathode design has a shorted Kanthal heater wire system that is connected to Molybdenum posts. Kanthal is a high affordable and widely available commercial of the shelf heating wire.
2.2.1	Three more design options will be analysed in which the LaB_6 emitter pellet will be directly heated by graphite elements. The first on uses round graphite blocks that house the emitter pellet inline of the heater circuit.
2.2.2	In a second graphite element cathode design the LaB_6 emitter pellet is installed as such, that it has faces which do not lie inline of the heater circuit.
2.2.3	Another graphite element cathode design makes use of graphite needle tips instead of block elements in order to enhance the thermal performance.
3.1	Commercial of the shelf LaB_6 thermionic cathodes are also explored in order to obtain reference comparison to other design options. The Kimball Physics ES-440 LaB_6 thermionic cathode uses a 1.78 mm diameter emitter pellet.
3.2	Heat Wave Labs produce a LaB_6 thermionic cathode in a so called top hat configuration, with a extending flat cylindrical emitter outside the heater circuit.
3.3	Another COTS cathode is given by AP Tech and makes use of clamping a top hat LaB_6 emitter in between graphite blocks and Rhenium shunts.

Before the design options will be further analysed in Chapter 5, the used materials in the LaB_6 thermionic cathodes are first described next in Section 4.3.

4.3. MATERIALS

This section deals with the various materials that are used in order to realise the cathode design options that have been discussed in Section 4.2. The main materials share the properties that they have good electric insulation, high operating temperature, good electric conduction and high or low thermal conductivity. In addition to that, materials are investigated which might not be a primary choice for usage (e.g. because of affordability reasons), but have interesting properties as well. Table 4.3 gives an overview of the investigated materials and their properties. The ones that are listed are (from left to right), the coefficient of thermal expansion, the thermal conductivity, the electrical resistivity, the maximum operating temperature, the absorptivity and the emissivity. Most values are taken from manufacturer brochures or databases such as *The Engineering Toolbox*[7], the National Institute of Standards and Technology (NIST[8]) and the Solar Absorptance and Thermal Emittance of Some Common Spacecraft Thermal Control Coatings [26]. However, not all values (for e.g. spectral absorptivity and emissivity) are to be found.

Table 4.3: Cathode design options material properties

Material	CTE [μm/mK]	k [W/mK]	ρ [Ωm]	T_{max} [K]	α [-]	ϵ [-]
Aluminium	23.1	237	$2.8 \cdot 10^{-8}$	933	0.2	0.1
Aluminium Nitride	4.5	210	Strong dielectric	2050	0.9	0.1
Aluminium Oxide	8.1	30	Strong dielectric	2000	0.4	0.4
Boron Nitride	3 - 4	33 - 50	Strong dielectric	3100	0.4	0.6
Copper	16.5	386	$1.678 \cdot 10^{-8}$	1358	0.3	0.2
Graphite	7.9 - 8.4	400	$5 - 9 \cdot 10^{-6}$	3800	0.8	0.8
Kanthal A1	11 - 15	13	1.45	1773	0.8	0.8
Lanthanum	12.1	13.4	$6.2 \cdot 10^{-7}$	1193	-	-
Lanthanum Hexaboride	6.2	47	$5 \cdot 10^{-7}$	2528	0.8	0.8
Macor	12.6	1.46	Strong dielectric	1273	0.2	0.8
Magnesium Oxide	10	45 - 60	Strong dielectric	3098	0.09	0.9
Molybdenum	4.8	138	$5.34 \cdot 10^{-8}$	2896	0.2	0.2
Rhenium	6.2	48	$1.93 \cdot 10^{-7}$	3459	-	-
Steel	11 - 12.5	43	$6.9 \cdot 10^{-7}$	1640	0.2	0.2
Tantalum	6.3	57.5	$1.31 \cdot 10^{-7}$	3290	0.4	0.05
Tungsten	4.5	173	$5.6 \cdot 10^{-8}$	3695	0.35	0.35
Zirconium Oxide	10.3	2.5	Strong dielectric	2400	0.23	0.88

The LaB_6 emitter pellet has dimensions of 3 mm in diameter and 2 mm in height and is currently in the smallest form available from the supplier Sindlhauser Materials GmbH[9]. According to competitor LaB_6 thermionic cathode manufacturers current emission rates of 20 - 30 A/cm^2 are achievable, which results in emission currents for this pellet in the range of 0.5 - 0.75 A, depending on the orientation. In most design options Boron Nitride is used to realise a ceramic base, Macor discs are used to install cathode components and graphite and Molybdenum elements are used in order to realise electrical and thermal contacts.

4.4. DISCUSSION

With the requirements that are given in Section 4.1 taken into account, the cathode design options that are given earlier in Section 4.2 will be realised using various materials out of the list in Table 4.3. Hence, this table will remain an important reference throughout the manufacturing phases. The goal of the to be conducted vacuum chamber tests is to realise the requirements posed in Table 4.1 These tests are required in order to verify whether a LaB_6 thermionic cathode can be realised as a subsystem for the low complexity, affordable and high efficiency multistage plasma thruster. With this amount of emission current the required thrust of 200 μN can be achieved with the micro electric thruster. The design options and their vacuum chamber tests will be discussed next in Chapter 5.

[7] `https://www.engineeringtoolbox.com/` | Visited on 29 March 2018
[8] `https://www.nist.gov/` | Visited on 29 March 2018
[9] `http://www.sindlhauser.de/de/` | Visited on 29 March 2018

5

VACUUM CHAMBER TEST CAMPAIGN

This chapter elaborates on the vacuum chamber tests that are conducted on various cathode test setups. The goal of these tests is to measure and evaluate the performance of the cathodes. By using a vacuum chamber, the environment of space can be simulated. First, the use of the vacuum chamber and the micro Newton thruster test facility are described in Section 5.1. Next to that, the executed test modes are described in Section 5.2. Afterwards, the conducted vacuum chamber tests are discussed in Sections 5.3 to 5.7. Finally, conclusions on the test results are given in Section 5.8.

In order to give an overview of the conducted vacuum chamber tests on the various design options throughout the vacuum chamber test campaign, a test matrix is given. It can be seen in Table 5.1. This table lists the various tests, their description and test goal, and gives a reference to the appointed section. This chapter deals with various vacuum chamber tests on various cathode design options as well as iterations. One that is in particular interested in the final iteration is advised to read Section 5.5.6.

Table 5.1: Test matrix

Test ID	Test description	Reference
Graphite heater cathodes	Testing the current and updated design of a LaB_6 thermionic cathode.	Section 5.3
Kanthal wire and Tungsten bulb cathodes	Investigating new design option cathodes with Kanthal heater wire and evaluating Tungsten bulb cathode performance.	Section 5.4
Direct heated cathodes	Investigating new design option cathodes that are directly heated by graphite elements.	Section 5.5
COTS Kimball Physics cathode	Obtaining a comparison for a commercial of the shelf LaB_6 thermionic cathode.	Section 5.6
Thruster mode cathode	Testing the graphite element directly heated cathode in a thruster mode setup with the xenon engineering model electric thruster.	Section 5.7

5.1. VACUUM CHAMBER TESTING

This part will describe the information on the use and preparation of simulated environments in order to test space hard ware, in particular the use of a vacuum chamber. The absence of air and the exposure to radiation contributes to a cruel environment. In addition to that, there are large temperature differences on the material surfaces of a spacecraft. These are aspects that need to be taken into account when performing simulated vacuum chamber tests on spacecraft components. Next to that, this section will elaborate on the test facility that is used in order to measure the performance of the micro electric thruster system as well as its subsystems such as e.g. the cathode. The micro newton test facility is established in order to perform independent micro-Newton thruster developments for space applications. It characteristics are as such that they comply with the requirements of the Euclid[1], NGGM[2], and the LISA missions. This includes highly precise direct thrust measurements in order to characterise thrust noise as well as absolute thrust measurements of the investigated micro propulsion systems.

First, the testing of these components in the simulated space environments is discussed in Section 5.1.1. In addition to that, the thrust measurement system is treated in Section 5.1.2. Afterwards, the plasma diagnostics system is described in Section 5.1.3 [12]. Next, Section 5.1.4 discusses the preparation of the vacuum chamber tests. Finally, the test execution is treated in Section 5.1.5.

[1] `http://sci.esa.int/euclid/` | Visited on 12 October 2017
[2] Next Generation Gravity Mission [27]

5.1.1. SIMULATED TEST ENVIRONMENT

At the point in the design process where the analytic models have been made in order to gain a better understanding of a complex topic, testing can be performed in order to get a close experience to real world conditions. These conditions include the environments that a spacecraft experiences during its lifetime. This includes the Earth's atmosphere at e.g. manufacturing and launch site locations, the Earth's upper atmosphere, regions beyond Earth's atmosphere and the deep space regions. What can be concluded from this is that a spacecraft component (i.e. hardware) does not only need to be able to survive in the harsh conditions of space, but also the ones on e.g. a warm and humid day or on a cold and dry day, depending on the launch site.

Next to that, immediate pressure drops and changes in temperature need to be taken into account, as space hardware can be subjected to temperatures ranging from 115 K to 400 K for Low Earth Orbits (LEO) and to temperatures as low as 3 K for deep space. In addition, effects such as both solar and cosmic radiation start to play a role when the space hardware is located outside the protection of Earth's atmosphere. Three main types of testing that are performed by space agencies such as ESA and NASA are listed and evaluated below [28, 29].

- **Qualification Testing -** Qualification testing is performed in order to subject the hardware to the most extreme conditions that it will experience during operation. These involve the cold and hot case thermal tests, but e.g. also shaker vibration and vacuum testing.
- **Acceptance Testing -** Acceptance testing is used in order to prove that the space hardware can operate under its stated operating conditions for a given amount of time.
- **Evaluation Testing -** Evaluation testing involves the experimental testing part for the largest amount. It is used a.o. in order to test theories and methods, prove the accuracy of an analysis under controlled conditions or to assist a design team to obtain knowledge on the test hardware.

For vacuum chamber testing, the aspects that need to be controlled inside the vacuum chamber are the humidity and the air pressure. How this is done is described in the next part.

Humidity describes the moisture levels inside the vacuum chamber. The hardware is tested for different humidity levels in order to verify whether a component is able to operate after being in a moist environment for a long time. This could for example be a (bad ventilated) storage area, or a hot day at a launch site (e.g. Kennedy Space Centre, Florida, USA). It is possible to control the humidity inside a vacuum chamber by a combination of a freezer and convection oven. These are computer controlled, in order to allow the test to cycle through a various range of humidity profiles. Acceptance values for the tested components depend on the purpose and use and can be found in the European Cooperation for Space Standardisation (ECSS) [30, 31].

Air Pressure is lowered to a very low level by using various equipment. This is a sequential process in which different types of pumps are used in order to reduce the pressure of gas molecules inside the chamber below ambient pressure. The vacuum pressure[3] range is divided into the following four categories that can be seen in Table 5.2 [28].

Table 5.2: Vacuum levels

Vacuum Level	Range [Torr]	Range [mbar]
Low vacuum	760 to 1	1013.25 to 1.33
Medium vacuum	1 to 10^{-3}	1.33 to $1.33 \cdot 10^{-3}$
High vacuum	10^{-3} to 10^{-7}	$1.33 \cdot 10^{-3}$ to $1.33 \cdot 10^{-7}$
Ultra high vacuum	$<10^{-7}$	$<1.33 \cdot 10^{-7}$

The vacuum chamber consists out of a 1500 l vacuum tank, that can be evacuated to $2 \cdot 10^{-7}$ mbar without any gas ballast (by e.g. an operating electric thruster inside). This is realised using a 5.5 l/s forepump, two 700 l/s turbopumps and a helium operated cryopump that has a pumping speed of 10,000 l/s. Combined, the whole vacuum chamber has a pumping capability of 11400 l/s. Figure 5.1 gives an overview of the vacuum chamber by means of a schematic. The tested leaking rate of the vacuum chamber is less than 10^{-9} mbar l/s. In this configuration, a minimum pressure of $1.2 \cdot 10^{-7}$ mbar can be reached. If a thruster with a mass flow of 0.5 sccm (e.g. μHEMPT) is in operation inside the chamber, then a minimum pressure of $3.5 \cdot 10^{-6}$ mbar can be reached, since propellant particles need to be pumped out in this case. Most micro electric thrusters operate with a propellant flow of less than 0.5 sccm. Therefore, the required pumping speed of in the 10^4 mbar l/s range has been realised [32–34].

[3] 1 Torr = 133.3 Pa

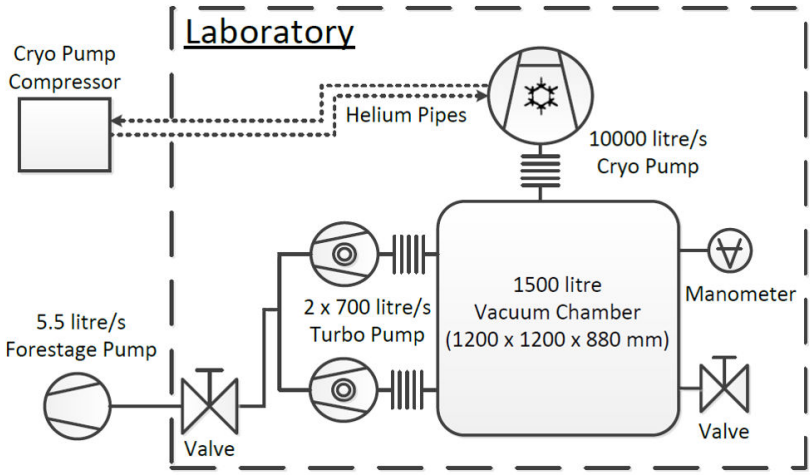

Figure 5.1: Schematic vacuum chamber [5]

All these characteristics follow from recommendations of the American Institute of Aeronautics and Astronautics (AIAA), the National Aeronautics and Space Administration (NASA) and the European Space Agency (ESA). With these pressure ranges it is possible to test a various range of electric thrusters, such as Hall Effect thrusters that are usually tested in the 10^{-5} mbar regime [35], or gyroscopic inertial thrusters that are tested in the 10^{-6} mbar range [36]. At a pressure of 10^{-5} mbar, space components can be qualified officially [37]. In order to measure the pressure inside the vacuum chamber a Pirani/Bayard-Alpert manometer system is used. This system combines two measurement principles in one device. For initial low pressures, the Pirani element is used to measure pressures down to 10^{-3} mbar. Afterwards, for lower pressures, the hot cathode gauge (i.e. Bayard Alpert manometer) takes over in order to provide accurate pressure measurements down to 10^{-10} mbar with an accuracy in the range of 3 - 6 % [5, 38].

Next to that, it is important that the vacuum chamber is large enough in order to avoid negative influences from the chamber walls to the thruster. In addition to that, it needs to be capable to house all the required test and measurement equipment. Nevertheless, large vacuum tanks are expensive in terms of purchasing, operating costs (as a larger volume need to be evacuated) and maintenance. Taking these aspects into account, a 1500 l vacuum tank has been established. Figure 5.2 shows the vacuum chamber at Airbus and next to that, Figure 5.3 shows the inside of the chamber. The vacuum chamber can be accessed by two doors; on the front and the rear side. This has been realised in order to gain easy access to any instrument and test equipment inside the chamber. Furthermore, the noise background is an important aspect to the noise sensitive thrust measurements. In order to obtain high accurate measurements in micro Newton propulsion systems in a vacuum chamber, the chamber needs to decoupled from the ground to minimise background noise. Therefore, it is put on four vibration damping systems in a rectangular formation. In addition to that, the fore stage rotary vane pump is placed outside of the facility in a separate container since it creates a large amount of vibrations and noise. Finally, the vacuum chamber is constructed as such, that it can be easily modified and adjusted to user requirements [39–42].

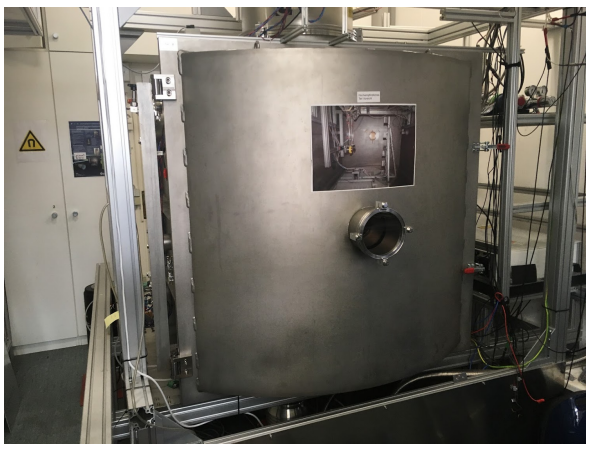

Figure 5.2: Vacuum chamber at Airbus

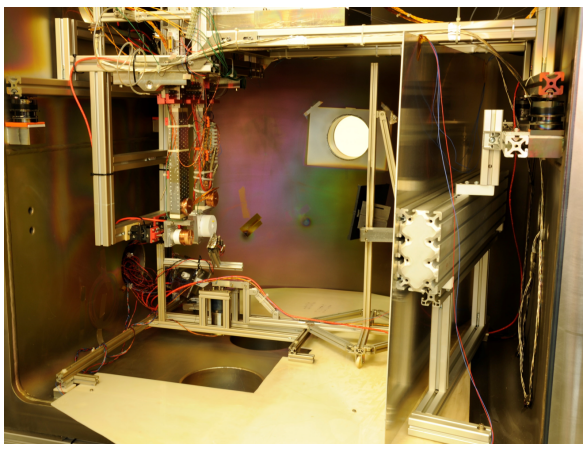

Figure 5.3: Vacuum chamber interior

5.1.2. THRUST BALANCE

The thrust of the micro propulsion systems inside the vacuum chamber is measured by means of a direct thrust measurement that is realised using a double pendulum thrust balance that has a sub-μN accuracy of 0.1 μN. Next to that, it is able to perform thrust noise measurement with high precision. These high resolution requirements are established so that highly precise attitude and orbit control system (AOCS) thrusters can be tested. These include candidates for ESA's Laser Interferometer Space Antenna (LISA) mission, down scaled micro propulsion systems for CubeSat applications and future space missions. The measurable thrust range is from 0 - 1500 μN [43, 44].

The thrust balance consists out of two identical hanging pendulums. One acts as a measurement pendulum, whereas the other acts as a reference pendulum. This is illustrated in Figure 5.4. The thrust measurement is realised by using a heterodyne laser interferometer on the pendulums as the measurement pendulum is deflected by the thrust of the micro propulsion system and the reference pendulum is not. Using the translation difference x between the two and the predetermined spring constant k, the thrust can be obtained by using Hooke's law in Equation (5.1). With the assumption that both (identical) pendulums are equally influenced by external noise and using the relative difference in translation, external noise contributors can be excluded. This noise can come from various contributors that have been discussed earlier such as e.g. seismic noise. Since both pendulums are equally affected by this, the noise will not be measured. In this manner, high resolutions in the pico-metre regime would be possible theoretically. Nevertheless, because of background that is unpreventable, translations in the nanometre regime are measurable. These correlate to a thrust accuracy of 0.1 μN. Furthermore, eigenfrequencies and other highly frequent noise contributors are damped by using an eddy current break in the upper part of the pendulum system [5].

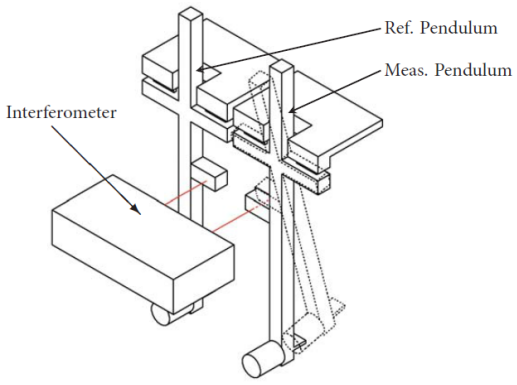

Figure 5.4: Thrust balance schematic [5]

$$F = -kx \tag{5.1}$$

The spring system consists out of 20 leaf springs, that besides spring damping provide a support of the pendulum to the thruster balance structure. Using a symmetric spring setup for the both the measurement and the reference pendulum, the deviation of both spring constants due to thermal expansion is minimised. Nonetheless, a calibration is required in order to be able to precisely determine the spring constant so that highly accurate thrust measurements can be performed. The calibration is performed by applying a highly accurate electrostatic force on the pendulums. This is realised by applying a predefined voltage on the electrostatic comb on the backside of the pendulum. In this manner the spring constant is evaluated by applying different voltages and thus electrostatic forces. The estimated maximum uncertainty that includes the calibration process and the overall relative error in the measurement chain is 3.78 % [5].

5.1.3. PLASMA DIAGNOSTICS SYSTEM

In order to measure the electric parameters of the propulsion system under test including basic ion plume properties, a plasma diagnostics system is used. It consists out of a patented gridless retarding potential analyser system. The instruments on the plasma diagnostics system are mounted on rotatable jib arm in order to allow for 180^o plasma plume measurements. The rotation is controlled by a stepper motor (Phytron VSS 52 [45]) that has a resolution of 200 steps and a step accuracy of 5% for 1.8^o. The stepper motor is operated by a digital controller that can provide a step resolution of 1/256. In addition to that, the stepper motor is connected to the jib arm by means of a transmission that has a gear ration of $1:256$. Hence, the resolution that can be realised by the jib arm as a whole is $2.7 \cdot 10^{-5}\ ^o$. Furthermore, the measurement system can be easily adjusted in order to measure different thruster systems that each have their own specific characteristics. The system is shown in Figure 5.5. The probes are based on a design of the University of Giessen by H. P. Harmann [46], W. Gaertner [47] and P. Koehler [48–50].

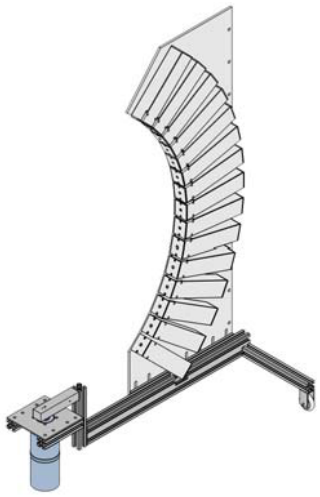

Figure 5.5: Plasma diagnostics system

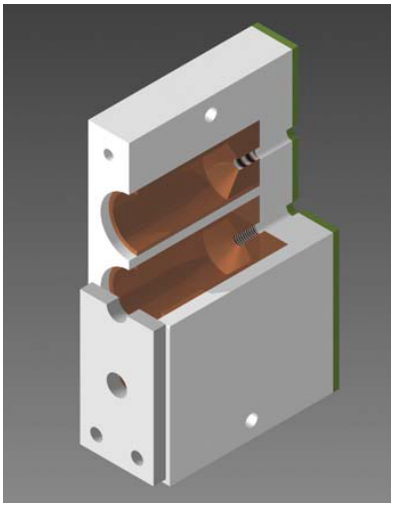

Figure 5.6: Faraday cups unit [5]

The novel energy selective Faraday probes that are placed on fifteen locations on the plasma diagnostics system as can be seen in Figure 5.5 are used in order to measure the ion current. With this setup a measurement of the ion current and ion energy at various measurements angles in two dimensions will be possible. The arrangement consists out of spherical configuration of 15 probes that can be used both as a gridless retarding potential analyser as well as a Faraday probe. It can perform measurements over $\pm 90^o$ in one direction and $\pm 45^o$ in the other angular direction. A electron shield made out of aluminium is used to prevent electron influx. In this manner, only the ion current from the ion plume will be detected by the cups. The Faraday cups are able to measure a current between 0 and 0.2 μA with a resolution of 15.3 pA and an accuracy of 0.5%. However, this resolution is affected by various noise sources such as electrical noise and ion beam divergence. Because of these effects, the resolution is limited to 600 pA. A three cup unit is displayed in Figure 5.6 [5].

The rear side of a Faraday cup unit houses an electronic circuit board. It is made sure that each probe has its own transimpedance amplifier, filter and gain amplifier. In this manner, the probes have their own independent electronic circuit for measurements. Next to that, the resistance on the circuit for each probe can be easily replaced in order to allow for various thrust range measurements. Hence, both the micro Newton as well as the mini Newton thrust ranges can be measured so that different ion thrusters can be tested inside the vacuum chamber at Airbus.

Furthermore, the retarding potential analyser (RPA) is used in the setup in order to obtain information about the ion energy. It is shown in more detail in Figures 5.7 and 5.8 respectively. The purpose of this device is to use a series of grids in order to selectively filter ions and determine the ion energy distribution. The first and outer grid of the system is exposed to the ion plume and its purpose is to protect the RPA from electron influx. The second grid acts as a retarding grid and slows down the incoming ions with respect to their energy. Furthermore, a secondary electron repelling grid is used in order to suppress secondary emission electrons that emanate from the first two grids and the collector. It is possible to adjust the voltage of a retarding grid in order to determine its retarding characteristics. Next, a copper plate acts as the ion collector. This can be seen in Figure 5.8. The design of the RPA that includes the size of the grids, the intermediate spacing and transparencies is based on published data by Gärtner, Böhm and Perrin [47, 50–52].

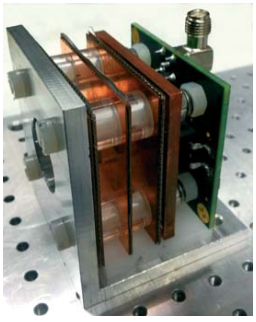

Figure 5.7: Retarding Potential Analyser

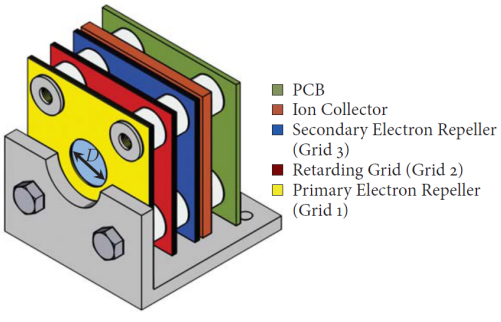

Figure 5.8: Retarding Potential Analyser schematic [5]

5.1.4. TEST PREPARATION

In order to have an efficient vacuum chamber test, it is important to have a good test preparation. This is realised by constructing a proper test manual, in which all the necessary actions are documented. It consists outs of a test setup, test parameters and test instrumentation. This involves applying the appropriate choice and layout of instrumentation both inside and outside the vacuum chamber. Depending on what the test engineers and scientists need to know, the test parameters and appropriate instrumentation is selected. For a vacuum chamber test this involves many temperature sensors, current sensors, voltage meters, pressure sensors, flow meters, humidity sensors, etc. The test manual structure can be seen in Figure 5.9. It is important to keep in mind that applying these sensors results in altering the reality. This is due to the fact that e.g. thermocouples affect surface temperatures and flow meters result in some degree of flow restriction. In addition to that, one needs to consider whether the designed test makes sense and will lead to the required test results. This will prevent unnecessary tests, time and costs.

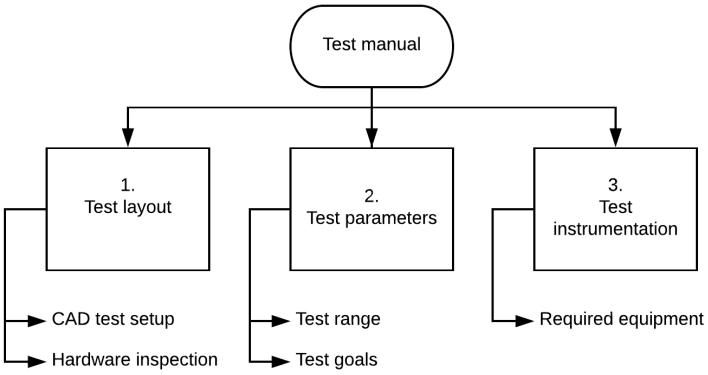

Figure 5.9: Test manual

Vacuum chamber tests are conducted within pressure vessels that are sealed from the atmospheric environment. The setup is often thermally insulated in order to prevent thermal interference with the atmospheric conditions. This results in a control volume that is often accomplished by a firm and heavy supporting structure. This structure is also referred to as the buildup. For the buildup it is important to be clean, well organised and easily accessible. In this manner, if problems or unknown test results occur, buildup problems can be easily ruled out and the main objective (the test data) can be analysed. Creating the proper buildup takes time and needs to be accounted for.

Furthermore, it is important to have a correct understanding on how the test hardware temperature is controlled. If heating or cooling methods are applied to quickly, then this can result in undesired thermal stresses and even fatigue in the material of the hardware due to thermal expansion aspects. In addition to that, it is important to have a material science engineer take a look at the type of material of the tested hardware. This is because of the fact that certain types of materials are able to break down at low pressures which can cause the inside of the thermal vacuum chamber to be coated with the tested material. Next to that, materials could release toxic fumes when exposed to these low pressures (and/or temperatures) [28, 29, 53].

In order to conclude the test, test requirements must have been established in such a way that one is able to check whether the tested hardware meets the required parameters. Here, it is important to remain strict and conclusive, even so when test results are very close the required ones, yet still outside the needed range. Since an improper design that would be supported by an incorrect performed test (i.e. a poor test) does not lead to an overall assured success of the hardware usage, the test rules need to be followed closely.

5.1.5. TEST EXECUTION

For the test execution it is important to be acquainted with both the test hardware and the test setup. This involves for project leads that have a dedicated test team to inform them well in time on new test hardware that is under development which requires testing. In this way, the test team can get informed on the to be tested hardware in such way, that they can prepare the test in a correct manner. This will result for them to be able to predict where problems can arise and what to about this in a better way. It involves adaptions that need to be made prior, during or after the test. A test team can even construct a so called problem shooting guide. With this, problems can be detected and resolved more easily, as they are being searched for and treated using a logical schematic. An example for such a schematic for the to be conducted tests is given in Figure 5.10. In the end, the test data needs to be stored and the test setup needs to be restored to its original one, after all problems and unknowns are dealt with. After these steps, the test setup is allowed to be used for future testing.

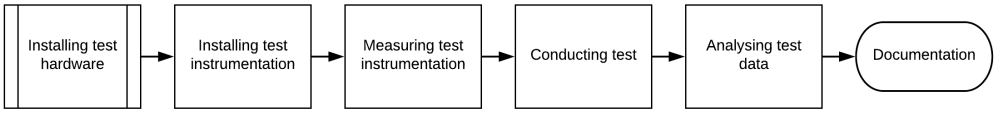

Figure 5.10: Test manual

One process that is often undergone in (thermal) vacuum chamber is the so called bake out. In this process the impurities embedded in the construction material of space hardware or support hardware such as gases, moisture, solvents and other substances that originate from the manufacturing process are forced out of the hardware by heating it within vacuum chamber. This is done in order to prevent the risks of outgassing of impurities in the vacuum of space that could end up to adhere to sensitive instrumentation such as optics.

As a side note, an important aspect to take into account when performing vacuum chamber tests is the "Corona" effect on charged electrical components that are at vacuum between 50 and $5 \cdot 10^{-4}$ Torr. It is an important effect because of the fact that it has shown to be capable of burning out circuit boards inside and outside of vacuum chambers in the past. In addition to that, a military satellite that was powered on during a thermal vacuum chamber test was ruined by this Corona effect. A Corona is also known as *metal vapour arching*. This arch is created in processes where an electric current or magnetic field is applied to an alloy. What happens is that the surface of the alloy starts to erode and that particles of this alloy will float away from the material and coat with anything within the vacuum chamber. This results in a target component where in between, an array of particles exists that are able to form a vapour (or plasma). In the case where sufficient electrical charge has been built up on either the test hardware or the target component, it is possible for an electrical arc to arise through the vapour. This is what is called a Corona. In order to avoid the corona effect, the inside chamber voltage is maintained below 80 Volt, if the chamber pressure is between 50 and $5 \cdot 10^{-4}$ Torr [28, 29, 53–55].

The vacuum chamber at Airbus has the possibility to store various sensors through a 4x 25-pins D-Sub connector flange. In this manner the sensors inside the chamber can be connected to controlling and data logging systems outside the chamber. The usage of these connections for the various conducted cathode vacuum chamber tests will be discussed in their test descriptions in Sections 5.3 to 5.6.

5.1.6. VACUUM CHAMBER CHARACTERISTICS

The test setup has been realised in order to be able to characterise the performance of various micro electric thrusters. In order to do so, high accuracy measurements of both the thrust and the ion plume are required. Table 5.3 gives a summary of the range, resolution and accuracy of the measured values of the equipment that is used in order to realise the measurements. It can be seen that for each measurement the resolution is small enough for the errors to have little effect on any measurement uncertainties that could occur.

Table 5.3: Test setup characteristics

Measurement System	Range	Resolution	Accuracy
Vacuum Chamber	P_{amb} - $1.2 \cdot 10^{-7}$ mbar	10^{-10} mbar	3 - 6 %
Vacuum Chamber (thruster operating)	P_{amb} - $3.5 \cdot 10^{-6}$ mbar	10^{-10} mbar	3 - 6 %
Thrust range	0 - 2500 μN	0.1 μN	3.78 %
Rotatable jib	0 -180^o	$2.7 \cdot 10^{-5}$ ^{o}	5 % for 1.8^o
Faraday cup	0 - 0.2 μA	600 pA	0.5 %

5.2. CATHODE TEST MODES

This section will discuss the modes in which the cathode can be tested in order to evaluate its performance. These are the diode mode and the thruster mode, which will be treated in Sections 5.2.1 and 5.2.2 respectively.

5.2.1. DIODE MODE

Diode mode testing is used in order to verify the functionality of the thermionic LaB_6 cathode. With this method, an aluminium part is installed in front of the cathode. Next, a high voltage is applied to this part in order to increase its potential. Hence, this part acts as an anode and is able to attract the emitted electrons by the emitter (cathode) in order to close the electrical circuit. This is shown in Figure 5.11, where the anode consists out of a cylindrical part of aluminium that is placed using spacers and insulating boron nitride (white) above the emitting cathode. The LaB_6 emitter is placed inside the graphite heater on the insulating macor discs. Furthermore, clamping of the electrical wires is realised in order to obtain a strain relieved test setup.

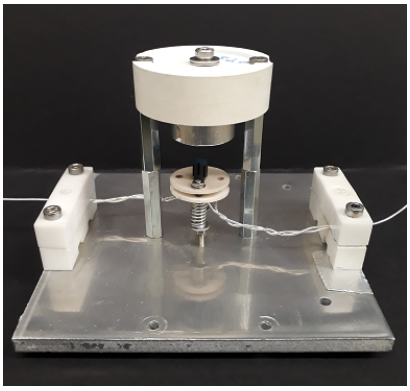

Figure 5.11: Diode mode testing [6]

The spacing between the emitter material and the anode is set to 4 mm initially. This has been done by taking the Child-Langmuir Equation (3.3) into account. The anode should not be placed too close to the emitter by 1 or 2 mm, because then radiative heat losses and sputtering will affect the performance. Both the graphite heater, the boron nitride spacer and the LaB_6 material have very high temperatures and as radiation heat losses scale with T^4 and $1/r^2$, the radiative heating of the anode material plays an important role in relation to the conductive heating of the emitter material. Next to that, sputtering and deposition of graphite particles on the surrounding parts will affect the performance if the distance d between the emitter and the anode is small [56].

5.2.2. THRUSTER MODE

In thruster mode testing the aluminium plate is removed and the thruster is installed in order to act as an anode. Hereby, the functionality of the micro thruster system as a whole can be tested, where the emitted electrons guided into the discharge chamber of the thruster by means of the applied magnetic field. This test mode is illustrated in Figure 5.12, in which tungsten bulbs are used as a cathode. Thruster mode testing is further elaborated on in Section 5.7.

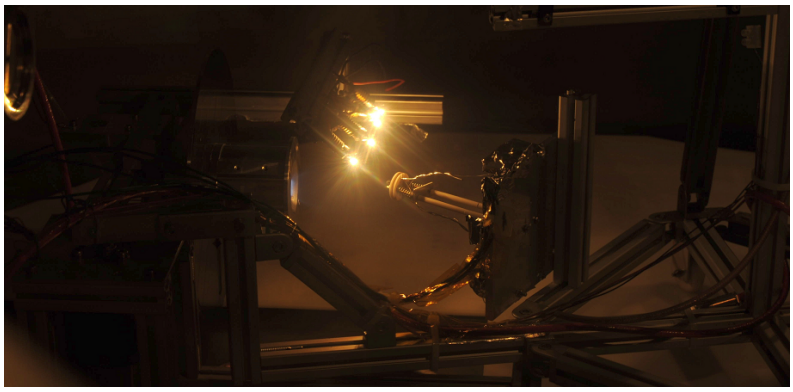

Figure 5.12: Thruster mode testing [6]

5.3. GRAPHITE HEATER LaB_6 THERMIONIC CATHODES

Now that the information on vacuum chamber testing is given in Section 5.1 and the test modes have been described in Section 5.2, the first cathode vacuum chamber test will be elaborated on. This test deals with the graphite heater and the LaB_6 emitter pellet placed into a spacer that is inserted into the heater. It is important to minimise poisoning due to contamination and therefore it is required to wear rubber gloves during working on the test setup and to carefully clean the components with isopropyl alcohol. The goal of the cathode vacuum chamber tests is to gain insight in the electrical performance of the emitter material. This involves obtaining the current emission that can be achieved for various heater input powers and anode voltage settings.

First, the test setup will be given in Section 5.3.1. Afterwards, the test instrumentation is discussed in Section 5.3.2. Subsequently, the test parameters are treated in Section 5.3.3. Next, Section 5.3.4 gives the test results and Section 5.3.5 discusses the next steps. Finally, Section 5.3.6 gives a discussion on the test results.

5.3.1. TEST SETUP

This section will describe the test configuration of the thermionic LaB_6 cathode vacuum chamber test. This is an updated version of the last test setup that has been conducted in previous work [6]. The main differences compared to that version are the use of an even smaller and thinner graphite heater, in order to increase the resistance and thus to enhance the heat generation by means of Ohmic heating. In addition to that, the LaB_6 emitter pellet is placed inside a boron nitride (BN) spacer in order to realise electrical insulation. This will prevent current running through the emitter directly instead of completing the full graphite heater path. The heater circuit and the cathode - anode circuits are two separated circuits that are connect to a shared star point ground, in order to avoid ground loops. This will be discussed in more detail in Section 5.3.2. Figure 5.13 gives an illustration of the test setup. Next to that, Figure 5.14 gives a detail view of how the LaB_6 emitter pellet is placed inside the BN spacer and inside the graphite heater. Summarising, the components that are used in order to realise this test configuration consist of:

- An aluminium base plate in order to install the test setup on.
- Two M2 rods in order to house the cathode setup.
- Four PTFE insulator blocks in order to strain relieve the circuit wiring to the heater.
- A graphite serpentine shaped heater in order to heat the emitter.
- A BN spacer to electrically insulate the emitter from the heater circuit.
- Silver wires with flat pressed ends in order to connect the graphite heater to the heater circuit.
- Two macor ceramic discs to house the cathode setup.
- Two springs in order to keep the graphite heater connected to the silver heater circuit lines.
- A tungsten wire to connect emitter to the ground and hence complete the cathode - anode circuit.
- Another PTFE block in order to house and insulate the ground line of the cathode - anode circuit.
- Screw-screw type connectors in order to connect the silver lines to the copper heater circuit input lines.

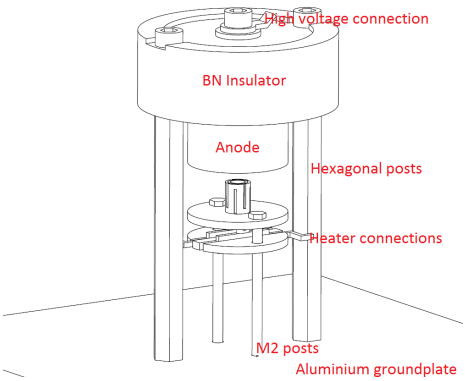

Figure 5.13: Graphite heater LaB_6 thermionic cathode setup

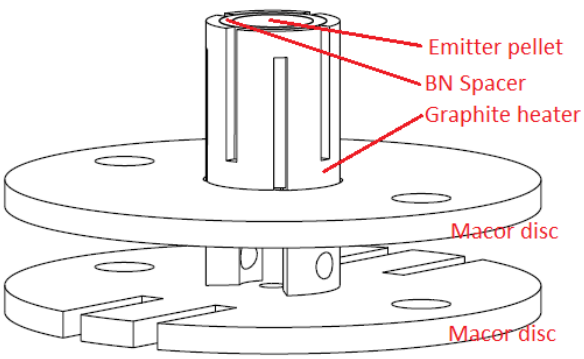

Figure 5.14: Cathode emitter insert detail

Figure 5.15 gives an illustration of the cathode test setup. On the left and right hand side it can be seen how four polytetrafluoroethylene (PTFE) insulator blocks are used in order to clamp the silver wires that provide the electrical connection to the graphite heater. The LaB_6 emitter is placed in the upper part of the BN spacer and is connected to the ground via a tungsten wire. On the upper end of the setup in Figure 5.15 the tungsten wire can be seen sticking out, before it is cut. Furthermore, it can be seen how the macor discs are mounted with nuts, springs and how the copper inserts reassure that the graphite heater will not be pressed out of the desired assembly.

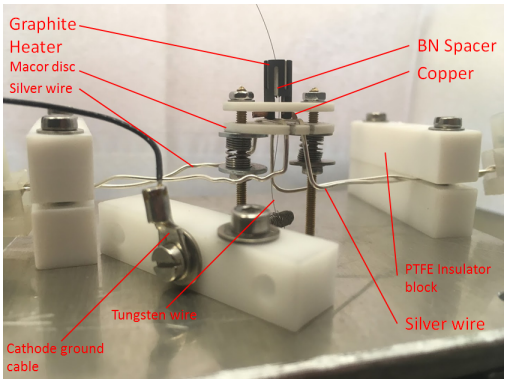

Figure 5.15: Thermionic LaB_6 cathode test setup illustration

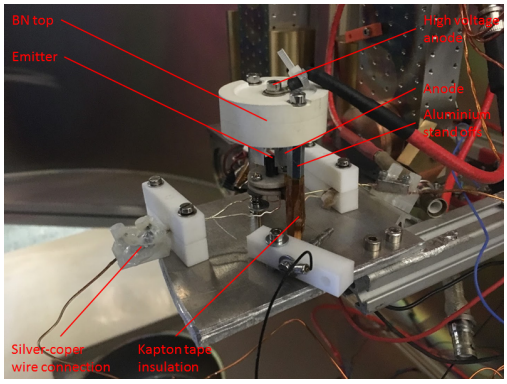

Figure 5.16: Cathode test setup

Next to that, Figure 5.16 illustrates how the high voltage line is connected to the anode. The boron nitride block on top is used in order to electrically insulate the anode from the rest of the test setup. It is kept in place by two aluminium stand offs that are screwed into the bottom mounting plate. Furthermore, an engraving has been made into the hollow cylinder anode in order to be able to visually inspect the LaB_6 emitter during the vacuum chamber test. This is because of the fact that both the graphite heater as well as the LaB_6 emitter will start to glow at high temperatures. In addition to that, one stand off is insulated with kapton tape in order to provide electrical insulation between the tungsten grounding wire and the stand off itself. Furthermore, it can be seen how the silver wires of the heater circuit are connected to the copper power lines by means of screw type wire connectors. The general test assembly is mounted on a Item profile so that it can be placed in front of the inspection window of the vacuum chamber.

The graphite heater has been realised as such, that it uses smooth and flat heating surfaces. These need to small in terms of cross sectional area and long in terms of length in order to increase the resistance and improve the heat generation. This is described by Equation (5.2), where ρ describes the material resistivity in Ωm, l the length and A the cross sectional area. For graphite the electrical resistivity and hence the resistance R decreases as its temperature increases up to 800 ^{o}C [57]. Hence at a constant current input I setting to the heater, the power input P will decrease, given by Equation (5.3).

$$R = \rho \cdot \frac{l}{A} \tag{5.2}$$

$$P = I^2 R \tag{5.3}$$

The graphite heater that can be seen in the test setup in Figure 5.15 is constructed from a 5 mm diameter and 10 mm long graphite tube. The width of the graphite long elements is equal to 1 mm in order to allow for possible manufacturing with tolerances. The legs of the heater have an increased thickness in order to lower the resistance and increase heat generation in the meandering part of the graphite heater, close to where the LaB_6 emitter is inserted into the BN spacer. The temperature of the graphite heater is determined in an iterative process, using the total heat balance for the graphite heater cathode system in Equation (5.4). It consists out of the radiation from the LaB_6 emitter pellet, the graphite heater itself and the heat conduction from the graphite heater towards the LaB_6 emitter.

$$P_{tot} = Q_{cond} + Q_{rad,LaB6} + Q_{rad,graphite} \tag{5.4}$$

According to previous work [6], a total input power of 20 W to the graphite heater leads to a heat radiation of the emitter of 1.37 W at 1400 K. Next to that, the conductive heat path equals 5.63 W and the graphite heater radiation is equal to 13 W. With an emitting area of the graphite heater of $6.28 \cdot 10^{-5}$ m^2, this results in a graphite heater temperature of 1462 K, according to Figure 5.18, which shows the graphite heater temperature vs its heat radiation. In order to verify this 20 W of input power, a thermal nodal model is evaluated which uses conductive and radiative heat flows. It can be seen in Figure 5.19. The thermal model evaluates the required emitter temperature in means of heat radiation. Therefore, the emitter temperature together with the material specific constants are the inputs, and the required heater power is the output of the thermal model. This value eventually relates to the cathode power requirement *HEMPT-CAT-002*. Figure 5.17 gives an overview of these steps.

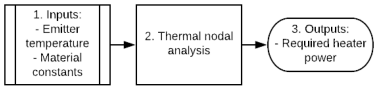

Figure 5.17: Thermal model analysis schematic

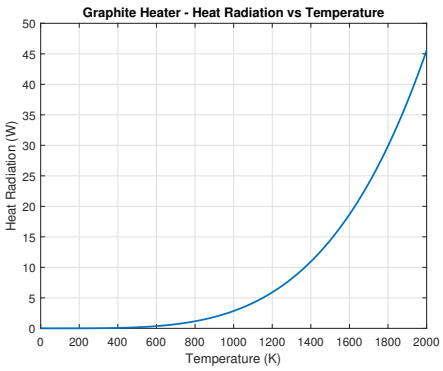

Figure 5.18: Graphite heater Temperature vs Heat radiation

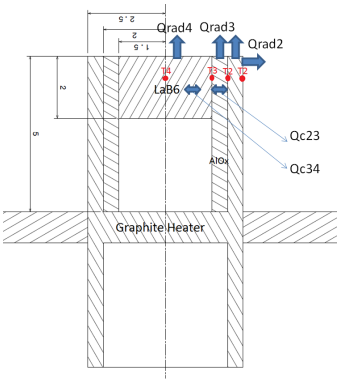

Figure 5.19: Thermal nodal network graphite heater cathode

The thermal balance which states that the input power has to equal the output power of the thermal system is evaluated in parts which begins with the heat radiation from the LaB_6 emitter pellet in Equation (5.5). The emissivity ϵ for the LaB_6 emitter is equal to 0.8 according to Table 4.3, its emitting area equals a circle with 3 mm diameter and the Stefan Boltzmann constant σ is equal to $5.67 \cdot 10^{-8}$ $Js^{-1}m^{-2}K^{-4}$.

$$Q_{rad4} = \epsilon A \sigma T_{LaB6}^4 = 0.8 \cdot \pi \cdot 0.0015^2 \cdot 5.67 \cdot 10^{-8} \cdot 1462^4 = 1.263 \text{ W} \tag{5.5}$$

Next, this radiative heat flow needs to come from and through the spacer, which for an Aluminium Oxide spacer is described by Equation (5.6) and evaluates the nodal temperature T_3 in Equation (5.7). According to table 4.3 the thermal conductivity k of LaB_6 is equal to 47 W/mK.

$$Q_{c34} = Q_{rad4} \tag{5.6}$$

$$Q_{c34} = \frac{kA}{l}\Delta T = \frac{47 \cdot 2\pi\left(\frac{0.0015}{2}\right) \cdot 0.002}{0.0015} \cdot (T_3 - T_4) \Rightarrow T_3 = 1404 \text{ K} \tag{5.7}$$

Next, the radiation by the Aluminium Oxide spacer on the top side of the system with emitting area A and emissivity ϵ is evaluated in Equation (5.8) order to determine conductive heat flow that is required through this spacer radially that eventually needs to flow to the LaB_6 emitter material in Equation (5.9) [58]. According to Table 4.3, the emissivity for Aluminium Oxide is equal to 0.4 and the thermal conductivity is equal to 30 W/mK.

$$Q_{rad3} = \epsilon A_{AlOx} \sigma T_3^4 = 0.4 \cdot \pi \cdot \left(r_{AlOx}^2 - r_{LaB6}^2\right) \cdot \sigma \cdot 1404^4 = 0.485 \text{ W} \tag{5.8}$$

$$Q_{c23} = Q_{rad3} + Q_{c34} = \frac{k\alpha d}{\log \frac{R_{out}}{R_{in}}}\Delta T = \frac{30 \cdot 2\pi \cdot 0.005}{\log \frac{0.002}{0.0015}} (T_2 - T_3) \Rightarrow T_2 = 1405 \text{ K} \tag{5.9}$$

Finally, the heat radiation on the graphite heater is evaluated with its emitting area A and emissivity ϵ in Equation (5.10). Afterwards, all the conductive and radiative heat flows are combined in order to establish the required input power on the cathode system in Equation (5.11). Here, it can be seen that the graphite heater will radiate at a temperature of 1405 K and that a total input power of 22.65 W will be required in order to obtain an emitter temperature of 1400 K.

$$Q_{rad2} = \epsilon \cdot A_{graphite} \cdot \sigma \cdot T_2^4 = 0.8 \cdot \left(\pi \cdot \left(r_{graphite}^2 - r_{alox}^2\right) + 2 \cdot \pi \cdot r_{graphite} \cdot h_{graphite}\right) \cdot \sigma \cdot 1405^4 = 17.89 \text{ W} \tag{5.10}$$

$$P_{in,tot} = Q_{rad4} + Q_{rad3} + Q_{rad2} + Q_{c34} + Q_{c23} = 22.65 \text{ W} \tag{5.11}$$

5.3.2. TEST INSTRUMENTATION

Now that the physical test setup of the cathode has been discussed, the test instrumentation will follow. This part describes all the sensors, installation and any electronic equipment that will be used during the vacuum chamber test of the cathode. The instrumentation that will be used consists out of the following items:

- **Vacuum Chamber -** The vacuum chamber has the properties that are listed in Table 5.4. It is desired to achieve the lowest pressure inside the vacuum chamber that is possible. In this manner the contamination risks on the LaB_6 emitter are minimised as much as possible. Hence, it is hypothesised that then the possible electron emission will be maximised.

Table 5.4: Vacuum chamber properties

Characteristic	Value
Leak rate	$<10^{-9}$ mbar l/s
Vacuum level	$1.2 \cdot 10^{-7}$ mbar
Capacity	1500 l

- **Graphite heater -** The heater is made from graphite since it has good thermal properties. It can be seen in Figure 5.20. It has a high electrical resistance when compared to other metals. Therefore, its heat generation is high when a potential is applied to it. In atmospheric conditions, graphite starts to react with oxygen at temperatures of 750 K in order to initiate combustion. However, in vacuum, graphite is resistant up to 3800 K. Therefore, it is an ideal material to be used as heater. By creating a narrow and long segment in the heater, the heat generation increases. Hence, the repeating pattern shape is a characteristic of these type of heaters [59]. Next to that, material studies by Goebel e.a. [60, 61] have shown that graphite has a high resistance to boron diffusion that could occur when operating LaB_6 or other boron compound emitters. This is due to the close packed hexagonal structure of the molecules.

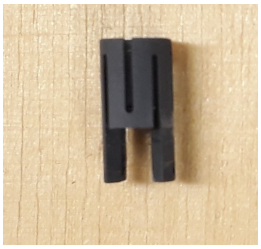

Figure 5.20: Graphite heater cathode test setup

- **Power Supply and High Voltage Supply -** This electrical type of equipment is used in order to regulate the power to the heater circuit and to apply the high potential to the anode. The power supply can be seen in Figure 5.21. It is a Rohde & Schwarz HAMEG HMP4040 programmable power supply. It has four programmable channels that can be put from 0 - 32 V and 0 - 10 A and have a maximal power output of 160 W. The total power output equals 384 W. In order to power the heater, two channels are used in parallel. This can be seen Figure 5.21 as well. Furthermore, in order to measure the anode current that is emitted from the cathode, the high voltage supply is used. It is illustrated in Figure 5.22. It is a type HCP 140 - 6500 from FuG Elektronik GmbH. The maximal output voltage is equal to 6.5 kV at 20 mA. With this machine, the emitted current can be read in the scale of micro Amps.

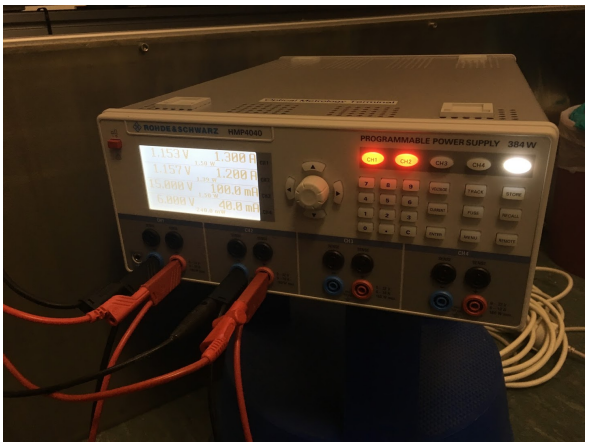

Figure 5.21: HMP4040 Power supply

Figure 5.22: FuG High voltage supply

- **Cabling -** In order to complete the heater circuit and the cathode circuit (which are two decoupled circuits), copper wires are used. The copper wires of the heater circuit are connected with screw type wire connectors that are insulated in a plastic. This can be seen in Figure 5.16. Next to that, the tungsten ground wire that is connected to the LaB_6 emitter is connected via a screw and a grounding cable. All cables are fed through the D-Sub connector flange in the wall of the vacuum chamber and to the electronic equipment. As mentioned earlier, it is important to have both circuits connected to the same star point ground in order to prevent any ground loops and measurement errors. This also includes the fact that both circuits are insulated from the chamber walls (which are connected to a separate grounding block and ground line). The electrical setup is illustrated in Figure 5.23 in more detail. It is illustrated how the LaB_6 emitter is heated by the graphite heater.

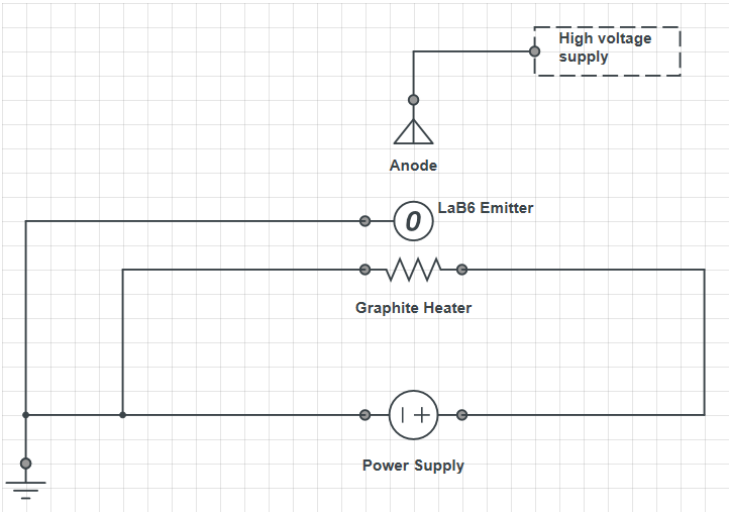

Figure 5.23: Electrical circuit graphite heater cathode

5.3.3. TEST PARAMETERS

Next, the test parameters for the cathode vacuum chamber test will be discussed. The goal of the test is to measure the anode current flow for various input heater power and anode voltage settings. The goal is to be able to achieve an anode current of 10 mA, with as little heater power as possible. In this manner, the required thrust of up to 200 μN can be achieved with the micro propulsion system [12]. In order to prepare the test setup in the vacuum chamber for the to be performed test, a bake out is performed at first. This is done in order to make sure that the maximum amount of particles, i.e. impurities embedded in the materials of the hardware such as gases, moisture, (cleaning) solvents and other substances that originate from the manufacturing process are forced out of the hardware by heating it within the operating vacuum chamber. Hence, afterwards the contamination is minimised and hence performance limitations are minimised as well. According to European Cooperation for Space Standardisation (ECCS) requirements, the cathode is undergoing a bake out of 60 minutes by having the graphite heater operate at an input power of 3 Watts [30].

Next, the heater power will be increased by 1 Watt every 5 minutes. In this manner, the heater and the other components are given time in order to adapt to the new conditions and settle in a thermal equilibrium. This time step is considered to be sufficient (in discussion with the engineering team), since all the components have very low thermal masses in the order of several milligrams. Simultaneously the input power to the heater circuit is recorded as well as the chamber pressure. Finally, at the point where current emission will be measured at first, a measurement series will be conducted at the given input power for a varying anode voltage in order to obtain an anode current emission characterisation. This will be done at a voltage range of 0 - 2000 V in steps of 200 V. In this manner, the emission current can be measured for various potentials, that would also occur in the plasma plume when operating in thruster mode. The initial anode potential is set to 500 V, since this has proven to be a good base for emission current initiation [5, 6].

5.3.4. TEST RESULTS

This section will give the test results for the first cathode vacuum chamber test that has been conducted. The goal of this part is present the findings in terms of current emission. Prior to this test, a current emission of 167 μA has been achieved in previous work [6]. Now that the test setup has been realised in the vacuum chamber, the electric connections have been measured, tested and approved, the vacuum chamber test is ready to be conducted. The test setup is located in front of an inspection window of the vacuum chamber, such that it can be easily inspected.

This is important, since it is known that the LaB_6 emitter material will anneal in red at a temperature of 1000 K [6]. Next to that, at the temperatures from 1000 K onwards, the initial current emission is expected according to Child's Langmuir relation (3.3). Furthermore, the graphite heater will anneal in orange and for higher temperatures in white. After a single day of pumping a pressure of $1.4 \cdot 10^{-6}$ mbar is reached which meets the 10^{-5} mbar requirement for space component qualification [37].

At 11:33 local time, the graphite heater power is put to 3 Watts in order to initiate a one hour bake out process. Afterwards, the heater input power is increased by steps of 1 and later 5 Watts every 5 minutes. At a heater power of 70 Watts (!) a red glowing emitter material is observed and a current emission initiates from 1 μA up to 5 μA, at a pressure of $4.7 \cdot 10^{-6}$ mbar. The anode potential at this point is equal to 507 V. Nonetheless, this is also the point where both the PTFE clamping blocks and the plastic screw screw type connectors start to melt due to the high line temperatures in the circuitry (more than 220 ^{o}C) and therefore the test is ended. This can be seen in Figure 5.16. It is found that despite the high input power, the emitter is brought to an emitting state and hence electron emitting temperature of 1000 K when it is realised in this decoupled heater and cathode - anode circuitry. Nonetheless, the heater resistance is low and thus the input power high.

5.3.5. NEXT STEPS

Since the input power for any current emission is rather high, compared to e.g. the range of 10 - 15 Watts that are being used for competitor COTS thermionic cathodes, some updates are considered for the next iteration. These adaptions to the setup and their impact on the performance are discussed in this part.

- **Doubling the copper heater circuit input power lines -** By doubling these lines, the resistance is halved and thus the power that is dissipated in this part is decreased. This causes the temperature of the copper lines to be lower and the power dissipation to be less.
- **Use of sense wires -** With the use of two additional copper lines from the sense ports of the power supply towards the connection point where the silver lines are connected to the copper heater circuit lines, the exact amount of power that is being put into that point can be measured and regulated. Hence, with this measure the power losses through the double copper input lines can be neglected and one is able to regulate the power into the heater more precise.
- **Aluminium Oxide spacer instead of Boron Nitride spacer -** During a design review it has been found that the coefficient of thermal expansion (CTE) of BN is much lower ($3 \cdot 10^{-6}$ m/mK)[4] than the one of graphite ($8.1 \cdot 10^{-6}$ m/mK)[5]. Therefore, it is argued that the graphite heater expands relatively more in the radial direction than that the BN spacer does, which causes the contact and hence the thermal conductive interface to decrease. Because of this reason it has been decided to change the BN spacer for an Aluminium Oxide spacer, which has a CTE of $8.1 \cdot 10^{-6}$ m/mK, which is equal to the one of graphite. In addition to that, the thermal conductivity of AlO is comparable to BN and the operating temperature is sufficiently high as well with 2000 ^{o}C.
- **Macor blocks instead of PTFE blocks -** In order to prevent the insulator blocks that are used to strain relieve the heater circuit on both sides of the aluminium base plate from melting by high line temperatures, the PTFE blocks are replaced by Macor blocks. Macor[6] is a ceramic that can withstand temperatures up to 1000 ^{o}C.

With these steps taken into account for the next design iteration and the vacuum chamber test, an anode current of 1 μA initiates at a heater power of 50 Watts. Next, the heater input power is increased as long as the emission retains a current value. For an input power of 66 Watts, the emission current increases from 17 up to 667 μA, at which it stabilises. The pressure at this point is equal to $1.9 \cdot 10^{-5}$ mbar. At this input power, the remaining PTFE block that is used to mount the grounding line of the cathode - anode circuit starts to melt by radiation and the test is ended. Despite the fact that a highest ever emission current has been achieved (compared to the 167 μA in an earlier stage [6]), the heater power to do so remains high and the emission current low.

Therefore, a different type of heater is investigated by the author which has meander shapes in the horizontal direction in order to lengthen the electrical path. Next to that, the cross sectional area is decreased to 0.5 x 0.5 mm in discussion with the technicians in the local workshop. The heater can be seen in Figure 5.24. With an electric resistivity of graphite that is equal to ρ = 8.89 Ωm and a total of n = 6 loops that create the heater path, the resistance is evaluated by Equations (5.12) and (5.13). It can be seen that with the increased heater path length and the decreased cross sectional area, the resistance of the heater is increased up to 6 Ω, whereas the current graphite heater has a resistance of 2 Ω.

[4] http://www.henze-bnp.com/PDF/HeBoSint_PI_GB.pdf | Visited on 14 December 2017

[5] http://poco.com/Portals/0/Literature/Semiconductor/IND-109441-0115.pdf | Visited on 14 December 2017

[6] https://www.corning.com/media/worldwide/csm/documents/71759a443535431395eb34ebead091cb.pdf | Visited on 14 December 2017

$$L = n \cdot 2\pi \cdot r_{avg} \tag{5.12}$$

$$R = \rho \frac{L}{A} = \rho \frac{L}{w \cdot h} = 6.03\ \Omega \tag{5.13}$$

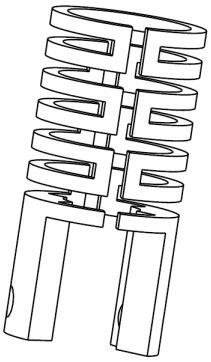

Figure 5.24: Improved graphite heater illustration

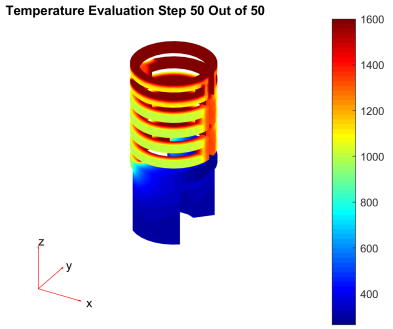

Figure 5.25: Improved graphite heater Temperature [K] distribution

Next to that, Figure 5.25 shows the Temperature [K] distribution. The boundary conditions are put to a 300 K temperature on the lower faces of the heater, i.e. the bottom of the legs, and a fixed temperature of 1600 K at the top side of the graphite heater. Next to that, it can radiate over all surfaces, except the inner side where heat flow towards the spacer and emitter is realised by conduction. It can be seen how the top ring reaches the high required temperatures. At this height the LaB_6 emitter is located. Nevertheless, the thin graphite sections are hard to manufacture. In discussion with the workshop team it has been found that it is possible to manufacture, but that it would also take a large amount of time as well as risk. Therefore it has been decided not to proceed with this heater concept.

5.3.6. DISCUSSION

The current parameters for the performance of the thermionic LaB_6 cathode with a graphite heater and a spacer insert made out of Aluminium Oxide are given in Table 5.5. Following up on the fact that relatively high input powers that are required in order to achieve relatively low emission current values, future design options are explored as well. These will be treated in Sections 5.4 up to 5.6.

Table 5.5: Thermionic cathode properties

Cathode type	Input power (W)	Emission current (mA)
Graphite heater	66	0.667

5.4. KANTHAL HEATER WIRE LaB_6 THERMIONIC CATHODES

The method of heating the LaB_6 emitter pellet with a Kanthal coil wire heater is one of the outcomes of the trade-off on the design options that are discussed in Chapter 4 and will be discussed in this section. First, the test setup will be given in Section 5.4.1. Afterwards, the test instrumentation is discussed in Section 5.4.2. Subsequently, the test parameters are treated in Section 5.4.3. Next, Section 5.4.4 gives the test results and Section 5.4.5 discusses the next steps. Finally, Section 5.4.6 gives a discussion on the test results.

5.4.1. TEST SETUP

The goal of the Kanthal heater coil is to heat the emitter by conduction as well as radiation to the required emitting temperatures of 1000 K and higher. Kanthal has a maximum operating temperature of 1400 ^oC, and therefore it should be capable of getting the LaB_6 emitter pellet that is placed inside the coil to an electron emitting state. The goal is to place the emitter pellet inside the coil, where the lower end has a tighter bend than the inner radius of 1.5 mm (which is equal to the radius of the LaB_6 pellet). The thickness of the Kanthal wire is equal to 24 AWG (All Wire Gauge), or 0.5106 mm. This means that at least five spirals are needed in order to wrap the 2 mm high LaB_6 pellet in order to maximise possible heat transfer to the emitter and minimise any other heat transfer (e.g. radiation to the environment). In general, Kanthal is a high resistance, affordable and efficient heating wire. More properties[7] of Kanthal wire are given in Table 5.6.

[7] `http://www.hi-tempproducts.com/pdf/the-kanthal-furnace-mini-handbook.pdf` | Visited on 24 January 2018

Table 5.6: Kanthal wire properties

Characteristic	Value
Maximum operating temperature [^{o}C]	1400
Melting point [^{o}C]	1500
Resistivity at 20 ^{o}C [Ω/mm^2/m]	1.45
Thermal conductivity [w/mK]	13
Coefficient of thermal expansion [m/mK]	$15 \cdot 10^{-6}$
Density [kg/m^3]	7100

Figure 5.26 gives a schematic of the Kanthal coil heater, whereas Figure 5.27 illustrates the Kanthal heater test setup. It can be seen how the macor blocks are used in order to electrically insulate the heater setup from the base plate and to strain relieve the circuitry. In addition to that, aluminium oxide tubes have been placed over the M2 rods in order to prevent electrical contact with the Kanthal wire. In addition to that, the purple LaB_6 pellet can be seen in the centre of the heater coil. Furthermore, a Macor disc is used in order to centre the cathode below the anode that will be placed later on.

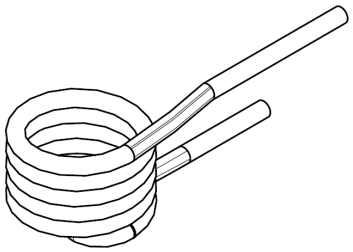

Figure 5.26: Kanthal wire coiled heater

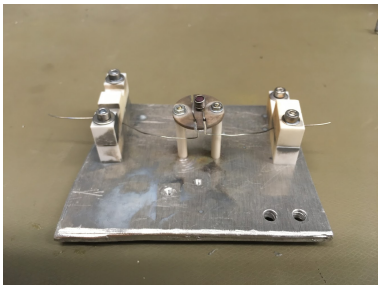

Figure 5.27: Kanthal wire cathode test setup

5.4.2. TEST INSTRUMENTATION

Whereas the electronic hardware that will regulate the input power and will measure the cathode emission current remains the same as before (Section 5.3.2), the heater circuit has now changed from a graphite heater to a Kanthal wire loop heater. It can be seen in Figure 5.27 how the input power lines will be connected on the left and right hand side. The orientation of the winded loop has been realised as such, that the current will run upwards through the loop. In this manner, the magnetic field that is realised by the current passing through the coil is directed upwards. This is illustrated in Figure 5.28. This magnetic field is able to help to guide the electrons to the anode (and eventually to the thruster, when the cathode is installed at a location in front of the thruster that is lower than the discharge chamber). Next to that, the electrical schematic for the Kanthal cathode setup is given in Figure 5.29.

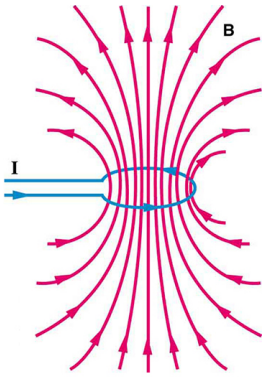

Figure 5.28: Wire loop magnetic field

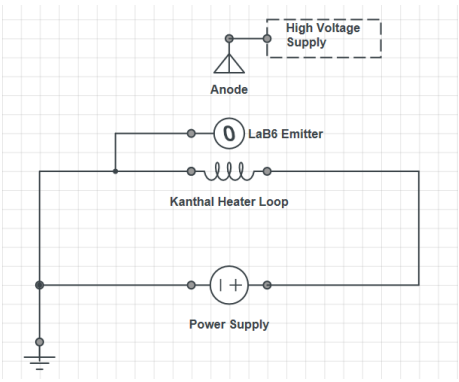

Figure 5.29: Kanthal wire cathode electrical diagram

The magnetic field is evaluated by Equation (5.14), starting from the Biot-Savart law. Here B equals the magnetic field in Tesla, μ_0 equals the magnetic permeability, I the current, R the radius of the loop, $\hat{r}$ the radial vector and L the length of the loop. For a loop radius of the Kanthal heater of 1.75 mm and a current throughput of 5 A this results in a magnetic field with strength of $1.8 \cdot 10^{-3}$ T. At a distance of 2 cm outside of the loop the axial magnetic field strength is then equal to 1.2 ·10−6 T.

When taking a closer look to the magnetic field that is generated with the Kanthal wire loop, it can be seen that the values are small and within the order of mT (refrigerator magnets). This is because of the small size of the loop and the relatively low current throughput. These values are low and can be surpassed easily by permanent Neodymium and Samarium Cobalt magnets that can go up to the 10^0 T range (loudspeaker magnets) and above which are used in hospitals (magnetic resonance imaging) [62, 63].

$$dB = \frac{\mu_0 I d\vec{L} \times \vec{r}}{4\pi R^2} = \frac{\mu_0 I dL \sin\theta}{4\pi R^2} \quad \Rightarrow \quad B = \frac{\mu_0 I}{4\pi R^2} \oint dL = \frac{\mu_0 I}{4\pi R^2} \cdot 2\pi R = \frac{\mu_0 I}{2R} \tag{5.14}$$

5.4.3. TEST PARAMETERS

Initially, the setup will be baked out at a low power setting for 60 minutes. Afterwards, the power is gradually increased in equal time steps in order to get the Kanthal wire glowing and to heat up the LaB_6 emitter pellet. Similar to with the graphite heater cathode setup in Section 5.3, the goal is to measure the current emission as soon as it has initiated for various anode input potentials ranging from 0 - 2000 V.

5.4.4. TEST RESULTS

With the bake out performed for 60 minutes at a total power of 129 mW, the power is increased very 10 minutes by 150 mW. At an input power of 1502 mW, the Kanthal wire is lit up and reaches it maximum operating temperature. At this instant, current emission starts from several μA and reaches the value of 3.8 mA after 60 minutes (at the constant power setting). This can be seen in Figure 5.30. While operating at the same input power setting for over 60 minutes, eventually the Kanthal wire burns through close to the AlO insulated spacer tube around the M2 rod.

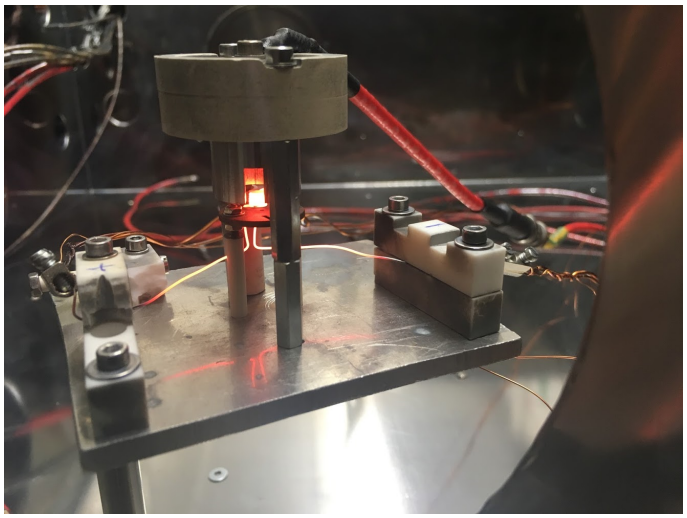

Figure 5.30: Kanthal heater cathode vacuum chamber test

5.4.5. NEXT STEPS

It has been found out that the Kanthal wire is not able to operate for a long time at a high throughput setting. Eventually, it will burn through at the hottest point while operating at this setting. Therefore, for the final iteration of the Kanthal wire heater, the following adaptions have been made:

- **Shortening the Kanthal wire -** The goal is to shorten the extensions of Kanthal wire from the coil itself and therefore concentrate the heat generation at the coil. In this manner heat radiation losses from superfluous (hot) Kanthal wire are minimised. In addition to that, the hottest location will be close to the LaB_6 emitter pellet that requires to be heated.
- **Introduction of Molybdenum posts -** Molybdenum 2 mm diameter posts are used in order to coil up the Kanthal wire and connect the heater circuit to the copper input lines. Molybdenum is known for its low electrical resistance and a high maximum temperature. Therefore, it is an ideal material to be used in a high aspect ratio configuration (with 2 mm diameter and 20 mm length) in order to act as an intersection in between the hot Kanthal wire and the copper input lines. Copper has a melting temperature of 1085 ^{o}C, whereas the Kanthal is operating at temperatures around 1400 ^{o}C. Therefore, with the Molybdenum posts the two can be safely connected.

- **Decreasing the input power increments -** The goal of this measure is to lower the increments of the input power in order to achieve current emission at a fixed power setting, without reaching the maximum operating temperature (and hence power setting) in a too early stage. This means that the cathode is given time to initiate current emission as the input power to the Kanthal heater coil is gradually increased.

- **Additional AlO spacers -** More AlO spacers have been used in order to reassure that the Kanthal wire heater circuit is not capable of shorting with the rest of the test setup. This can be seen in Figure 5.31.

With the adaptions made to the Kanthal wire heater coil setup, a current emission initiates at an input power of 882.4 mW. Due to the shortening of the Kanthal wire the required power to obtain current emission is lower than before. At this instant the pressure is equal to $8.9 \cdot 10^{-6}$ mbar and the anode potential equals 804 V. From this point onwards that current emission has initiated, it is recorded versus time. After 38 minutes a maximum value of 1.821 mA of current emission is achieved. This can be seen in Figure 5.32. After that operating time (at a constant power input), the heater wire burns through and the test is ended. This can be seen in more detail in Figure 5.33.

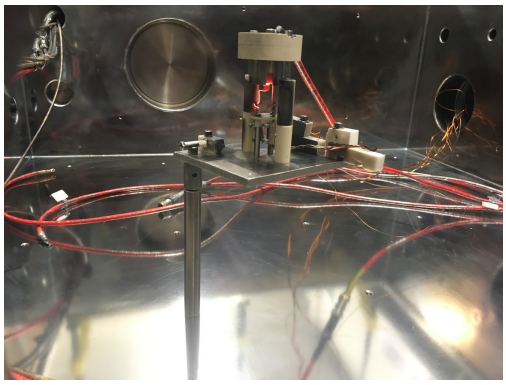

Figure 5.31: Kanthal wire coiled heater on Molybdenum posts

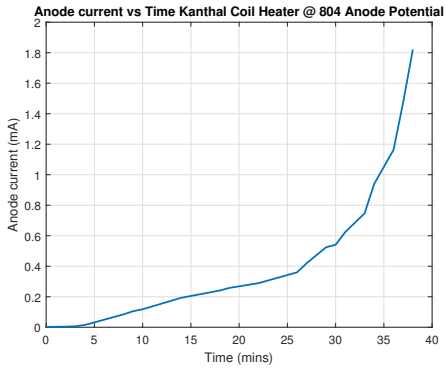

Figure 5.32: Kanthal wire emission current vs time

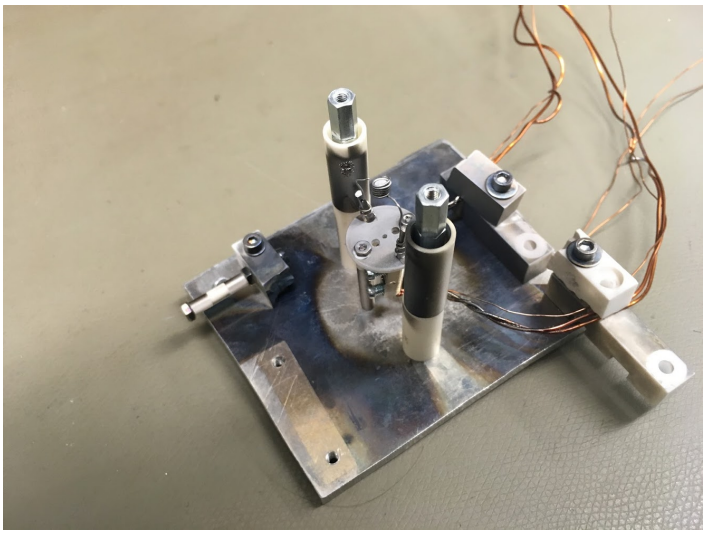

Figure 5.33: Kanthal wire burnt through

Kanthal wire current emission verification

Since glowing wires such as e.g. Tungsten and Rhenium filaments are known to emit electrons themselves at high operating temperatures, it will be checked for whether it is actually the LaB_6 pellet that is emitting electrons or not. This will be done in a stand alone test without the emitter placed inside the Kanthal coil heater. In addition to that, a light bulb is added in order to verify the test setup, from which it is known that a current emission of 5 mA per 1 Watt of input power can be achieved. Furthermore, another test object is included, which is a welded Tungsten Rhenium thermocouple. The goal of this is to check whether it can be used for both a temperature reading as well as a heating wire. The setup can be seen in Figure 5.34.

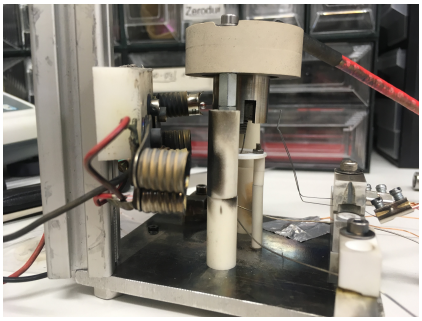

Figure 5.34: Tungsten bulb, Kanthal heater and T-Re thermocouple

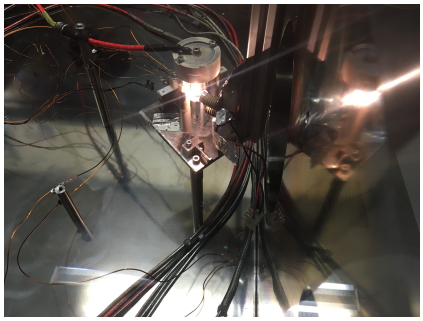

Figure 5.35: Tungsten bulb operation

On the left hand side of Figure 5.34 one can see the cracked 1.2 W and 12 V COTS light bulb that contains a Tungsten wire. In the centre of the test setup the Kanthal wire coil is placed and on the right hand side of the anode the Tungsten - Rhenium thermocouple is installed. First, the bulb is tested and it returns the expected current emission. The pressure at this moment is equal to $6.9 \cdot 10^{-6}$ mbar and the anode potential equals 604 V. The operating Tungsten bulb can be seen in Figure 5.35. It is important to mention that at the current vacuum chamber pressure the Tungsten filament has enhanced characteristics compared to in its own bulb glass, where the pressure is only several millibars. Therefore, the bulb can be run at higher operating voltages than the 12 V indicated by the manufacturer. It would be e.g. possible to operate the bulb at 18 V and 500 mA for a week long, compared to the 12 V and 100 mA that are advised by the manufacturer [64].

In order to obtain reference current emission characteristics for the thermionic LaB_6 cathode, a characterisation for the Tungsten bulb is carried out. This is done by measuring the anode current for an input power of 2 and 3 Watts respectively and changing the anode potential from 0 - 2000 V. In addition to that, for an anode potential of 604 V and a pressure of $6.9 \cdot 10^{-6}$ mbar, anode currents of 10 and 15 mA are reached for input powers of 2 and 3 Watts respectively. Furthermore, Figures 5.36 and 5.37 show the graphs for the anode current versus anode potential for 2 and 3 Watts of input power respectively.

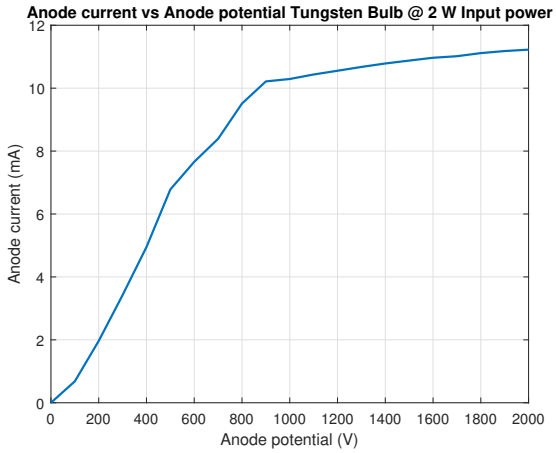

Figure 5.36: Tungsten bulb current emission for 2 Watts input power

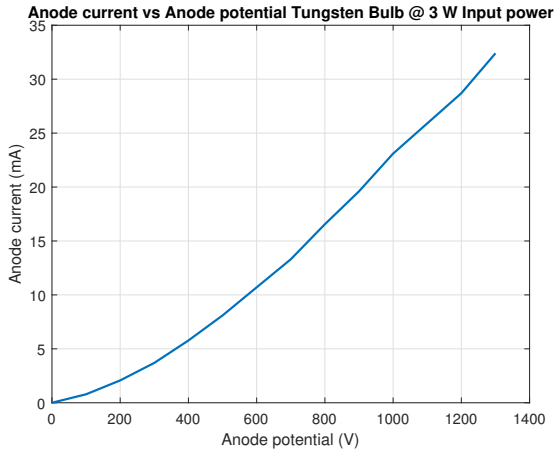

Figure 5.37: Tungsten bulb current emission for 3 Watts input power

What is interesting to see and can be especially shown in Figure 5.36 is how the current emission reaches its limit value as the anode potential is increased even more. This shows the space charge limitation that is reached by terms of the Child-Langmuir relation in Equation (3.3). It indicates that for a constant power setting the amount of electrons that can exist in the volume that contains the cathode and anode is finite. This will be shown later on for the thermionic cathode design as well.

Next, the tungsten rhenium filament is tested and as expected, the input power can be turned off after which the change of voltage on the circuit can be read with a multi-meter in order to obtain a temperature read out according to the calibration of tungsten rhenium filament thermocouples. In addition to that, the glowing filament emits electrons, but at a very low rate compared to the input power (0.058 mA for 22 W of input power). Its operation can be seen in Figure 5.38. Hence it is concluded to not be used as a primary electron emission source. It will also not be used as a heater coil due to high heat radiation losses and heater circuit shorts due to direct contact with the electron emitter.

Furthermore, the Kanthal wire coil without the LaB_6 insert is tested and as with the other two filaments it is the case that it emits electrons. An electron emission of 1.1 mA is reached for an input power of 1.3 Watts, without operating at a long time. This is a value in same order of magnitude as with the other Kanthal wire cathode tests, that did contain the Lab_6 emitter insert. At this point the pressure is equal to $2.4 \cdot 10{-}5$ mbar and the anode potential equals 604 V. Its operation can be seen in Figure 5.39. The test indicates that the Kanthal wire is the primary source of electron emission and the LaB_6 emitter has not been activated in terms of electron emission.

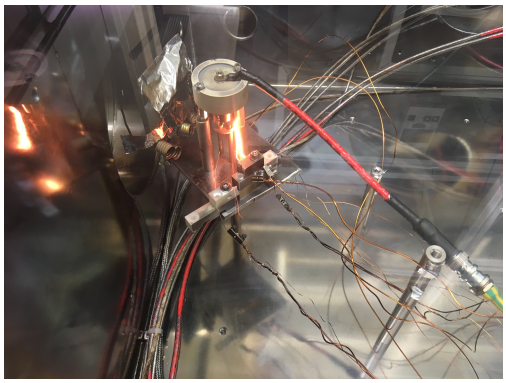

Figure 5.38: Tungsten Rhenium thermocouple operation

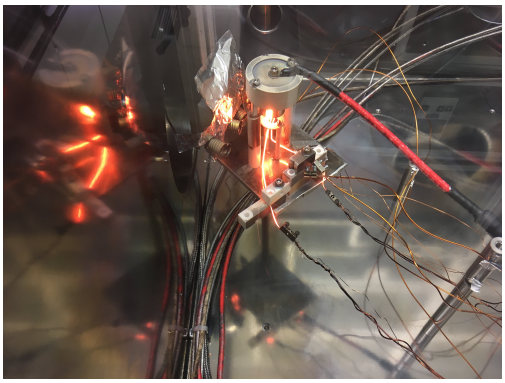

Figure 5.39: Kanthal wire coil operation

5.4.6. DISCUSSION

Despite the fact that Kanthal wire proves to be an affordable heating wire with suitable characteristics, it turns out that it cannot be operated for a long period (i.e. more than 30 minutes) on or near its maximum operating limit. In addition to that, conducted vacuum chamber testing has shown that it has actually not been capable of initiation current emission from the LaB_6 emitter insert inside the heater coil. Instead, the Kanthal wire itself has been emitting electrons at a rate of around 2 mA per 1 Watt of input power. Table 5.7 gives an overview of the cathode development thus far.

Table 5.7: LaB_6 Cathode development

Cathode type	Input power (W)	Emission current (mA)
Graphite heater	66	0.667
Kanthal heater coil	1.5	3.8
Kanthal heater with Mo. posts	0.9	1.8
Tungsten bulb	2.1	9.1
Tungsten bulb	2.9	15.6

The Tungsten light bulbs are a reasonable electron emission source because of the fact that they are widely available, affordable and have predictable characteristics. However, their lifetime is short as their evaporation rate is high. As an example, for every thruster mode test six Tungsten bulbs are replaced every single time. In addition to that, some of them have shown to fail in test with Iodine as a thruster propellant. Therefore, it is interesting in developing a thermionic LaB_6 cathode, which has a better lifetime and enhanced compatibility with eventual iodine thruster developments. Hence, in the next Section 5.5 the design option with a direct heating method is evaluated.

5.5. DIRECTLY HEATED LaB_6 THERMIONIC CATHODES

The method of directly heating the LaB_6 emitter pellet in a closed heater circuit originates from the competitor overview that has been performed during the literature study [25]. The goal is to place the emitter directly in the heater circuit and heat it by Ohmic heating. In this manner, emitted electrons are resupplied over the heater circuit. First, the test setup will be given in Section 5.5.1. Afterwards, the test instrumentation is discussed in Section 5.5.2. Subsequently, the test parameters are treated in Section 5.5.3. Next, Section 5.5.4 gives the test results and Section 5.5.5 discusses the next steps. Finally, Section 5.5.6 gives a discussion on the test results.

5.5.1. TEST SETUP

With an eye on the LaB_6 thermionic cathode development in other space industries, a direct heating cathode method has been established. The schematic can be seen in Figure 5.40. It consists out of two 2 mm diameter and 20 mm long Molybdenum posts, two 5 mm diameter and 3 mm high graphite cylinders with a cutout in order to house the LaB_6 emitter pellet. Furthermore, macor discs, M2 rods and a BN housing are used in order to assemble the cathode setup. AlO spacer tubes make sure that electrical insulation is maintained. The realisation of the test setup can be seen in Figure 5.41.

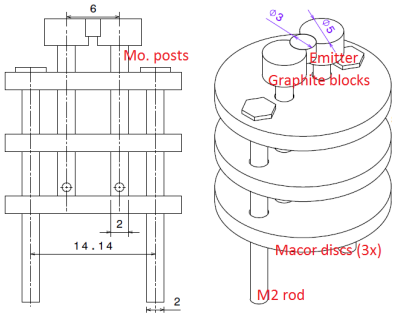

Figure 5.40: Round graphite blocks direct heated cathode setup

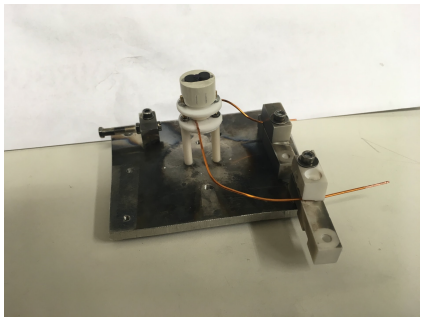

Figure 5.41: Round graphite blocks test setup

The graphite blocks are used for heat generation. In the setup, the graphite parts have the highest electrical resistivity of $6 \cdot 10^{-6}$ Ωm. In comparison to that, LaB_6 has an electrical resistivity of $5 \cdot 10^{-7}$ Ωm and Molybdenum has an electrical resistivity of $5.34 \cdot 10^{-8}$ Ωm. This makes the heat generation by Ohmic heating in the graphite parts the largest, which is beneficial for the heating of the LaB_6 emitter pellet. Next to that, the high operating temperatures of the emitter do not effect the cold ends of the Molybdenum posts that are connected to the copper input lines. Furthermore, with this test setup it can be checked for whether electron emission is possible in a directly heated method. In other words, the question whether electrons can be extracted from the emitter or if they are guided away through the heater circuit will be answered.

5.5.2. TEST INSTRUMENTATION

With a similar measurement setup as with the other vacuum chamber tests that have been discussed in Sections 5.3 to 5.4, only the electrical circuit is different than before. The two copper lines that can be seen in Figure 5.41 are connected to the copper input lines. Next to that, the cathode is directly heated and any emitted electrons can be directly resupplied over the heater circuit. As always, it is important to have a single star point ground for both the heater circuit as well as the cathode - anode circuit in order to avoid any ground loops. Furthermore, the thermocouple that has been tested for its functionality in Section 5.4.5 is placed along the centre line of the setup, below the emitter material. In this way, a feedback for the emitter material can be achieved. The calibration of the thermocouple is given by Table 5.8. The left column indicates the temperature in Fahrenheit, while the right column indicates the value of the potential that is read over the thermocouple by a multi-meter. Furthermore the theoretical potential is given in the second column and the difference to the measured one. It has been determined that with a value of 18 mV, a temperature of 1800 ^{o}F (i.e. 982 ^{o}C) should be reached. At this temperature, according to the possible emission current for LaB_6 in Figure 3.2, the 3 mm diameter emitter should be capable of emitting 70 μA of emission current. The electrical diagram for the round graphite blocks cathode setup can be seen in Figure 5.42.

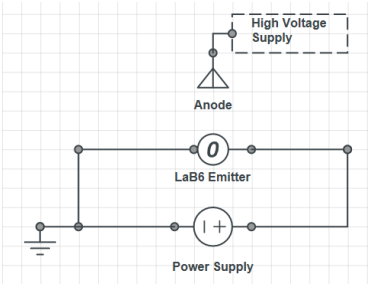

Figure 5.42: Round graphite blocks electrical diagram

Table 5.8: Calibration thermocouple

T (F)	Th. Pot. (mV)	Δ (μV)	Meas. Pot. (mV)
600	5.150	-1.1	5.139
800	7.241	-2.9	7.272
1000	9.393	4.5	9.442
1200	11.563	4.5	11.612
1400	13.723	3.1	13.756
1600	15.852	2.2	15.875
1800	**17.933**	**-0.6**	**17.927**
2000	19.952	-1.4	19.938

5.5.3. TEST PARAMETERS

Similar to other conducted cathode tests, the goal is to measure the cathode emission current for various heater input powers and for various anode potential settings in the range of 0 - 2000 V. In order to do so, first electron emission needs to be achieved. Therefore, the heater input power is gradually increased in steps of 5 Watts per 5 minutes. In this way, the temperature can stabilise before a next increment is applied. First, a bake out of 60 minutes at a power setting of 5 Watts is performed in order to outgas any particles and volatiles of the test setup.

5.5.4. TEST RESULTS

As the power to the cathode circuit is increased, the graphite blocks and the LaB_6 emitter pellet start to glow. This occurs at a power input of 11.6 Watts. At this moment, the anode current is 0, the pressure is equal to $8.1 \cdot 10^{-6}$ mbar and the anode potential equals 604 V. The thermocouple gives a reading of 5 mV, i.e. 590 ^{o}F (i.e. 310 ^{o}C). This moment can be seen in Figure 5.43. Next, the power is increased and increased, but however, no current emission is achieved. Even with three input channels on the power supply giving a total input power of 104 Watts to the cathode circuit, no current emission occurs. At that stage, the thermocouple gives a reading of 13.35 mV, which equals to 1370 ^{o}F (i.e. 743 ^{o}C). This can be seen in Figure 5.44. Despite the fact that the whole system is glowing strongly (which is even enhanced visually by the lighting in Figure 5.44), it appears that the temperature that is reached on the emitter is not high enough for current emission.

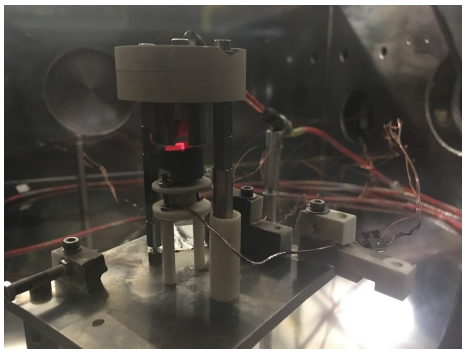

Figure 5.43: Round graphite blocks cathode at 11 Watt input power

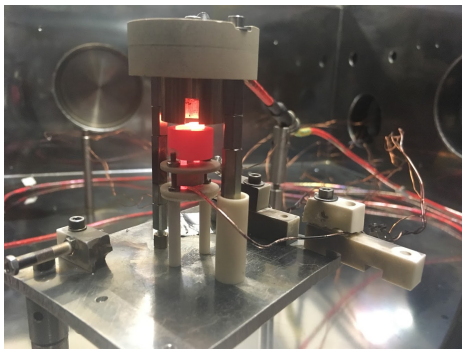

Figure 5.44: Round graphite blocks cathode at 104 Watt input power

5.5.5. NEXT STEPS

On one side, it is argued that the cathode does not emit any current because of the fact that it has not been brought initial emitting state temperatures of 1800 ^{o}F. On the other hand, it is argued that it could be possible for any high kinetic energy containing electrons to flow back directly into the heater circuit, as the graphite blocks are tightly enclosing the LaB_6 emitter pellet. This is an effect that can be seen from competitor thermionic cathodes, where all the emitting surfaces of the cathodes are extending from the heater circuit. Taking both aspects into account, the next iteration of the directly heated cathode by graphite elements is based on the following items:

- **Improving the heater characteristics -** With a decrease in the cross sectional area of the current that is flowing through the heater path, the resistance can be increased and the heat generation is increased as well.
- **Placing the LaB_6 emitter outside the heater circuit current path -** As the emitter pellet has faces that are outside of the direct heating current path, it can be checked for whether current emission to the anode is possible, instead of any electrons flowing directly back into the heater circuit itself.
- **Removing the BN housing around the cathode -** Even though the BN housing has a low thermal conductivity, it still inflicts a relatively large thermal mass that is heated and a heat radiation loss as it is emits heat. Hence, in the next setup the housing of the cathode will not be directly on or over the hot components such as the graphite and emitter elements.

Horizontal cathode circuit with round graphite blocks

With the above mentioned aspects taken into account, a BN base is designed and developed that is capable of fixing the LaB_6 emitter pellet in free space, using threaded Molybdenum posts and graphite inserts that increase the heat generation towards the emitter. This can be seen in Figure 5.45. In this setup, the left and right Molybdenum posts are turned towards each other using the bolts. Next to that, the emitter can be placed in an orientation in which it has faces that are extending from the heater circuit. In other words, if the emitter is brought to proper temperatures in order to emit electrons, they can vacate the emitter material from those surfaces. In the setup in Figure 5.45, this is the circumferential surface area of the LaB_6 pellet.

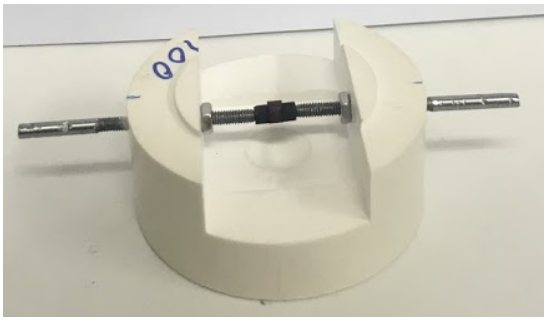

Figure 5.45: LaB_6 emitter pellet clamped in between graphite blocks

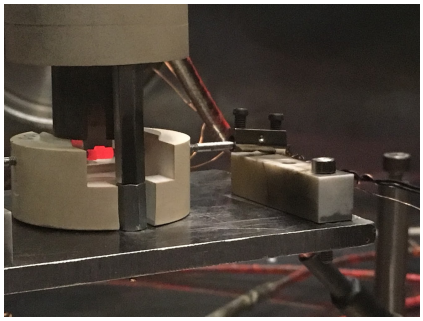

Figure 5.46: Round graphite blocks and LaB_6 emitter pellet

Using a thermal nodal network model it will be checked for whether the emitter can be brought to an emitting temperature of 1600 K. At this temperature, it is able to emit with 0.4 A/cm^2 over the circumferential area of the pellet and the remaining side faces, which results in an emission current of 10 mA. The current emission vs temperature plot that is used for this can be seen in Figure 3.2. The thermal nodal network model can be seen in Figure 5.47. This figure also indicates the dimensions (in mm), thermal conductivities (in W/mK) and electrical resistivity values (in Ωm) of the three materials that are used. The nodal temperatures T_1, T_2 and T_3 are for the LaB_6 emitter pellet, the graphite round elements and the end of the Molybdenum posts respectively.

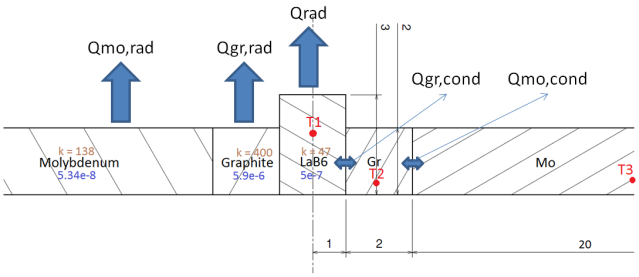

Figure 5.47: Thermal nodal network model round graphite elements heating

The first step is to determine the heat radiation from the LaB_6 emitter pellet at an temperature of 1600 K. This is done in Equation (5.15). Next, the required power throughput through the graphite elements and Molybdenum posts is determined. Accordingly, the heat radiation losses are taken into account. The temperature at a graphite element is determined with Equation (5.16).

$$Q_{rad} = \epsilon A \sigma T^4 = 0.8 \cdot 2.67 \cdot 10^{-5} \cdot \sigma \cdot 1600^4 = 7.94 \text{ W} \tag{5.15}$$

$$Q_{gr,cond} = \frac{kA}{l} \Delta T = \frac{400 \cdot \pi \cdot 0.001^2}{0.002} (T_{LaB6} - T_2) \Rightarrow T_2 = 1594 \text{ K} \tag{5.16}$$

Next, the temperature at the end of the Molybdenum posts is determined in order to evaluate the thermal network. In order to do so, the required throughput in terms of thermal energy is determined first. This consists out of the radiating emitter pellet, the radiating graphite blocks and the conductive heat that is passed on through the graphite elements. The graphite element radiation is given by Equation (5.17). The temperature T used is an average of the graphite element temperature on the one end and the LaB_6 emitter temperature on the other end. The temperature on the far end of the Molybdenum post is given by Equation (5.18).

$$Q_{gr,rad} = \epsilon A \sigma T^4 = 0.85 \cdot 2\pi \cdot 0.001 \cdot 0.002 \cdot \sigma \cdot \left(\frac{T_{LaB6} + 1594}{2} \right)^4 = 3.71 \text{ W} \tag{5.17}$$

$$Q_{mo,cond} = \frac{Q_{rad}}{2} + Q_{gr,rad} = \frac{kA}{l} \Delta T = \frac{138 \cdot \pi \cdot 0.001^2}{0.020} (T_2 - T_3) \Rightarrow T_3 = 1240 \text{ K} \tag{5.18}$$

The temperature of 1240 K is safe to connect copper input lines to since copper has a melting temperature of 1358 K. In order to obtain the total input power, the radiation of the Molybdenum rods needs to be taken into account.

This term is evaluated in Equation (5.19). Next to that, the input power to the round graphite heating element cathode is determined in Equation (5.20). The total amount of input power to get the LaB_6 emitter pellet to 1600 K is equal to 26.83 W.

$$Q_{mo,rad} = \epsilon A \sigma T^4 = 0.2 \cdot 2\pi \cdot 0.001 \cdot 0.020 \cdot \sigma \cdot \left(\frac{T_2 + T_3}{2} \right)^4 = 5.74 \text{ W} \tag{5.19}$$

$$P_{in,tot} = Q_{rad} + 2 \cdot Q_{rad,gr} + 2 \cdot Q_{rad,mo} = 26.83 \text{ W} \tag{5.20}$$

The setup with the LaB_6 emitter clamped in between the two round graphite blocks is baked out in a vacuum chamber test at an input power of 3 Watts. Next, the input power is increased by steps of 3 Watts every 15 minutes. At an input power of 14 Watts the graphite blocks and the LaB_6 emitter pellet start to anneal in orange. This can be seen in Figure 5.46. At this moment, the pressure is equal to $5.3 \cdot 10^{-6}$ and the anode potential equals 600 V. However, the current emission remains zero until an input power of 40 Watts, where it initiates and rise up to 0.5 mA. Hence, it shows that it is possible to emit and achieve electron flow. Nonetheless, the heat generation is not high enough in order to achieve the desired 10 mA of cathode anode current.

Horizontal cathode circuit with graphite needle tips

From the test with the round graphite blocks clamping the LaB_6 emitter pellet it has turned out that glowing can be achieved, but not in a sufficient way in order to extract the desired amount of electrons. Therefore, the graphite blocks are replaced by graphite needle tips, in order to increase the heat generation as the cross sectional area through the needle tip is decreased. With needle tips, the cross sectional area towards the emitter of the graphite elements can be decreased, which results in an increased resistance and thus heat generation.

The graphite needle tips are constructed from 5 mm graphite rods and using a pencil sharpener. This results in a 16 degrees half cone angle at the tip of the needle. Next to that, a 2 mm deep and 2 mm diameter pocket is created along the centre line at the 5 mm diameter surface in order to insert the Molybdenum posts. The geometry of the needle can be varied and this method allows for a straight forwards first iteration. Now that the round graphite blocks are replaced by graphite needle tips, the thermal model needs to be iterated as well. In order to prepare the conical section for thermal modelling, it has been segmented into small finite elements that consist out of rectangular blocks. In this manner, the conduction and radiation can be evaluated per element and eventually integrated to obtain an accurate result. Figure 5.48 gives an illustration of how the graphite needle with half cone angle θ is divided into segments that will be used as rectangular elements with width x_n and height y_n.

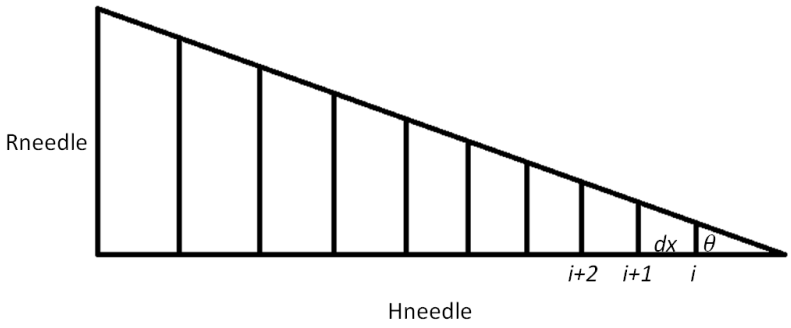

Figure 5.48: Graphite needle tip element by element analysis

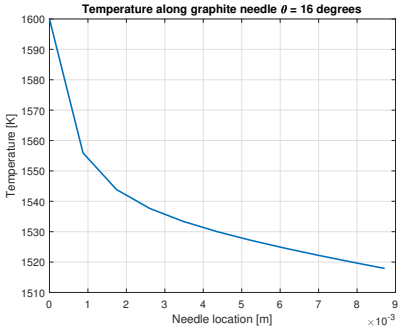

Figure 5.49: Needle Temperature vs Location

First, the width and height of the elements are determined. These are then used to determine the conduction and radiation for each element in a similar manner as before with the round graphite blocks. These values will be different for each element, because of the fact that the both the cross sectional area as well as the free radiating area increase. Figure 5.49 shows how the temperature from the needle tip at 1600 K decreases along the graphite needle length. At the end and hence the largest diameter section of the graphite needle the temperature is used to determine the temperature at the end of the Molybdenum posts. This is equal to 476.2 K. The temperature drop is much larger than before, because the total heat radiation along the (larger) graphite needle element is larger as well. In order to determine the total input power to the graphite needle tip cathode to get the LaB_6 emitter pellet to 1600 K, the Molybdenum heat radiation needs to be taken into account as well. Doing so, it is found that a total input power of 55.5 W is required. This will be taken into account when performing the vacuum chamber diode mode test. Figure 5.50 gives an overview of the test setup. Next to that, Figure 5.51 gives an illustration of the realised test setup.

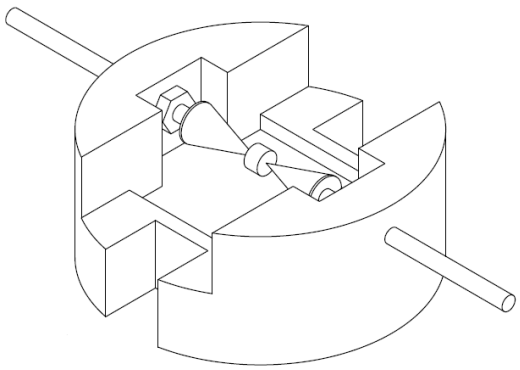

Figure 5.50: Graphite needle tips setup

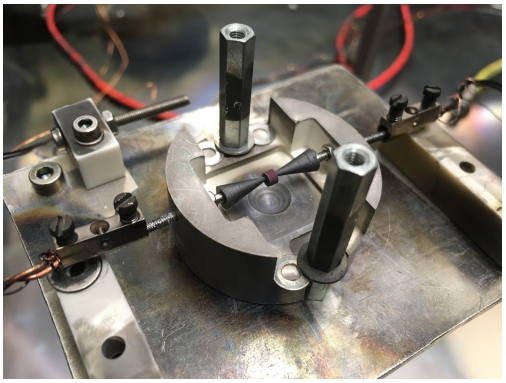

Figure 5.51: Detail view graphite needle tips cathode

First, the setup is baked out at an input power of 5 Watts. Next, the input power is increased in steps of 5 Watts every 15 minutes. The time steps are sufficiently large enough in order to reach thermal stability and to give electron emission time to initiate at a fixed input power setting. At an input power of 16 Watts the needle tips and the LaB_6 emitter pellet start to anneal in orange. At this moment, the pressure is equal to $5.2 \cdot 10^{-6}$ mbar and the anode potential equals 658 V. With the graphite needle tip cathode the glowing that is achieved on both the graphite needle tips as well as the LaB_6 emitter pellet is brighter than ever before. In addition to that, the glowing is stronger near the tip of the graphite needle than at its larger diameter cross sections. The glowing can be seen in Figure 5.52. Next, at an input power of 53 Watts current emission initiates with 3 μA and is slowly increasing. In the next 67 minutes the input power is kept at a constant setting and the emission current is measured. In this time period, a maximum current of 45 mA is achieved. The emission current versus time plot can be seen in Figure 5.54. At the end of the 67 minutes, the inside thread of the anode has reached that high temperatures that it is no longer to carry itself on the bolt and it drops down, shorting the cathode - anode circuit. This can be seen in Figure 5.53.

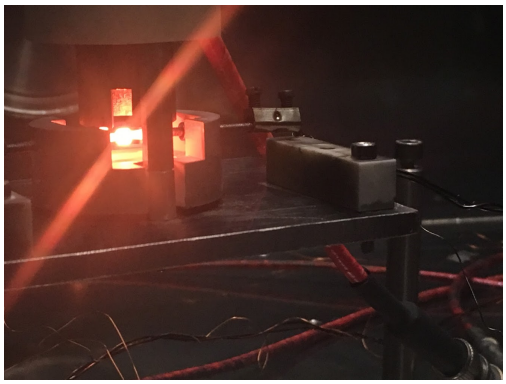

Figure 5.52: Graphite needle tips and LaB_6 emitter glowing

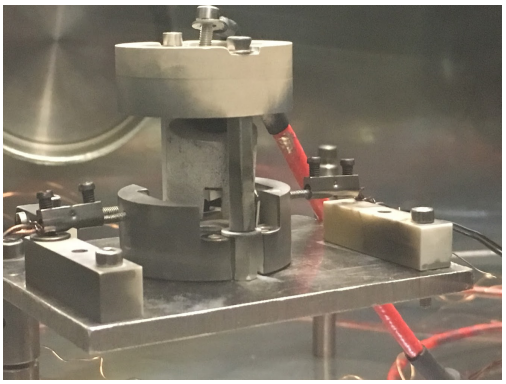

Figure 5.53: Anode fallen down onto cathode heater circuit

In a similar test a similar amount of electron emission has been achieved, namely 64 mA for an input power of 56 Watts. Similarly, the pressure inside the vacuum chamber is equal to $7.1 \cdot 10^{-6}$ mbar and the anode potential equals 658 V. The anode current development over time can be seen in Figure 5.55. The amount of emission current that can be achieved is now higher than the required 10 mA according to the requirement *HEMPT-CAT-001*. Therefore as a continuation, for the next iteration a BN cover lid is created so that the anode is not able to come down from the bolt that it is hanging on. In this manner, the varying input powers and anode potentials can be applied in order to obtain a characterisation of the graphite needle tip cathode.

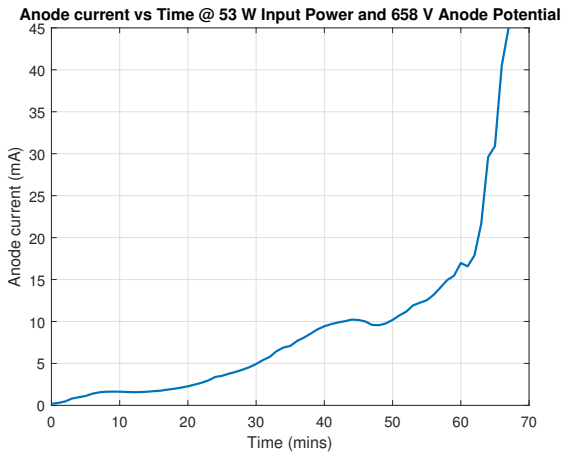

Figure 5.54: Anode current vs Time for graphite needle tips cathode

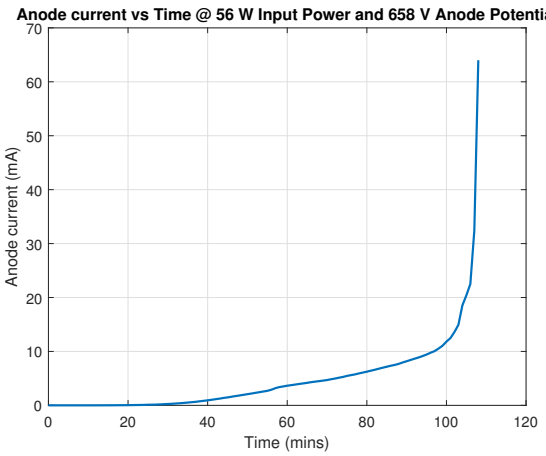

Figure 5.55: Anode current vs Time - Test 2

Graphite needle tip characterisation

Now that the graphite needle tip cathode is able to achieve a decent amount of electron emission, it will be tested for various input powers and anode potential settings. In this manner, a characterisation of the cathode can be made and it can be compared with COTS thermionic cathodes and future iterations. In order to recap the test parameters from Section 5.5.3; the graphite needle tip cathode will be tested for fixed power settings and varying the anode potential from 0 - 2000 V. In addition to that, the anode current will be measured for a fixed anode potential setting and varying the input power. In this manner, the space charge limitation according to the Child-Langmuir relation in Equation (3.3) as well as the physical electron emission according to the Richardson relation in Equation (3.1) can be analysed.

First, the graphite needle tip cathode is operated at a fixed power setting of 40 Watts. Next, the anode potential is increased from 0 Volts up to 2000 Volts in steps of 100 V. The result can be seen in Figure 5.56. Above an anode potential of 1500 V discharging sparks are occurring and hence the possible voltage that can be put is limited. The graphs for input powers of 45, 50 and 55 Watts can be seen in Figures 5.57, 5.58 and 5.59 respectively. For the last measurement series at an input power of 55 Watts these discharge sparks occurred even earlier and the measurement is therefore performed up to 1200 V. A lower power setting than 40 Watts has not been measured, because of the fact that with 40 Watts of input power the emission current at a high anode potential of 1500 V is already limited to 7 mA. Hence despite the fact that the required input power in order to meet the required emission current is high, it can be achieved and further testing and development on this iteration is continued. In addition to that, it can be seen, especially from the first two measurements in Figures 5.56 and 5.57, how initially the anode current increases in the convex part before it goes over an inflection point and changes to the concave part of the graph. Here, space charge limitation becomes visible. In other words, for a fixed power setting there cannot be a higher emission current (i.e. amount of electrons) existing in between the cathode and anode.

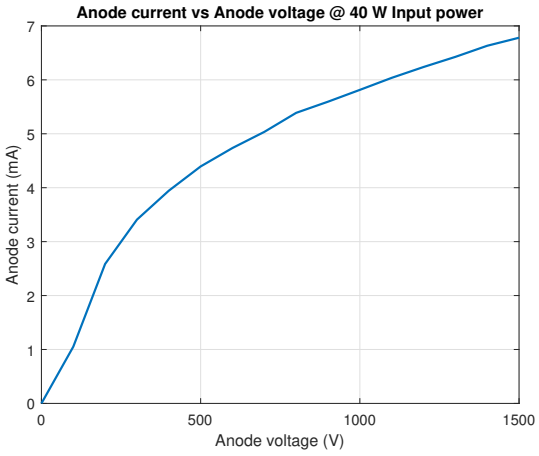

Figure 5.56: Anode current vs Anode voltage - 40 W

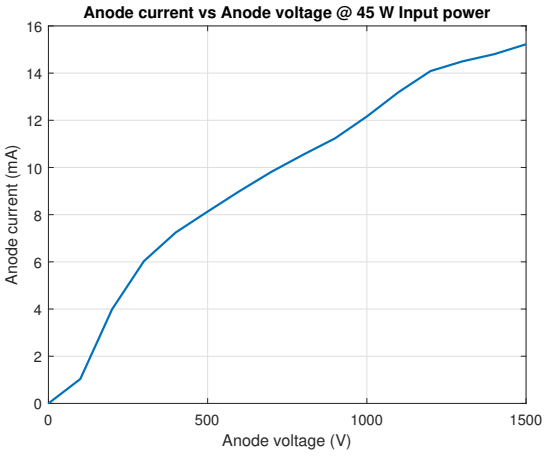

Figure 5.57: Anode current vs Anode voltage - 45 W

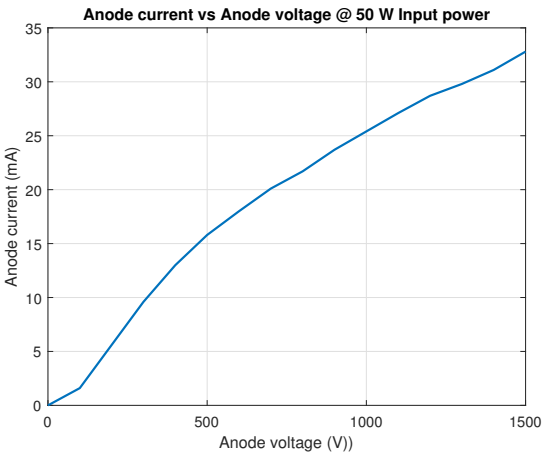

Figure 5.58: Anode current vs Anode voltage - 50 W

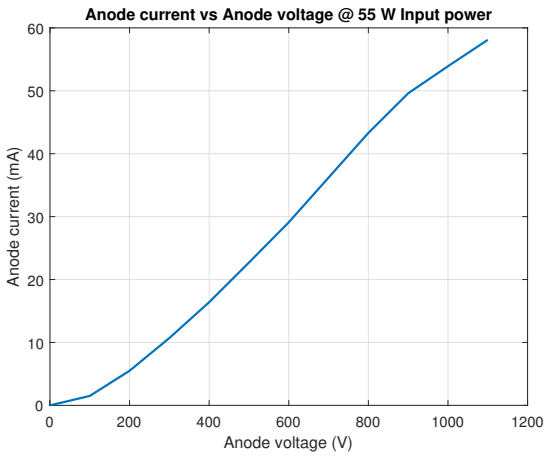

Figure 5.59: Anode current vs Anode voltage - 55 W

In order to illustrate the behaviour of the anode current versus the anode potential for the different power settings, they have been put into a single graph. This can be seen in Figure 5.60. Again, it can be seen from the graphs how they will reach their asymptotic limit at some point as the space charge between the cathode and anode is limited. This behaviour is expected according to the Chlid-Langmuir relation that describes the existence of a finite amount of charges within a control volume. Furthermore, for a higher input power a higher amount of emission current can be achieved, as the emitting temperature will increase.

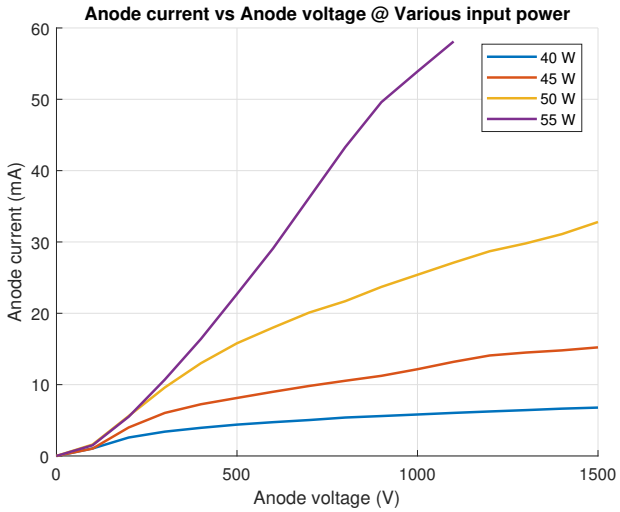

Figure 5.60: Anode current vs Anode Potential - 40, 45, 50 and 55 W

Next to that, the anode potential is kept at a constant value whereas the input power is varied. In this manner the physical amount of electrons that can be emitted from the LaB_6 emitter pellet can be characterised. This is also described by the Richardson relation in Equation (3.1). The limiting value of input is put to 55 Watts, since at this power setting the electron emission initiated and the load and hence heat generation on the D-sub feed through in terms of Amps is decent (28 A over a 25-pin D-Sub with 12 pins and 13 pins allocated to both sides of the circuit respectively). First, the emission current for an anode potential at 300 V is measured. The result can be seen in Figure 5.61. Afterwards, the same is performed for 400, 500 and 658 V (the initial setting). The graphs for these measurements are given in Figures 5.62, 5.63 and 5.64 respectively. A setting lower than 300 V has not been measured, because at 300 V the anode current limits to close to 3 mA.

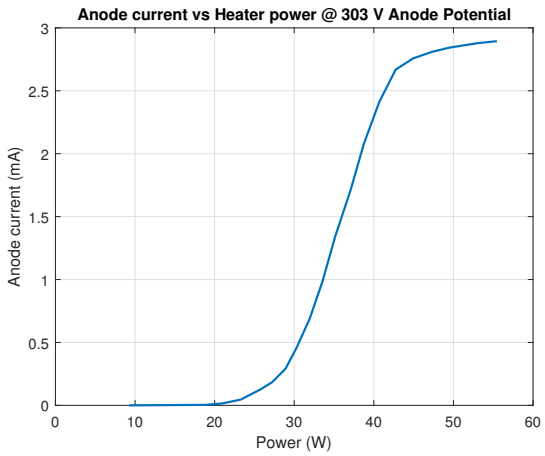

Figure 5.61: Anode current vs Input power - 303 V

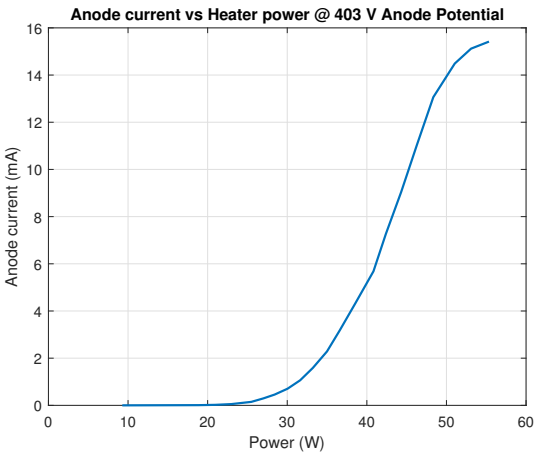

Figure 5.62: Anode current vs Input power - 403 V

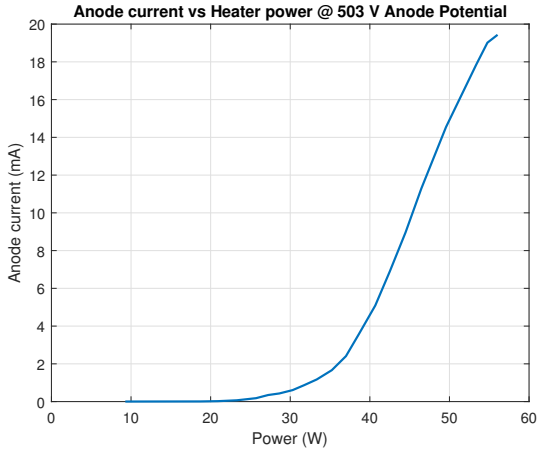

Figure 5.63: Anode current vs Input power - 503 V

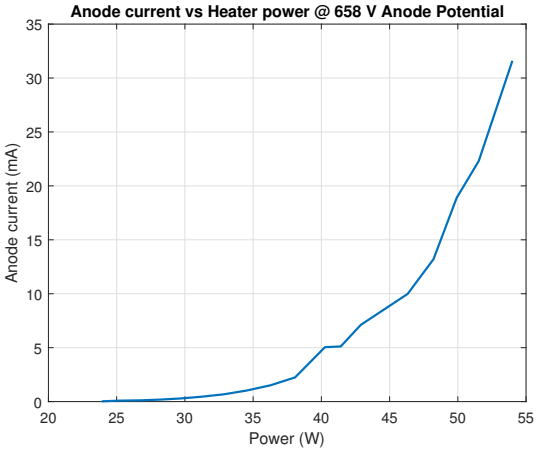

Figure 5.64: Anode current vs Input power - 658 V

For the two lower anode potential cases where in this case the anode potential equals 300 V and 400 V in Figures 5.61 and 5.62 respectively, the Richardson limitations can be seen to be reached. This means that as the input power to the LaB_6 emitter pellet is increased more and more while the anode potential is kept constant, the increment of electron emission decreases and decreases. This is because of the fact that it is physically impossible to extract any more electrons from the emitter for the constant level of anode potential. Figure 5.65 shows the graphs for the various potential settings combined in a singe plot. Only the high potential case of 658 V does not show the stabilising behaviour yet within the used input power range, whereas the other cases do.

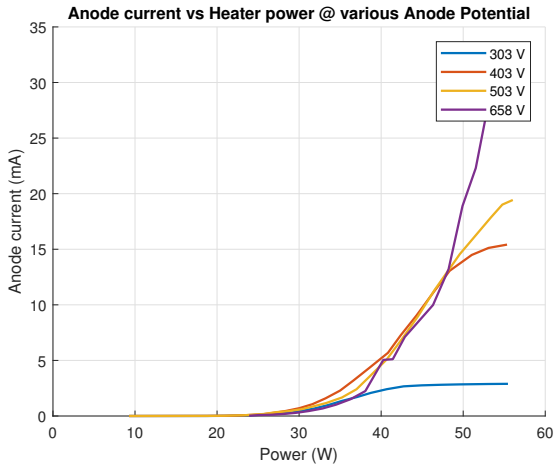

Figure 5.65: Anode current vs Input power - 300, 400, 500 and 658 V

5.5.6. DISCUSSION

With the graphite needle tip cathode configuration the desired amount of 10 mA of emission current can be achieved. Nonetheless, the required operating input power range of 1 - 15 Watts according to *HEMPT-CAT-002* is not met by far. Furthermore, emission currents up to 64 mA have been achieved. Next to that, a characterisation on the graphite needle tip cathode has been performed in order to obtain emission current characteristics for various input power and anode potential settings. These do not only give insight in the performance of the cathode, but also allow comparison with other thermionic LaB_6 cathodes. Furthermore, in this configuration it will be possible to test the cathode in thruster mode in combination with a xenon propellant engineering model electric thruster. Table 5.9 gives an overview of the cathode development.

Table 5.9: LaB_6 Cathode development

Cathode type	Input power (W)	Emission current (mA)
Graphite heater	66	0.667
Kanthal heater coil	1.5	3.8
Kanthal heater with Mo. posts	0.9	1.8
Tungsten bulb	2.1	9.1
Tungsten bulb	2.9	15.6
Graphite needle tip	56	64

5.6. COTS KIMBALL PHYSICS LaB_6 CATHODE

In order to obtain a performance comparison with the developed graphite needle tip LaB_6 cathode, a commercial of the shelf thermionic LaB_6 cathode is procured and tested. This is the Kimball Physics ES-440 High Current LaB_6 Crystal[8]. According to the manufacturer, it is capable of emitting up to 0.5 A of emission current at an input power of 10 Watts. The operating temperature is around 1800 K and the vacuum level that is required shall be equal to or lower than 10^{-7} Torr (i.e. $1.33 \cdot 10^{-7}$ mbar). First, the test setup will be given in Section 5.6.1. Afterwards, the test instrumentation is discussed in Section 5.6.2. Subsequently, the test parameters are treated in Section 5.6.3. Next, Section 5.6.4 gives the test results and Section 5.6.5 discusses the next steps. Finally, Section 5.6.6 gives a discussion on the test results.

5.6.1. TEST SETUP

The COTS Kimball Physics LaB_6 cathode will be tested in diode mode in order to obtain a characterisation for the electron emission. The cathode consists out of a 1.78 mm diameter flat cylinder LaB_6 single crystal emitter that is mounted in a Molybdenum guard ring. With Molybdenum wires it is connect to 1 mm diameter Molybdenum posts, which are fixed in a 12 mm diameter and 1 mm thick ceramic base. The cathode assembly can be seen in Figure 5.66. Next to that, Figure 5.67 gives a schematic overview of the cathode [3].

[8] `https://www.kimballphysics.com/downloadable/download/sample/sample_id/1291/` | Visited on 24 November 2017

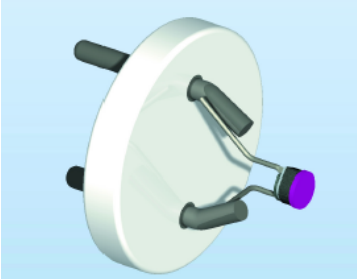

Figure 5.66: Kimball Physics COTS cathode [3]

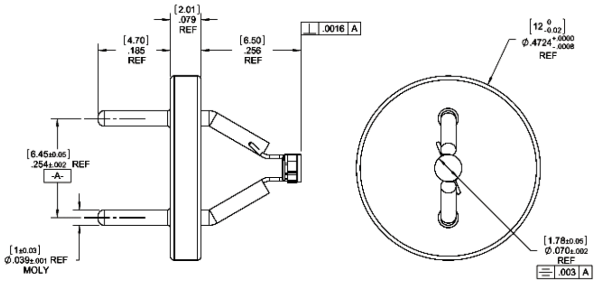

Figure 5.67: Kimball Physics COTS cathode schematic [3]

The diode mode test setup that is realised in order to test the COTS Kimball Physics cathode consists out of BN base that is able to both house and protect the cathode, if the anode is lowered. Nonetheless, this is not expected to happen because of the fact that the emitter itself is smaller compared to the 3 mm diameter LaB_6 emitter pellet and moreover, because of the fact that there are no relatively large hot graphite elements. The BN base has an outer diameter of 15 mm and an inner diameter of 13 mm in order to house the cathode. The fixation is realised by installation on 2 mm extending M2 posts from the ground plate and clamping from the front and rear side by bolts. Furthermore, cutouts are made in order to house and connect the screw screw type connectors to the Molybdenum posts of the cathode. The copper input lines are clamped in between Macor blocks in order to strain relieve and insulate the cathode heater circuit. Figures 5.68 and 5.69 give an overview of the setup, whereas Figure 5.70 shows how the connections are realised.

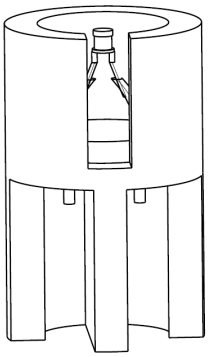

Figure 5.68: Isometric view

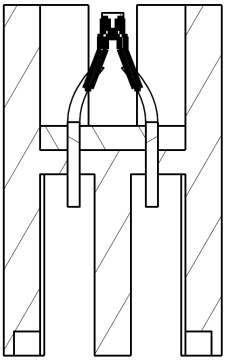

Figure 5.69: Section view

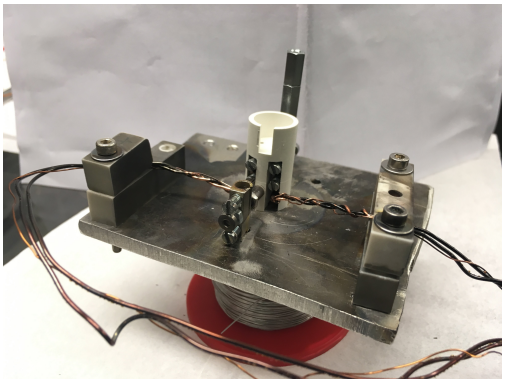

Figure 5.70: Kimball Physics COTS cathode connections

5.6.2. TEST INSTRUMENTATION

The test instrumentation in terms of test equipment remains unchanged. The anode is placed above the COTS Kimball Physics cathode and connected to the high voltage supply. Next to that, the heater circuit is closed with the screw screw type connectors that are attached to the Molybdenum posts of the cathode. As with previous tests, it remains important to have a shared star point ground for the two floating circuits, i.e. the heater circuit to the cathode and the cathode - anode high potential circuit. In this manner ground loops are prevented and measurements can be compared to other cathode diode mode tests.

5.6.3. TEST PARAMETERS

The goal of this COTS Kimball Physics cathode diode mode test is to evaluate the electron emission performance and to compare the performance with the graphite needle tip cathode. Therefore, its emission current is measured for four different power settings and varying anode potential, where for the lowest one of the four the emission current limits to a low absolute value. In addition to that, the anode potential is kept standard at 300, 400, 500 and 600 Volts in order to compare it with the graphite needle tip cathode performance from Section 5.5.5.

According to Kimball Physics, there are no requirements in order to start an activation process for the LaB_6 emitter crystal. Nevertheless, the assembly as a whole will outgas and therefore a bake out is required, as with all the other cathode vacuum chamber tests. Furthermore, Kimball Physics recommends to increase the heater power stepwise, while not letting the vacuum chamber pressure exceed $1 \cdot 10^{-7}$ Torr (i.e. $1.33 \cdot 10^{-7}$ mbar). As this pressure is lower than the achievable pressure in the vacuum chamber that is used, the operating pressure will be kept as close as possible to the minimum reached vacuum chamber pressure [65].

5.6.4. TEST RESULTS

In this section the test results for the COTS Kimball Physics cathode will be given. First, the cathode is baked out at an input power of 10 mW for 60 minutes. The pressure is equal to $5.5 \cdot 10^{-6}$ mbar and the anode potential equals 608 V. Afterwards, the input power is increased gradually and timely so that the vacuum chamber pressure remains as low as possible. In this manner the risk of poisoning the cathode by chemical reactions between e.g. La and O forming LaO is minimised.

Despite the fact that the recommended operating pressure of lower than 10^{-7} Torr by Kimball Physics can not be met in the used vacuum chamber, the cathode can be tested at the minimum pressure that is achievable. At an input power of 2.1 Watts the LaB_6 emitter starts to glow. This can be seen in Figure 5.71. At this moment the pressure inside the vacuum chamber is equal to $5.5 \cdot 10^{-6}$ mbar and the anode potential equals 608 V. Next, the COTS cathode starts to emit electrons up to 73 μA. The pressure has risen to $5.6 \cdot 10^{-6}$ mbar and the anode potential remains 608 V. At this point the glowing is clearly enhanced, which can be seen in Figure 5.72.

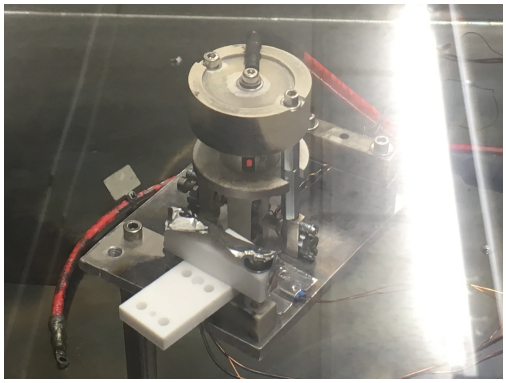

Figure 5.71: COTS Cathode glow initiation

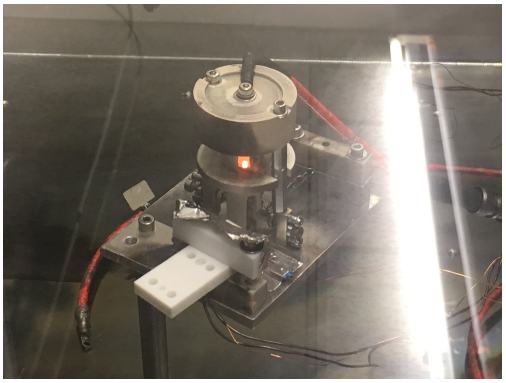

Figure 5.72: COTS Cathode enhanced glowing

As the anode potential remains equal to 608 V (the initial setting), the anode current is measured for various input power settings. This has been done up to an input power of 7 Watts. The reason for this is because at this input power already an anode current of 39 mA is reached, which supersedes the required 10 mA of emission current. Next to that the input power is reached with 7 A and 1 V, whereas the manufactures have calibrated an operating condition of 5.5 A and 1 V, with a maximum of 9 A and 2 V. In order to not put the COTS cathode to high loads, the measurements are carried out up to 7 W of total input power. The results for 300, 400, 500 and 600 V of anode potential and various input powers can be seen in Figures 5.73 to 5.76 respectively.

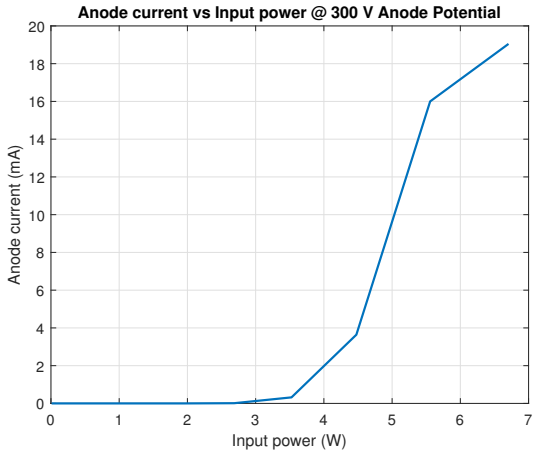

Figure 5.73: Anode current vs Input power - 300 V

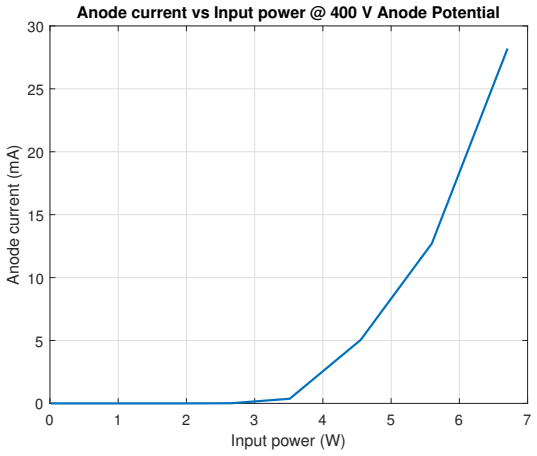

Figure 5.74: Anode current vs Input power - 400 V

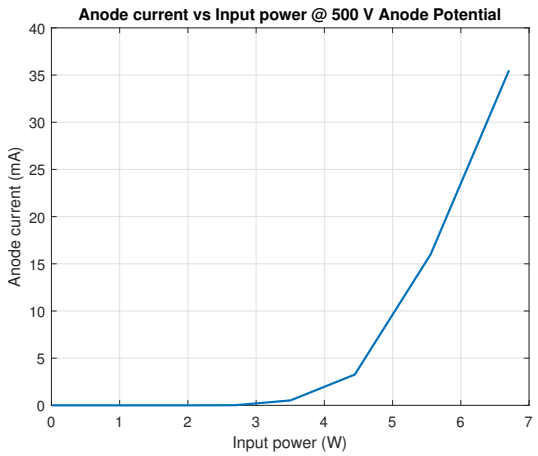

Figure 5.75: Anode current vs Input power - 500 V

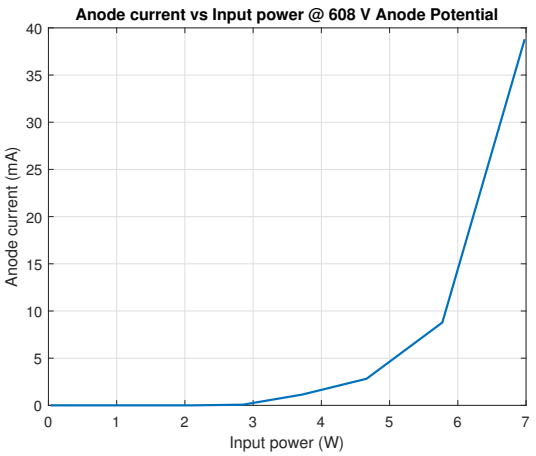

Figure 5.76: Anode current vs Input power - 658 V

Whereas, the space charge limitation is not as clearly visible for all the of the graphs in Figures 5.73 to 5.76, the asymptotic trend can be seen for the lower potential case of 300 V of anode potential in Figure 5.73. Here, the anode current will be limited despite the fact that the cathode power is increased. This is the result of Richardson limitation as described by the Richardson relation in Equation (3.1). Furthermore, the graphs have been combined into a single plot in Figure 5.77 in order to illustrate the behaviour. It can be seen how the limitations for the remaining curves will occur outside the 0 - 7 Watts input power range and how the same trend is followed.

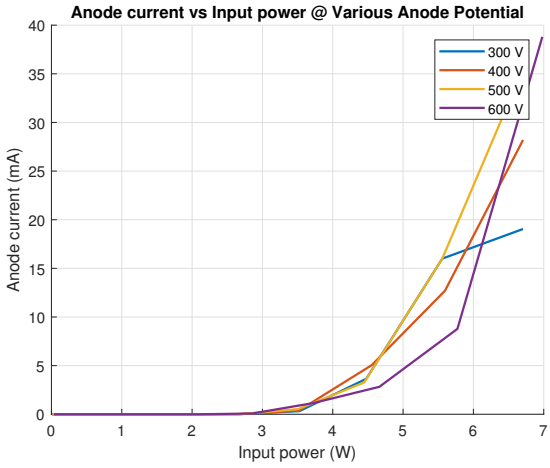

Figure 5.77: Anode current vs Input power - 300, 400, 500 and 600 V

Next to that, the emission current for the COTS Kimball Physics cathode is measured for the different power settings of 4, 5, 6 and 7 Watts, while varying the anode potential up to 1300 V. In any case, it is made sure to not put a high load on the anode. Therefore, the power that is going through the anode according to the anode potential and the anode current ($P = VI$), is limited to 25 Watts. In this manner, the load will not be high and there is no risk of the anode block of detaching or falling down [66]. The graphs for the 4 - 7 Watts of input power can be seen in Figures 5.78 to 5.81 respectively. In all of the graphs the limitation behaviour due to space charge limitation according to the Child-Langmuir relation in Equation (3.3) is visible. Despite the fact that anode potential is increased, the increment in emission current is limited and will eventually go to zero.

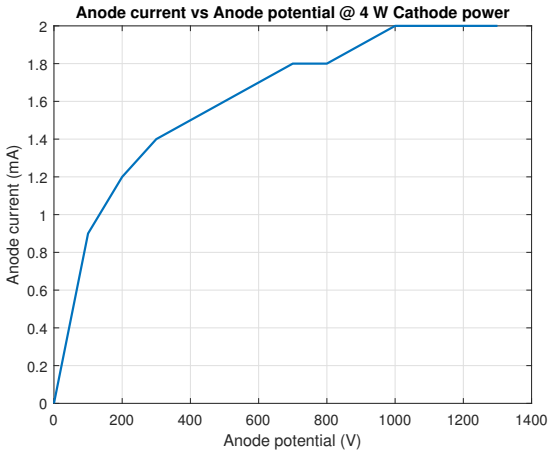

Figure 5.78: Anode current vs Anode potential - 4 Watts input power

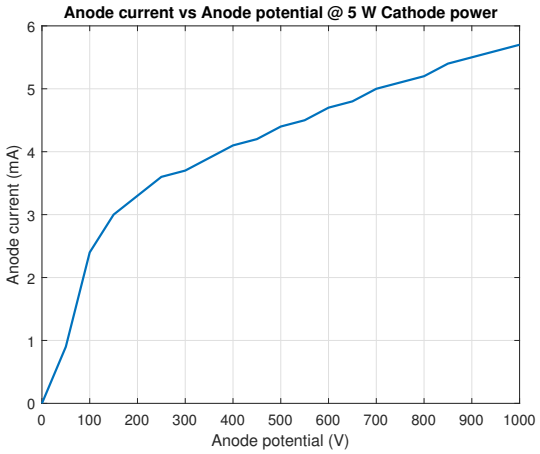

Figure 5.79: Anode current vs Anode potential - 5 Watts input power

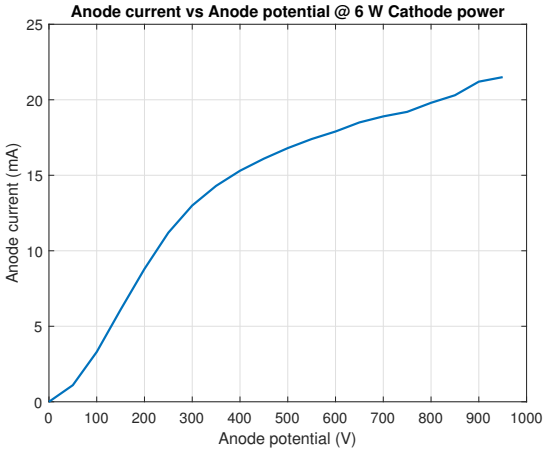

Figure 5.80: Anode current vs Anode potential - 6 Watts input power

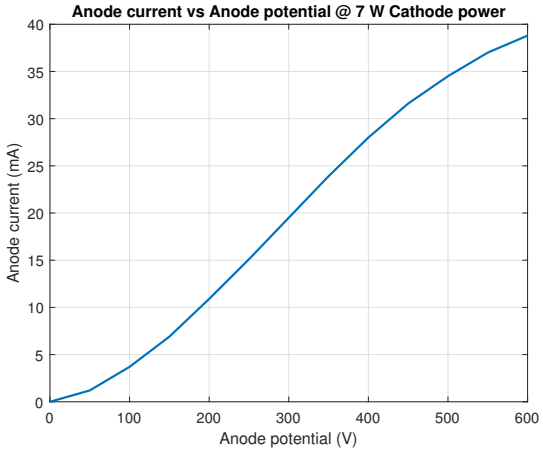

Figure 5.81: Anode current vs Anode potential - 7 Watts input power

Next to that, all of the graphs have been combined into a single plot. The result can be seen in Figure 5.82. In this plot, the limitation behaviour for the various cases due to space charge limitation effects can be clearly seen. Furthermore, it can be seen how the required current emission of 10 mA can be achieved for the required operating input power range of 1 - 15 W. Hence, the COTS Kimball Physics LaB_6 cathode proves to be a suitable candidate in order to operate with the micro electric thruster. This is mainly due do the much smaller emitting surface and the enhanced thermal design. Not only is the radiating area smaller compared to the graphite needle tip cathode, but also are the hot elements better insulated by means of the low emissivity Molybdenum guard ring.

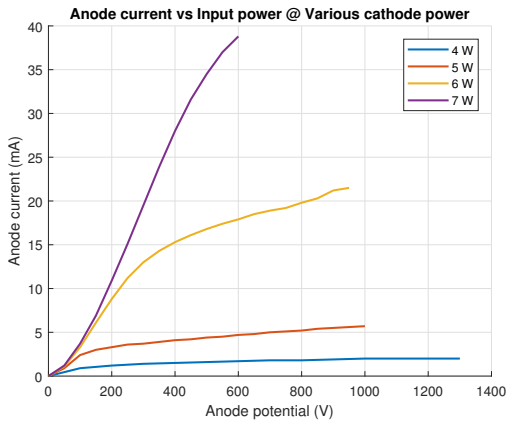

Figure 5.82: Anode current vs Anode potential - 4, 5, 6 and 7 Watts

5.6.5. NEXT STEPS

Furthermore, the COTS Kimball Physics cathode will be tested with a ring magnet in order to investigate whether electron emission is enhanced at lower potential settings. This is an important aspect since it is hypothesised that eventually the electrons can be guided along the magnetic field lines by the ring magnet towards the discharge chamber of the thruster. However, it remains important to keep the operating temperatures into account. This is because of the fact the magnets lose their magnetisation at their Curie temperature. For Samarium Cobalt magnets such as the ring magnet the Curie temperature is equal to 800 ^{o}C, whereas for Neodymium magnets it is equal to 320 ^{o}C. Initial thermal analysis has shown that the AlO spacer at 4.5 mm away of the 1800 K LaB_6 emitter achieves a temperature of 1400 K. Therefore, it is unlikely that (at least for nominal / high operating conditions, i.e. 7 Watts) there is any change in emission current. The ring magnet has an outer diameter of 14 mm, an inner diameter of 11 mm and a height of 3 mm. The test setup with the COTS cathode from Section 5.6.1 is adapted in the following ways:

- **BN base modified -** In order to house the ring magnet the BN top shell is removed. This is realised by the manufacturing of another similar BN cathode base.
- **AlO spacer tube added -** An Aluminium Oxide spacer tube is placed inside the ring magnet. In this manner, the Molybdenum legs of the COTS cathode are prevented from being shorted or affected by the ring magnet. In addition to that, the COTS cathode inside the tube is protected should the anode above detach.
- **Ring magnet added -** The ring magnet is placed around the AlO tube and lower than the LaB_6 emitting part. In this manner the magnetic field lines are diverging to the zenith direction and hence electrons have the capability of following them.

The resulting test setup in operation can be seen in Figure 5.83. The ring magnet is installed around the glowing AlO spacer tube. The BN disc is used to fixate and centralise those parts around the cathode. The test parameters are equal to the COTS cathode test without a magnet. In order to conduct the magnet COTS cathode test at equal cathode emission temperatures as without a magnet, the test is tuned as such that the equal emission current is reached for a fixed potential setting by varying the input power. Next, the cathode is tested for this equal temperature case regarding the ”magnetless“ COTS cathode test for the 4, 5, 6 and 7 Watt measurements. However, no change in emission current performance is measured. In addition to that, it is noted that the magnet has lost almost all of its magnetisation after the tests. It has only very little attraction to the whiteboard by now and is not capable any longer of adhering to it. Thus, the ring magnet has experienced temperatures close to or greater than its Curie temperature has no effects on enhancing (low potential) electron emission.

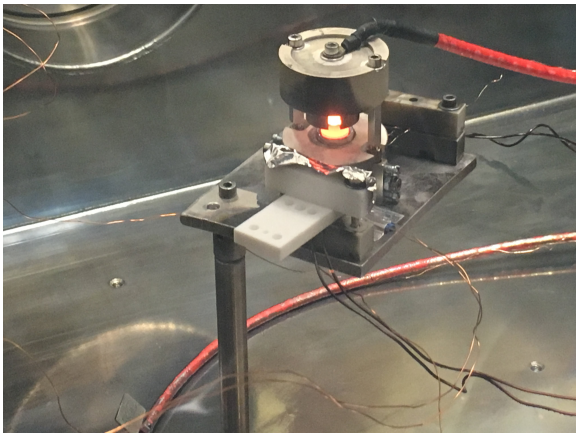

Figure 5.83: COTS Cathode magnet test

5.6.6. DISCUSSION

Current emission for the COTS Kimball Physics cathode is achieved in diode mode testing. Despite the fact that mentioned emission currents up to 0.5 A are not reached (nor 0.75 A with 30 A/cm^2 or 0.5 A if the 20 A/cm^2 emission characteristic is used), the COTS cathode provides sufficient emission current of 10 mA in order to be operated with the electric thruster. Moreover, the power levels that are required in order to achieve the desired emission current values are low and within the required range of 1 - 15 W. This is due to the fact that the efficiency and heat generation are of a high level. Table 5.10 shows the cathode development. The COTS cathode has been tested with a ring magnet in place as well, yet this showed no enhancement in electron emission.

Table 5.10: LaB_6 Cathode development

Cathode type	Input power (W)	Emission current (mA)
Graphite heater	66	0.667
Kanthal heater coil	1.5	3.8
Kanthal heater with Mo. posts	0.9	1.8
Tungsten bulb	2.1	9.1
Tungsten bulb	2.9	15.6
Graphite needle tip	56	64
COTS Kimball Physics	7	38.8

Due to the fact that other thermionic LaB_6 cathodes than the graphite needle tip cathode and the COTS Kimball Physics cathode do not produce the required emission current of 10 mA, they will not be continued in the design process. In order to continue the LaB_6 cathode feasibility operation with the micro electric thruster in place, a thruster mode test with the graphite needle tip cathode will be performed. This is discussed next in Section 5.7. The COTS cathode will remain to be evaluated in a thruster test in a later stage.

5.7. GRAPHITE NEEDLE TIP CATHODE THRUSTER MODE TEST

In the final test the graphite needle tip cathode is tested in thruster mode with the operable full scale xenon thruster engineering model. The goal of this test is to verify whether the realised cathode is able to provide a sufficient amount of electrons for the propellant ionisation process in the discharge chamber of the electric thruster. In terms of electron emission this should be possible since the required 10 mA is met, however in terms of power consumption the efficiency needs to be improved as mentioned before. In addition to that, neutralisation of the exiting plasma plume needs to be realised in order to safely keep the thruster running. This section described this thruster test. First, the test setup will be given in Section 5.7.1. Afterwards, the test instrumentation is discussed in Section 5.7.2. Subsequently, the test parameters are treated in Section 5.7.3. Next, Section 5.7.4 gives the test results and finally, Section 5.7.5 gives a discussion on the test results.

5.7.1. TEST SETUP

The graphite needle tip cathode and its base are mounted on an aluminium base plate that is placed below and in front of the micro electric thruster's discharge chamber. In this manner it is placed outside the plasma plume and plasma sputtering effects are minimised. The copper input lines to the cathode are clamped in between macor blocks and the ground plate as well as the thruster are grounded in order to prevent static discharges. Furthermore, tungsten bulbs (6) are installed next to the thruster and six more are added from a neighbouring thruster setup. According to Section 5.4.5, the tungsten bulbs are capable of emitting 5 mA with 1 Watt input power. The bulbs are used in order to start the thruster for the first time. The setup can be seen in Figure 5.84.

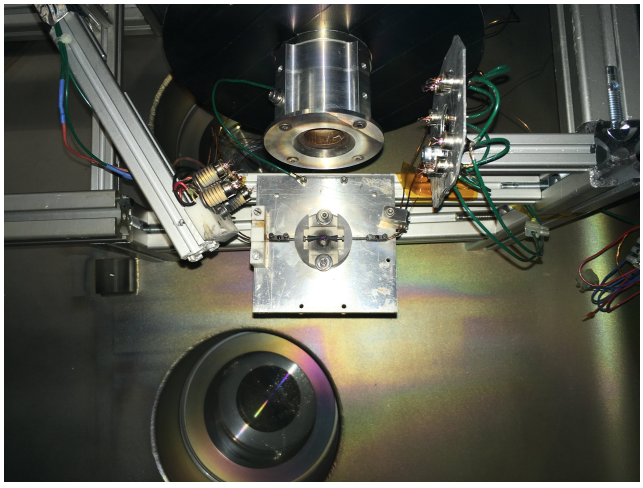

Figure 5.84: Thruster mode cathode setup

5.7.2. TEST INSTRUMENTATION

Now that the graphite needle tip cathode is tested in thruster mode, there are some changes that have been made in the instrumentation. These include the vacuum chamber, the electric thruster that is added and the use of the tungsten bulbs as additional cathode. They are shortly described below:

- **Vacuum chamber -** First of all, the large thruster vacuum chamber is used. This is the same chamber that is described in Section 5.1.1 and has the capability of reaching a vacuum in the order of the 10^{-7} mbar range. Next to that, a xenon micro electric thruster can be operated with a mass flow of 2 sccm while the vacuum chamber pressure can be maintained in the 10^{-5} mbar range.
- **Xenon electric thruster -** An operable engineering model xenon propellant micro electric thruster is installed in the vacuum chamber and acts as anode. Emitted electrons from the cathode are guided into the discharge chamber of the thruster and as they collide with xenon particles, ionisation is realised. The high kinetic energy electrons are not capable of crossing the magnetic bottles that are induced by the permanent magnets and the ionisation process is enhanced even more in these areas. The high potential on the anode inside the thruster is again realised by a FuG high voltage supply.
- **Tungsten bulbs cathode -** The tungsten bulbs are used with the xenon thruster in order to start it up for the first time. This means that the bulbs will be lit in order to emit electrons and the thruster can be charged as the anode potential is applied and the xenon mass flow is started.

5.7.3. TEST PARAMETERS

As mentioned earlier, the primary goal of the thruster mode test is to verify whether the xenon thruster can be operated with the graphite needle tip cathode. Therefore, the xenon thruster is started with the tungsten bulbs at first, after which the graphite needle tip cathode is activated. Afterwards, the tungsten bulbs will be slowly put out by reducing the input voltage on them. This is **1)** of the 3 items that will be tested. The test flow is thus as follows:

1. **Pump down the vacuum chamber -** First, the vacuum chamber is pumped down to a pressure in the order of the 10^{-7} mbar range.
2. **Activate the tungsten bulbs -** Next, the tungsten bulbs are activated in order to start electron emission. They will operate on 1 Watt for each of the six bulbs in order to start up the thruster.
3. **Prepare the xenon thruster -** By applying a high potential of 700 V on the anode inside the thruster in the discharge chamber, the thruster is ready for propellant ionisation and start-up.
4. **Start the xenon thruster -** Subsequently, the xenon thruster is started by applying a xenon mass flow of 2 sccm through the anode into the discharge chamber. The vacuum chamber pressure will rise into the 10^{-5} mbar range.
5. **Start the graphite needle tip cathode -** Now, the graphite needle tip cathode is started by applying the bake out process at first and afterwards increasing the input power up to 56 Watts.
6. **Turn off the tungsten bulbs -** Finally, the tungsten bulbs are slowly shut down by decreasing the input voltage on them.

Next to that, the second item **2)** that will be tested for is whether the xenon thruster can be started up with the graphite needle tip cathode solely operating. For this to occur, it needs to be capable of emitting sufficient electrons to start the ionisation process in the discharge chamber of the electric thruster.

Furthermore, **3)** the cathode emission current as well as the neutralisation current will be measured during thruster operation as the anode potential in the electric thruster is varied from 400 up to 1000 V. In this way the thruster will keep running during the measurement series.

5.7.4. TEST RESULTS

According to the three test objectives discussed in Section 5.7.3, the xenon thruster test with the graphite needle tip cathode is executed. The graphite needle tip cathode is baked out at an input power of 3.5 Watts for 60 minutes. The pressure is equal to $9.8 \cdot 10^{-7}$ at this point and the anode potential inside the discharge chamber equals 700 V. At an input power of 16 Watts, the LaB_6 pellet starts to glow in orange slightly. Afterwards, the thruster is started again, this time while the Tungsten bulbs are on as well as the graphite needle tip cathode. The xenon mass flow is equal to 2 sscm, the pressure rises to $3.7 \cdot 10^{-5}$ mbar and the anode current is equal to 63 mA. Figure 5.85 shows the xenon thruster operating with only the tungsten bulbs activated, whereas Figure 5.86 shows the thruster in operation with the graphite needle tip cathode activated as well as the tungsten bulbs. Next to the cathodes, the characteristic blue ion plasma plume can be seen as the charged propellant particles radiate as they are accelerated.

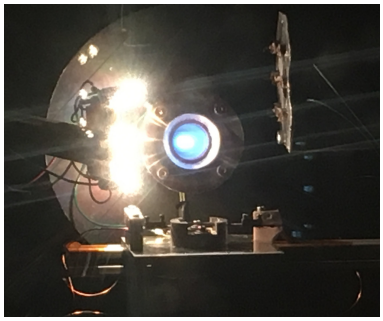

Figure 5.85: Xenon thruster with tungsten bulbs activated

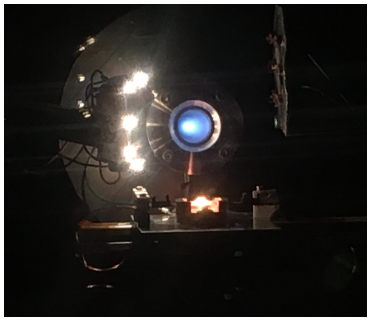

Figure 5.86: Xenon thruster with added graphite needle tip cathode

Subsequently, the voltage on the tungsten bulbs is gradually turned down and the thruster keeps running. This means it can be operated in a steady state where the graphite needle tip cathode is providing both electrons for the discharge chamber as well as for neutralisation of the exiting plasma plume. The graphite needle tip cathode is operating at 63 Watts at this moment, and the pressure inside the vacuum chamber is equal to $3.7 \cdot 10^{-5}$ mbar. The anode potential (i.e. high voltage, HV) equals 700 V and the anode current is equal to 63 mA (I1). In thruster mode, this is the current of the ion beam, i.e. the ionisation current. The actual cathode current, i.e. the current that is emitted by the cathode, is measured to be 5 mA (I2). This amount of current is measured directly on the cathode with a multi-meter and the amount is sufficient to start the ionisation process and realise the 63 mA of ion beam current on the anode. The difference between the two, 58 mA, flows over the walls of the vacuum chamber to the ground (I3). In space however, the vacuum volume is not limited and therefore this 58 mA of current needs to be able to originate from the cathode in order to neutralise the exiting beam. The process is illustrated in Figure 5.87. Next to that, the xenon thruster that is operating with the graphite needle tip cathode can be seen in Figure 5.88.

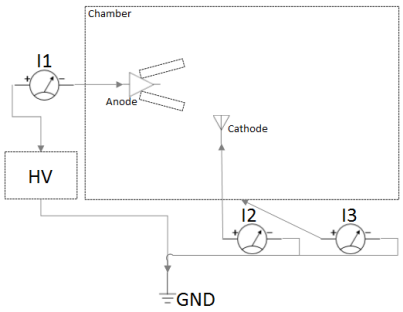

Figure 5.87: Schematic of current flow in thruster mode testing

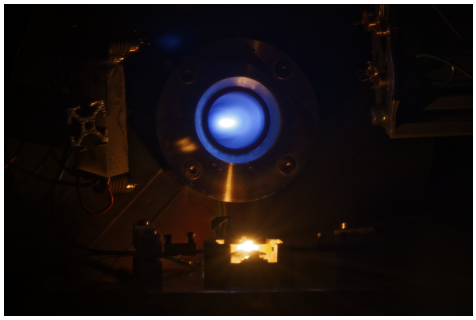

Figure 5.88: Xenon thruster with graphite needle tip cathode

The next test item is to verify whether the thruster can be started with the graphite needle tip cathode in place. In order to do so, the mass flow of xenon is reduced to 0 sccm and the thruster is hence turned off. Next, the thruster is started with 700 V of anode potential and a mass flow of 2 sccm of xenon. Afterwards, the thruster runs stable. Subsequently, the measurement series for varying the anode potential from 400 to 1000 V is carried out. This is done for a mass flow of 1.6 sccm of xenon. The resulting changes in anode and cathode current (I1) and (I2) in Figure 5.87 can be seen in Figure 5.89. At a mass flow of 2 sccm there are multiple discharge sparks occurring on the inside vacuum chamber walls. This can be seen in Figure 5.90. Hence, the measurement series is cancelled for the 2 sccm mass flow case.

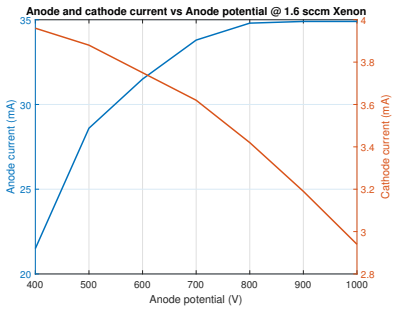

Figure 5.89: Anode and Cathode current vs Anode potential

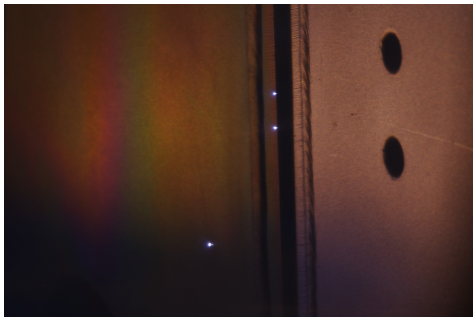

Figure 5.90: Discharge sparks on the vacuum chamber inside walls

From Figure 5.89 it can be seen how the anode current increases as the anode potential is increased. This illustrates that the ionisation process is enhanced at a higher potential, which is described by the Child-Langmuir relation in Equation (3.3). Next to that, the cathode current decreases as the anode potential is increased. This is because of the fact that the ionisation inside the discharge chamber is enhanced at higher anode potentials, and less electrons are required in order to ionise the constant feed of xenon propellant.

5.7.5. DISCUSSION

The graphite needle tip cathode has been tested in thruster mode with the full scale xenon engineering model electric thruster in place. In terms of current emission, propellant ionisation and hence thruster operation the test has been a success. Nonetheless, in terms of power consumption further iterations and improvements are necessary to successfully implement the cathode into the system with the required operating range of 1 - 15 W. Next to that, the thruster is able to be started with a xenon mass flow of 2 sccm with this cathode in place. Hence, the electron emission by the cathode is sufficient for start-up and stable thruster operation, both at 1.6 and 2.0 sccm of xenon. In addition to that, it concludes a proof of concept of an emitting LaB_6 pellet as electron source for propellant ionisation as well as plasma plume neutralisation. An important aspect to keep in mind is that in space there is no possibility for any static spark discharge as they do occur inside a vacuum chamber. Therefore, it remains highly important for any cathode in electric thrusters that is also used as a neutraliser for the plasma plume to be able to emit sufficient electrons in order to neutralise the plume. Otherwise, the spacecraft will become electrically charged which will affect the equipment on board. Furthermore, the emission current of the graphite needle tip cathode is sufficient for it to be operated in thruster mode with the miniaturised high efficiency multistage plasma thruster as well.

5.8. CATHODE TESTS CONCLUSION

This section will elaborate on the conclusions and recommendations that can be made on the vacuum chamber test campaign. In this campaign various design options for a LaB_6 thermionic cathode have been tested. These include indirect as well as direct heating configurations. The main aspects are shortly described below:

- **Graphite heater with BN spacer -** The design iteration that has been continued upon involves a graphite heater with a Boron Nitride spacer inside, into which the LaB_6 emitter pellet is placed. In this manner the heater circuit is decoupled from the cathode - anode circuit. Grounding of the emitter pellet is realised via a separate Tungsten wire.
- **Graphite heater with AlO spacer -** In this iteration the BN spacer is replaced by an Aluminium Oxide spacer, which has a similar coefficient of thermal expansion as the graphite heater. In this manner, the thermal contact required for heat conduction is maintained. An emission current of 667 μA is achieved, which is not close to the required 10 mA. In addition to that, the input power is high with 66 Watts.
- **Kanthal wire heater -** The Kanthal heating wire coiled around the LaB_6 emitter pellet proves to be a feasible and mainly affordable thermionic cathode solution. Nevertheless, the Kanthal is unable to operate for a long time (>60 minutes) near its maximum operating limit at 1400 ^{o}C. In addition to that, it has been discovered that the achieved emission current of 3.8 mA for an input power of 1.5 Watts is actually originating from the Kanthal wire itself instead of from the LaB_6 emitter pellet.
- **COTS Kimball Physics cathode -** The commercial of the shelf LaB_6 thermionic cathode from Kimball Physics has a high efficiency. This is indicated by the fact that an electron emission of 38.8 mA can be reached with an input power of only 7 Watts. This is due to the thin Molybdenum guard ring, wires and posts that are used in order to maximise heat generation. A subsequent test with a magnet ring in place has shown no enhancements in electron emission at low (and any other) anode potential settings.
- **Molybdenum rods and graphite heating elements -** With Molybdenum rods and graphite needle tips the LaB_6 emitter pellet can be heated sufficiently in order to initiate electron emission and achieve an anode current of up to 64 mA for an input power of 56 Watts. This graphite needle tip cathode is able to provide a sufficient amount of electrons in order to both start up and to run the xenon micro electric thruster in a stable configuration. Hence, electric thruster applications for future space missions such as OneWeb e.a. that involve orbit raising with electric thrusters will be realisable. Nonetheless, power consumption remains to be improved on and taken into account, as the power requirements are not yet met.

From the test campaign it can be concluded that direct heating of the LaB_6 emitter pellet is the most effective way in order to get it to emitting temperatures. In addition to that, it is recommended that the emitter has faces which do not lie directly in the heater current path. In this manner, the excited electrons in terms of given kinetic energy can actually exit the emitter instead of flowing back directly into the heater circuit. This can be realised by heating the emitter in a needle tip configuration, or by configuring it as such to have a top planar emitting surface.

Furthermore, the input power for the graphite needle tip cathode remains high when it is compared to other COTS cathodes or even to the tested COTS Kimball Physics cathode in Section 5.6. The main reasons for the high power input are the large heat radiation losses that originate from mainly the graphite needle tips and the LaB_6 emitter pellet. Due to the fact that the operating temperatures are high (in the order of 1800 K) and these losses scale with the fourth power of the temperature, the radiation is high. This can be minimised by shielding the cathode withing thin steel or molybdenum heat shields. Thin, because in this manner the thermal masses remain low and there is not a lot of energy lost in heating these. Next to that, these materials can deal with high temperatures (of more than 1500 K) and have a low emissivity. In that manner, they do not radiate a large amount of heat to space in the form of heat losses. In addition to that, the COTS Kimball Physics cathode has a smaller LaB_6 emitter pellet (1.78 mm diameter by 1 mm height, compared to 3 mm diameter by 2 mm height), which is beneficial in terms of heating but in terms of heat radiation losses as well. This is due to the lower thermal mass and lower emitting area for radiation.

The free radiating space of the emitter pellet influences the electron emission area as well. Therefore, this needs to be taken into account so that the required amount of electron current remains achievable. In an improved setup, direct heating is applied from the sides or even from the bottom of the LaB_6 emitter pellet. In this manner, heat shielding can be realised as well. Next to that, molybdenum parts need to be small, yet large enough to carry the required heating current while minimising heat radiation to the environment (despite its low emissivity). A possible option would be to insert the LaB_6 emitter pellet into a thin molybdenum tube, that is welded with thin molybdenum wires to molybdenum connection posts.

In terms of a compliance check and in order to refer back to the posed requirements in Section 4.1 a short outlook is given here. Considering the performed cathode development the emission current of 10 mA is achieved so that eventually thruster mode testing is possible, successful and the posed 200 μN of thrust can be realised. However, the current power input to the cathode system is high and outside of the required 1 - 15 W range. Therefore, improvements are required in terms of efficiency in order to get the power input down. Hence in future design iterations the thermal aspects such as conductive and radiative heat losses need to be taken into account in order to optimise the total system efficiency.

6

STORAGE

This Chapter will elaborate on the storage options that have been considered. These are analysed in order to be able to store cathodes in such a way that prevents them from oxidising and poisoning. Mainly this involves storing them in an oxygen free environment. This is necessary in order to be able to store the cathodes for a sufficient amount of time prior to shipment to the customer. First, Section 6.1 elaborates on the various storage options that are analysed. Afterwards, the selected storage method is described in Section 6.2.

6.1. CATHODE STORAGE

For the storage of the cathodes there exists several options. These are treated in this section. The main purpose of the storage is to be able to store flight model cathodes for a long time period, prior to the point in time where they are shipped to the customer. According to the MetOp-SG Cleanliness Requirement Specification [67], the supplier shall be able to store unassembled components for a maximum period of 10 years. The goal of the storage method is to prevent the cathodes from poisoning by oxidation reactions with atmospheric particles. Several applicable storage options are discussed in Section 6.1.1. Afterwards, a trade-off is given in Section 6.1.2.

6.1.1. STORAGE METHODS

- **Nitrogen purged box -** nitrogen is used as a standard for contamination free storage as it is a relatively inert gas. Therefore, it does not react with stored materials and it does not carry moisture. Hence, it is a good candidate for isolation. Despite that fact that the gas argon is advised to be used in a sealed box within a low offgassing transport box, similar performance can be reached with using Nitrogen which comes at a better price [68].

  For long term storage that is required (around 2 years), nitrogen purged boxes are a good candidate because they limit organic recontamination that is possible due to the use of hardware before launch and the opening of boxes if needed. A nitrogen controlled cabinet is able to be automatically regulated by a nitrogen purge controller. This controller makes sure that the desired nitrogen levels inside the box are maintained. An example of such a nitrogen purged box can be seen in Figure 6.1.

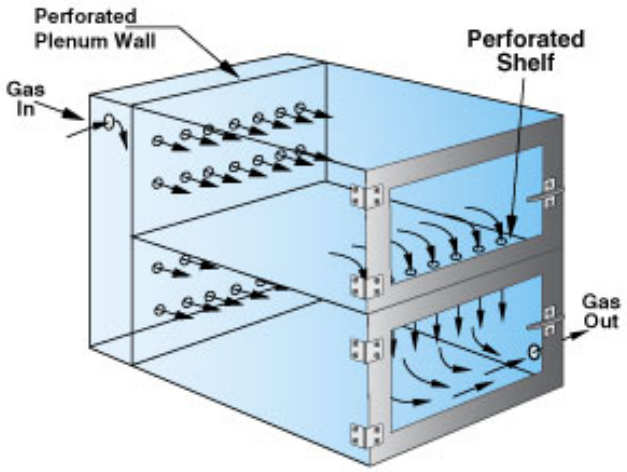

Figure 6.1: Nitrogen purged box schematic

From Figure 6.1 it can be seen how the nitrogen enters the box, pushes out the oxygen and settles at a local atmosphere that contains a high percentage of nitrogen. The nitrogen is able to push out the oxygen in this manner since its specific weight is larger than oxygen. This is due to the fact that atmospheric air contains 21% oxygen (O_2) and 78% nitrogen (N_2) [69]. Hence, the relative specific weights for oxygen and nitrogen are evaluated in Equations (6.1) and (6.2) respectively to illustrate this.

$$0.21 \cdot 2 \cdot 16 = 6.72 \quad \text{kg/mol} \qquad (6.1) \qquad\qquad 0.78 \cdot 2 \cdot 14 = 21.84 \quad \text{kg/mol} \qquad (6.2)$$

In this manner, the nitrogen is able to force out all moisture and contamination loaded air. With the use of *Really Useful Boxes*[1] the cathodes can be easily placed and ordered. Furthermore, the MetOp-SG Cleanliness Requirement Specification requires the components to be stored in an area that is maintained between 17 ^{o}C and 27 ^{o}C. In this way, chemical reactions catalysis are avoided when temperatures would be too high. Next to that, certain electronic reactions that would occur on certain technologies at low temperatures are avoided as well. In addition, it is mentioned that parts encapsulated in plastic packages are to be stored in either nitrogen, dry and ionised air or dry packs [67].

- **Vacuum bags -** These can be used in order to create a vacuum inside the bag in which the cathode is placed. With the removal of oxygen, the oxidation and poisoning on the cathode materials is minimised. Nonetheless, it is expected that it is difficult to generate a very high level vacuum inside a bag with e.g. a vacuum cleaner that is used in order to pump the air out. Therefore, a small of amount of air will remain inside the bag which is able to cause oxidation on the cathode. Hence, this option is not treated in more detail.

- **Nitrogen purged bags -** Another promising option is to used nitrogen purged bags. This option is used for more applications in the space industry in order to store items in a nitrogen rich and pure environment. Again because of the fact that nitrogen has a higher specific gravity than oxygen, a bag can be purged with nitrogen in order to force the oxygen out on top. There are several types of sealant bags that can be used for this application. They will be discussed later in this part. For now, an electrostatic discharge (ESD) bag is taken as an example to illustrate the process. It can be seen in Figure 6.2.

Figure 6.2: ESD Bag with sealer

As can be seen from Figure 6.2, the goal is to purge gaseous nitrogen (GN2) in on one side of the bag, have the centre part sealed, and to let the O2 flow out on the other side of the bag. The process can be repeated by using a secondary bag, in order to enhance the nitrogen rich environment in total. Additionally, desiccants can be put (if required). Next to the ESD bags, different types of sealant bags can be used, as long as they are hydrophobic and have a proper sealing application.

- **Immersed bath -** The cathode can be immersed in a bath of a different type of liquid than water (without O-atoms). In this way, it is sealed from these atoms and prevents the oxidation to form the e.g. LaO layer on the emitter material.

- **Grease -** This works good for e.g. copper tubing as it can be easily applied. Nonetheless, it is not convenient to apply a good layer of grease on the small cathode materials and completely isolate them from air in that way.

[1] `http://www.staples.de/plastikboxen/cbs/7355695.html?promoCode=400600999&Effort_Code=WW&Find_Number=7355695&mT=0` | Visited on 04 April 2018

- **Zinc/Tin Oxide protection layer -** This methods creates e.g. a protective ZnO layer on the hardware, but these metals have low thermal conductivity and could therefore affect the thermal performance to such an extent that this option is not suitable for thermal applications.

6.1.2. TRADE-OFF

In order to select the proper storage method for cathode systems, a trade off is performed. The candidates that are mentioned earlier in Section 6.1.1 are weighed for the following five trade criteria:

1. Performance
2. Affordability
3. Compatibility
4. Lifetime
5. Complexity

Above mentioned trade criteria are now used in order to generate a graphical trade-off for the different cathode storage options types. For the graphical trade off, the grading criteria are defined from best to worst as excellent (green), good (blue), correctable (yellow) and unacceptable (red). These are listed in Table 6.1.

Table 6.1: Ratings Graphical Trade-off

Graded	Colour
Excellent	Green (G)
Good	Blue (B)
Correctable	Yellow (Y)
Unacceptable	Red (R)

These ratings will be used for the graphical trade-off, which can be seen in Table 6.2. In this table the trade criteria are listed in the first row and the design options are listed in the first column. Vacuum bags have been used in the past in order to store space hardware. They are an affordable and cost effective solution, but nonetheless they remained to show a form of oxidisation on the objects inside. This is most likely because of the fact that they cannot be made completely vacuum or at least to a sufficient vacuum level. The downside of the immersed bath and grease options is that the cathode needs to go through the cleaning process again, prior to shipment. This can be expensive both in terms of time and cost.

Therefore, one is looking for a commercial of the shelf solution. This can be realised by nitrogen purged boxes. They allow for multiple cathodes storage, while they can be opened at any time. This is because of the fact that an automatic nitrogen purge controller is able to control the nitrogen based atmosphere inside the chamber. Another advantage is the durability and versatility of the system. It can be operated with different gasses if needed and it will last for a long time. Another suitable option that is selected for discussion are the nitrogen purged bags. This method has the advantage that it is cost advantageous and that the materials required in order to use the method are in house at Airbus by the largest amount or can be procured. These involve the sealant bags, the nitrogen gas supply, the pressure relievers and regulator on the nitrogen gas supply.

Table 6.2: Graphical trade-off cathode storage options

Criteria ⇒ Cathode Type ⇓	Performance	Affordability	Compatibility	Lifetime	Complexity
Nitrogen purged box	Good (G)	Acceptable (B)	Good (G)	Good (G)	Acceptable (B)
Vacuum bags	Reasonable (Y)	COTS (G)	Good (G)	Reasonable (Y)	Low (G)
Nitrogen purged bags	Reasonable (Y)	COTS (G)	Good (G)	Reasonable (Y)	Low (G)
Immersed bath	Acceptable (B)	Reasonable (Y)	Low (R)	Good (G)	Low (G)
Grease	Low (R)	Acceptable (B)	Low (R)	Reasonable (Y)	Acceptable (B)
Zinc/Tin oxide layer	Low (R)	Reasonable (Y)	Reasonable (Y)	Good (G)	High (R)

6.2. STORAGE PROCEDURE

This section will elaborate on the selected storage procedure. It will use nitrogen purged bags and boxes in order to store cathode components. An example of an ESD bag that can be used for such an application has been given in Figure 6.2. Next to that, different types of sealant bags can be used, as long as they are hydrophobic and have a proper sealing mechanism. The steps that are to be taken in order to purge the bag and store cathode are evaluated below.

1. First, one needs to make sure that the components that will be used in order to purge the nitrogen into the required bag are clean. This involves cleaning the nitrogen purge hose tip with isopropyl alcohol (IPA). Next to that, the inside of the bag should be clean and free from any contaminants and loose materials. Furthermore, it is important for the operator to wear latex gloves at all times because of the fact that human skin is acidic.
2. Next, the cathode is put into the seal bag inside a box. As much as air as possible is forced out of the bag manually. Two small openings should be made in order to allow for the nitrogen hose tip to enter the bag and for a secondary (partial) hose/pipe to allow for the oxygen to escape the bag. This is illustrated in Figure 6.2. In this figure it can be seen how the nitrogen enters the bag on one side and forces the lighter oxygen out on the other side

Figure 6.3: Pressure reliever and nitrogen flow regulator

   The nitrogen is purged into the bag by using a regulated control valve that is attached to the nitrogen gas bottle. The nitrogen bottle is equipped with a pressure reliever in order to let the pressure drop from 200 bars to 1-10 bars. In this way, the nitrogen can be manually purged into the bag until it is full. Figure 6.3 illustrates the pressure reliever with the attached nitrogen “fill” hose.
3. As the bag is completely filled with nitrogen, the nitrogen filler and the Oxygen escape tube need to be removed. Next, the bag can be sealed.
4. Afterwards, the process explained in steps 2 and 3 above can be repeated if required, in order to generate an even higher level nitrogen environment. On the other side, one can choose for the option to put the nitrogen purged bag into another seal bag with desiccant or a plastic box (also with desiccant), for final storage.

7

COMMERCIAL FEASIBILITY ANALYSIS

The goal of this chapter is to analyse the strategic context and commercial potential of the cathode development within Airbus. Next to that, it will be shown how the cathode development project will be conceived to lead to a commercial exploitation. In order to do so, the target users and customers will be addressed first in Section 7.1. Next to that, the competition will be described in Section 7.2. Subsequently, Section 7.3 deals with the strengths, weaknesses, opportunities and threats analysis. Furthermore, the financial and market objectives are addressed in Section 7.4. Next, the cost and pricing is discussed in Section 7.5. Afterwards, the migration plan will be evaluated in Section 7.6. In addition to that, the partnering suppliers will be treated in Section 7.7. Finally, conclusions are given in Section 7.8.

7.1. TARGET CUSTOMERS

The number of small satellites seeking launch continues to grow. The projected growth for the next years can be seen in Figure 7.1. Therefore, new opportunities are emerging to fly these satellites as secondary payloads on several launchers systems. As already briefly addressed first in the Introduction in Chapter 1, satellites are becoming smaller and more powerful with high performance instruments and even propulsion systems for orbit keeping. This leads to the fact that micro electric thruster systems will start to play an even more important role on these satellites in the near future [7, 70–72].

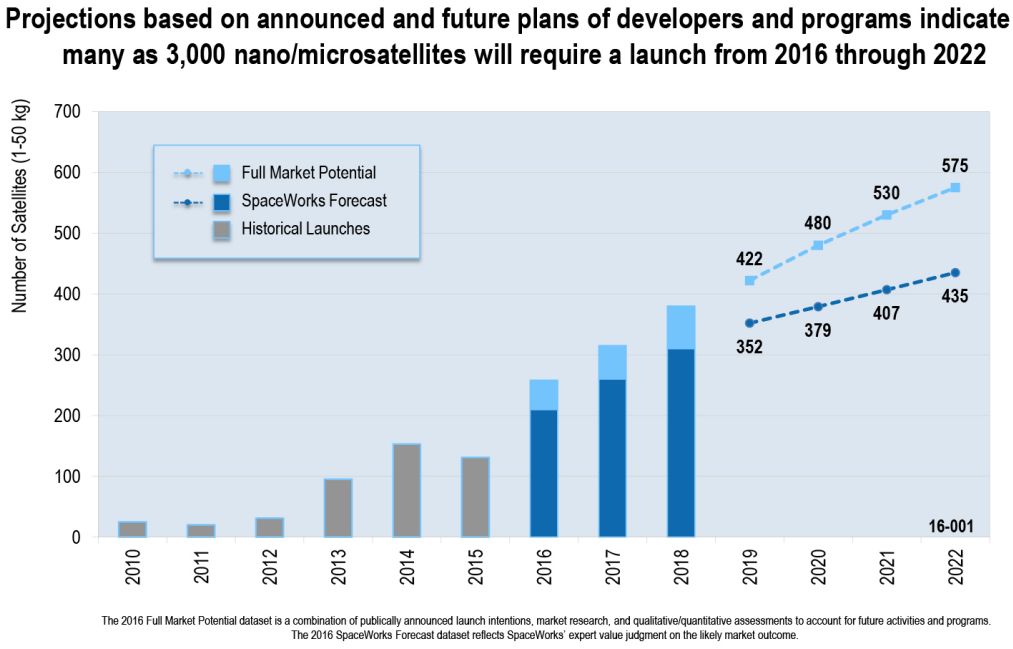

Figure 7.1: Projected satellite market for nano- and microsatellites [7]

There exist many commercial companies and research institutes that are developing in the small satellite technology and that require micro electric propulsion systems and therefore suitable, efficient and affordable cathodes. The flexible and deployable solar panel technology is a promising development that allows for power budgeting solutions for the electric thrusters. Example companies that are active in developing CubeSats are listed below:

1. **Airbus contracts -** With the acquisition of e.g. Astrium, the Cassidian divisions, Dutch Space and others, the consortium of Airbus[1] is growing significantly over the last few years. With contracts for ESA such as the Laser Interferometer Space Antenna (LISA), BepiColombo and the Multi-Purpose Crew Vehicle (MPCV), Airbus is performing a lot of development in the space sector. Sites are located in France, Germany, Netherlands, Spain, and the United Kingdom.

2. **Clyde Space -** The company Clyde Space[2] is one of world leading innovators and suppliers of CubeSats and small satellite systems. Clyde Space is located in Glasgow in the United Kingdom. The productivity is high, with on average six flight-ready CubeSats being manufactured each month in 2016 in the on-site clean room. The sales are for the largest part outside of the European Union, with 80%. Nonetheless, the market within the European Union is growing.

3. **Delft University of Technology -** Amongst many other universities all over the world, there is a technical university that has a miniaturised satellite program. Delft University of Technology[3] has carried out a CubeSat program named Delfi. Nowadays, the research lies within further miniaturised satellites even smaller than CubeSats, so called PocketQubes that consist out of 5 cm cubic units. They provide a good platform for demonstrating miniaturised space systems for a low cost.

4. **GOMspace -** The company GOMspace[4] is a globally leading designer, integrator and manufacturer of high-end nanosatellites. These are in the form of CubeSats and are designed for customers that are in the academic, commercial and government markets. GOMspace is specialised in space systems integration, nanosatellite subsystems and advanced miniaturised radio technology. The company is located in Denmark and has a subsidiary, Nanospace, in Sweden.

5. **Innovative Solutions In Space (ISIS) -** ISIS[5] is located in Delft, The Netherlands. They are specialised in the assembly, integration and testing of CubeSat structures. In addition to that, a lot of breadboard testing is performed on the in-house soldered print boards that are also assembled into the CubeSat. Furthermore, they provide launch services for CubeSats with the ISILaunch branch.

6. **OHB SE -** OHB[6] is an European multinational technology cooperation. The headquarters are located in Bremen in Germany. Next to that, they have sites in Italy, Luxembourg, Sweden, France and Belgium. The company specialises in space systems, aerospace and industrial products. One of the main products is the fully integrated spacecraft.

7. **PlanetLabs (Planet) -** Planet[7] is founded in 2010 by a team of ex-NASA scientists. Planet has locations in the United States of America, The Netherlands, Germany and Canada. Their mission is to image the entire Earth every day. In this manner, global change can made visible, accessible and actionable. This will be done using constellations of CubeSats that are capable of monitoring the entire globe. In this manner, a lot of space missions can be realised that are specialised in aspects such as fire detection, forest growth and health management, container ship tracking and counteracting piracy and global weather forecasting.

8. **Spire -** Spire Global, Inc.[8] is a company in the United States of America that specialises in gathering timely based worldwide weather data. It has sites in the United States of American and in the United Kingdom. The goal is to provide the Earth with a network of satellites that are capable of gathering worldwide atmospheric data. This data will be used in order to accurately predict the weather. In order to maintain such a network of satellites, new ones have to be sent up in order to replace the deorbiting ones or they need to be equipped with an orbit keeping subsystem. In any case, micro electric propulsion systems will play an important role for these (near future) CubeSats.

9. **Thales Alenia Space -** With the acquisition of Alcatel, Leonardo and Telespazio, the Franco-Italian aerospace manufacturer Thales Alenia Space[9] is formed. It has sites across Europe in France, Italy, the United Kingdom, Spain, Belgium, Germany and Poland. The company is specialised in the development of multi purpose logistic modules that are used to transport cargo inside the Space Shuttle orbiters. Next to that, they have worked on various modules for the International Space Station. In addition to that, they are involved in many space projects with other companies such as the ones in this list.

[1] `http://www.airbus.com/` | Visited on 04 April 2018
[2] `https://www.clyde.space/` | Visited on 04 April 2018
[3] `https://www.tudelft.nl/` | Visited on 04 April 2018
[4] `https://gomspace.com/home.aspx` | Visited on 04 April 2018
[5] `https://www.isispace.nl/` | Visited on 04 April 2018
[6] `https://www.ohb.de/index-english.html` | Visited on 04 April 2018
[7] `https://www.planet.com/` | Visited on 04 April 2018
[8] `https://spire.com/` | Visited on 04 April 2018
[9] `https://www.thalesgroup.com/en` | Visited on 04 April 2018

10. **TNO -** The Netherlands Organisation for Applied Scientific Research, or TNO[10] focuses on applied science. They have locations throughout many cities within The Netherlands. One of the topics in which TNO is specialised is space and scientific instrumentation. Many optical instruments are required to operate at very low temperatures in order to minimise thermal noise on the detector. Hence, thermal control is an important issue. Not only is it important to keep the instrument cool using cold fingers or cryocoolers, but also to be able to control the temperature profile across the whole structure of the satellite. In addition to that, precise orbit control is important in order to obtain high accuracy measurements.

7.2. COMPETITION

In this section an assessment of the competition is given. Next to that, the positioning of Airbus with respect to the market and in the value chain is presented. Nowadays, the trend in micro electric propulsion systems goes to high efficiency, low weight, affordable and low complexity systems. In this manner, future miniaturisation for CubeSats and mass production for satellite constellations will be realisable.

There exist various companies that are developing micro electric thrusters. Most of them are however located in the United States of America. In Europe, currently only Airbus, ThrustME (France), Deutsches Zentrum für Luft- und Raumfahrt (DLR) and Enpulsion are developing on electric thrusters and cathode systems. This makes it an interesting technology to develop, especially for sales to customers within Europe. In order to be complete, a list is given that denotes competitive products from competing companies:

1. **Airbus -** Airbus[11] is developing on the μHEMPT in Friedrichshafen and the larger electric thruster, the HEMPT in Lampoldshausen. The size, and thrust ranges vary from design to design according to the applications of the thruster. In addition to that, the telecommunications satellite Eutelsat-172B that is built for Eutelsat by Airbus has successfully reached its target orbit by climbing from its initial orbit while using solely electric thrusters. At this moment, these are used to keep the satellite into this target orbit.

2. **ThrustMe -** ThrustMe[12] is located in France and is developing on radio frequency gridded ion thrusters. They are capable of realising complete thruster modules for advanced small satellites as well as modules that fit into a one unit (1U) CubeSat. The acceleration grids are biased with radio frequency voltages across a capacitor. In this manner, the realised plasma acts as a diode as the mass of the ions and electrons is different. Next to that, the capacitor charges itself. Hence, the direct current voltage is capable of accelerating the charged ions constantly while electrons can only exit the grid during a short time period that is in correspondence with the RF cycle. In this manner the complexity is kept low, while the performance and the efficiency is kept high.

   Another interesting point to mention is that on 13 February 2018 Innovative Solutions In Space and ThrustMe have signed a Memorandum of Understanding[13] related to the use of an advance electric propulsion system for ISIS CubeSats. This is due to the fact that the developments in the CubeSat world tend to move towards larger constellations for commercial purposes and the demand for propulsion systems increases.

3. **Deutsches Zentrum für Luft- und Raumfahrt -** DLR[14] has various locations in Germany and is currently developing on electric propulsion with their Electric Propulsion Innovation & Competitiveness (EPIC) EU project. This project is under development with partners such as Agenzia Spaziale Italiana, Belgian Science Policy, Centre National d'Etudes Spatiales and UK Space Agency.

4. **OHB -** The German firm OHB is developing Electra[15], which will be a telecommunications satellite with solely electric propulsion. In this manner the amounts of fuel needed is lowered significantly, which leaves more room for revenue making equipment. The launch is planned for in the year 2022. The satellite is part of the European Space Angency's (ESA) Advanced Research in Telecommunications Systems (ARTES[16]) programme.

5. **Enpulsion -** Enpulsion[17] is an Austrian start up company that is developing Field Emission Electric Propulsion (FEEP) thrusters. These are designed for various satellites with a weight from 3 up to 100 kilograms. The success of the thruster concept consists out of the possibility of being modular and clustering pre-qualified building blocks with the proprietary Indium-FEEP technology. In this manner a custom electric propulsion solution can be offered for a wide range of space applications.

[10] https://www.tno.nl/en/ | Visited on 04 April 2018
[11] http://www.airbus.com/ | Visited on 04 April 2018
[12] http://thrustme.fr/ | Visited on 04 April 2018
[13] https://www.isispace.nl/thrustme-isis-sign-mou-offer-advanced-small-satellite-capabilities/ | 18 February 2018
[14] http://www.dlr.de/rd/en/desktopdefault.aspx/tabid-2266/3398_read-44284/ | Visited on 04 April 2018
[15] https://www.ohb-system.de/electra-358.html | Visited on 04 April 2018
[16] https://artes.esa.int/ | Visited on 04 April 2018
[17] https://enpulsion.com/ | Visited on 04 April 2018

7.3. SWOT ANALYSIS

The goal of this section is to give a Strengths, Weaknesses, Opportunities and Threats (SWOT) diagram for the LaB_6 thermionic cathode. In this manner, information can be provided on the selling factors such as existing intellectual property rights, know-how and technology against products of competitors. Next to that, the commercial pool and its difficulties can be addressed. The SWOT diagram for the LaB_6 thermionic cathode can be seen in Table 7.1.

Table 7.1: SWOT Analysis LaB_6 thermionic cathode

Strengths	**Weaknesses**
• High electron emission • Light weight • Low complexity • Superior flexibility in desired ceramic base configurations • Long heritage of LaB_6 thermionic cathodes at Airbus • End-to-end service	• Requires high operating temperatures ($\geq$ 1300 K) • LaB_6 crystal easily poisoned and damaged • High operating power and power requirement not yet met • Single supplier dependency (Airbus in Europe)
Opportunities	**Threats**
• Single supplier dependency (Airbus in Europe) • Production on large scale highly possible • Qualification is required to improve TRL • Lower cost and lead times with increased production • Reliable product, many applications • In-house complete development of a full system • Increase of in-house intellectual property right (IPR) • Not only product delivery but also support	• Brittle cathode assembly; assembly requires careful operations • Contamination and poisoning issues need to be addressed • Requires proper storage and transport • Competitor products entering the market

7.4. FINANCIAL AND MARKET OBJECTIVES

This section will deal with the analysis of the financial and market objectives in terms of sales volume, market share and predicted market penetration. This is done both with and without the proposed development. As has been mentioned earlier in Section 7.1, the market for thermionic LaB_6 cathodes is wide open in Europe. There are more companies that are developing these, which are mainly based in the United States of America or Russia. Hence, for European space projects it is interesting to develop in this new technology.

With this open market the market share will be very large at the point when the thermionic LaB_6 cathodes is brought to the market. Not only will this be beneficial for the possible sales volume, but also for the predicted market penetration. Being the only supplier that is capable of producing thermionic LaB_6 cathodes in different kind of configurations depending on the client's requirements is a good position to be in. It is expected that in the first year up to five thermionic LaB_6 cathodes are going to be sold. In the subsequent year, the goal is to sell five to fifteen of them. In the near future, it is expected that the sales will grow even more. This is because of the fact that not only the reputation will grow due to the fact being the sole supplier, but also due to the fact that the prices will drop because of the learning effect in the production of the thermionic LaB_6 cathodes in all sorts of configurations.

With the remaining resources from the internal research and development project in thermionic LaB_6 cathodes within Airbus the goal is to establish a commercial strategy of how these cathodes are going to be sold. By attending conferences and referencing the thermionic LaB_6 cathodes in other ongoing partnering projects the name, purpose and performance of these cathodes can be shared and promoted. The main idea to always keep in mind is that the technology is very promising as the performance is high, the affordability is high, the weight is low and the complexity is low. Hence, these thermionic LaB_6 cathodes are interesting for many space applications in the near future.

7.5. COST AND PRICING

This section elaborates on the assessment of the investment and costs as well as the corresponding pricing strategy. The costs are divided into two segments, the non-recurring and the recurring costs. They will be discussed in Sections 7.5.1 and 7.5.2 respectively. Afterwards, the total costs are summarised in Section 7.5.3.

7.5.1. NON-RECURRING COSTS

The non-recurring costs of a system include all the costs that are associated with the design, development and qualification of the system. Next to that, they include the breadboard article (or prototype), engineering model, qualification unit and multi-subsystem wraps. The multi-subsystem wraps are costs related to integrating two or more subsystems (not applicable for the thermionic LaB_6 cathodes project) [1].

The non-recurring costs are concluded by executing thermal vacuum chamber tests on the thermionic LaB_6 cathodes and establishing their characterisation. Their functions are tested on the breadboard / prototype models. Next, the form, compliance and versatility is confirmed by the engineering model of each type. The next step is to perform qualification tests in order to establish a flight unit equivalent component. The qualification will be discussed in more detail in Section 7.6. In conclusion, the non-recurring costs consists out of the required vacuum chamber testing and evaluation which in terms of a two work days are evaluated at 800 EUR.

7.5.2. RECURRING COSTS

The recurring costs are the costs that are associated with the production of the actual unit(s) that will be flown in space (i.e. the flight models). These costs include flight hardware and multi-subsystem wraps. These costs are primarily material costs, which will be dealt with next. However, one should keep in mind the optional quality assurance and mechanical tests that are to be performed according to the client's requirements. These tests can be required if a client requires an extraordinary design or configuration of a thermionic LaB_6 cathode. Therefore, these (optional) tests have been included in the timeline schedule for the production of thermionic LaB_6 cathodes. This timeline can be seen in Figure 7.2.

Next, the material costs will be discussed. For a graphite needle tip cathode that is installed with molybdenum posts and on a boron nitride ceramic base, the costs are evaluated. BN materials are procured from Henze BNP[18]. Next to that, the molybdenum material is purchased via Metall Maier[19] and the graphite material comes from Graphite24[20]. The main cost driver for the thermionic LaB−6 cathode in terms of material costs is the LaB_6 emitter pellet itself. These are purchased from Sindlhauser Materials GmbH[21] and drive up the materials costs for a thermionic LaB_6 cathode. The total material cost equals 654 EUR and is summarised in Table 7.2.

Table 7.2: Thermionic LaB_6 cathode material cost

Material	**Cost** [EUR]
HeBoSint C100	100
Molybdenum rod	39
Bolts and nuts	5
Graphite rod	10
LaB_6 emitter (5x)	500
Total	**654**

As can be seen from Table 7.2, the LaB_6 emitter material costs for the thermionic LaB_6 cathodes is a large cost driver. This is also one of the contributors on which a large amount can be saved. For the current cathodes the material is ordered from Sindlhauser and it requires a single LaB_6 emitter pellet to realise a LaB_6 thermionic cathode. If the Lab_6 thermionic cathodes will be made in larger numbers, then also the material can be bought in larger portions, which will lower the price. Next to that, the material can be bought in bulk directly. In this manner it is expected that this price post can be lowered even more by factors in the range of 10 to 20% [1].

In order to give a projected timeline of the production process of a thermionic LaB_6 cathode, Figure 7.2 is given. This timeline shows the activities that are required to be performed after the order has come in for a thermionic LaB_6 cathode. In about 23 weeks, or just over five months, a cathode can be assembled, tested and delivered to the client. If there is not any additional quality assurance (QA) or mechanical testing required, then this time frame can be

[18] https://www.henze-bnp.de/HeBoSint-Bornitrid-Sinterkoerper.php | Visited on 04 April 2018
[19] https://www.sintermetallshop.de/ | Visited on 04 April 2018
[20] http://www.graphite24.de/ | Visited on 04 April 2018
[21] http://www.sindlhauser.de/de/ | Visited on 04 April 2018

even reduced to 15 weeks. This depends on the client's requirements and the configuration of the thermionic LaB_6 cathode.

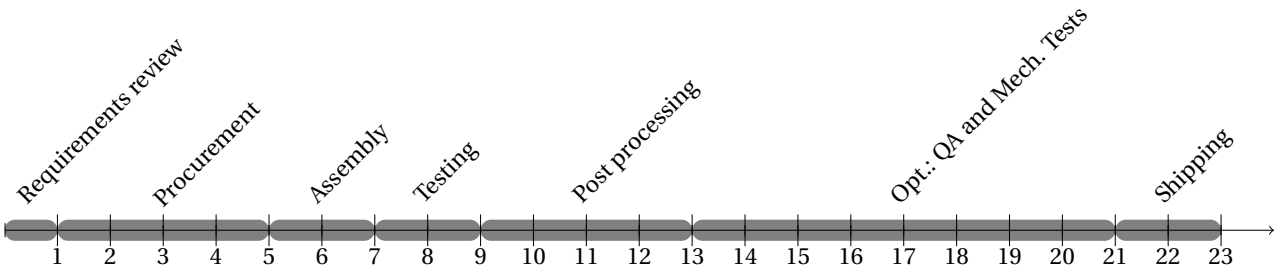

Figure 7.2: Timeline thermionic LaB_6 cathodes production process (in weeks)

7.5.3. TOTAL COSTS

The goal is to sell thermionic LaB_6 cathodes at a price of 1500 EUR. This price has been established by adding the non-recurring and recurring costs, while adding a profit margin. It is also based on the projected sales that are discussed further on. In addition to that, it establishes a competitive price with the market competitors that have been discussed in the literature study report [25].

The goal for the sales is to sell at least five thermionic LaB_6 cathodes. Addressed companies are (amongst others) the ones that are discussed in Section 7.1. In the subsequent years, with heritage and reputation taken into account, the goal is to sell five to fifteen thermionic LaB_6 cathodes. In the near future, the sales are expected to increase even more as has been illustrated in Section 7.1 with Figure 7.1.

7.6. MIGRATION PLAN

In this section, the steps from the validation of the intended development to the full operational deployment and service provision will be discussed. Next to that, the market strategy with the corresponding distribution channels and service provision is evaluated. The first step towards operational deployment and service of the thermionic LaB_6 cathodes are the qualification testing and acceptance testing. In this manner, the TRL can be increased from 4 to 6. With qualification testing the hardware is exposed to the most extreme conditions that it will experience during operations. This involves both the hottest and the coldest case in a thermal test. Next to that, it compromises shaker vibration and vacuum testing. Furthermore, contamination and outgassing issues have to be addressed in these tests [28, 29].

Acceptance testing is performed in order to prove that the space hardware (i.e. the thermionic LaB_6 cathodes) are capable of operating under their required operating conditions for a given amount of time. These tests involve thermal cycling testing, in order to show that the thermionic LaB_6 cathode is capable of operating for a required time period (corresponding to the satellite's lifetime). Preliminary tests that dealt with this aspect have already been performed at Airbus. Future thermal vacuum chamber and thermal cycling tests can be conducted on-site at Airbus.

Finally, evaluation testing will be performed. These tests involve the experimental testing for the largest amount. They conclude the mechanical tests that have already been performed in order to obtain more knowledge on the thermionic LaB_6 cathode mechanical characteristics. As these tests are performed and evaluated, the product heads towards full operational deployment in space applications. With clients all over the world, as mentioned in Section 7.1, the distribution channels are endless and many sales are going to be made.

7.7. SUPPLIERS

This section discusses the policy in terms of relations with suppliers that exists in order to achieve the objectives that are described in Section 7.4 (Financial and Market Objectives). In order to accomplish the market objectives of selling multiple thermionic LaB_6 cathodes in the near future, the required material will be required to be bought in by bulk. In this manner, the price drops and the stock of the required material will not deplete. This will prevent delivery delays. The required materials for the thermionic LaB_6 cathodes and their availability are discussed below:

1. **Boron Nitride -** Boron Nitride in the form of HeBoSint C100 can be easily procured in bulk material from Henze BNP. In addition to that, many other suppliers are available for the easily machinable high temperature ceramic.
2. **Molybdenum -** Molybdenum is neither an expensive nor difficult obtainable metal and is currently procured via Metall Maier. Just as with Boron Nitride, it can be easily procured from other suppliers which is favourable in order to not be dependent on a single supplier.
3. **Bolts and nuts -** The isometric bolts and nuts that are needed for creating a single thermionic LaB_6 cathode can be ordered from any general hardware store. These parts have a low price and will therefore not be addressed further in this part.
4. **Graphite -** Graphite is also a common material and can be procured via a wide range of suppliers. Currently it is purchased from Graphite24. The costs are low and the quantities are high, which is favourable for large scale cathode production.
5. **Lanthanum Hexaboride -** The LaB_6 emitter material is the most expensive material that is required in order to realise thermionic LaB_6 cathodes. Hence, it is advised to explore the market and find alternative suppliers in order to not be dependent on a single one. In addition to that, appropriate deals can be made in terms of purchasing higher quantities for a lower price. Currently, the emitter material is purchased via Sindlhauser Materials GmbH.

7.8. CONCLUSION

Thermionic LaB_6 cathodes prove to be a promising solution in micro electric propulsion applications. Not only are they very lightweight, but they also have a high efficiency, affordability and a low complexity. This allows for a high emission current from the thermionic LaB_6 cathode. Using straight forward manufacturing materials, the price is kept low, the weight is kept low and the performance is kept high. The current TRL of the thermionic LaB_6 cathodes is 4. After the commercialisation and qualification the TRL can be increased to 6. At that level, the thermionic LaB_6 cathodes prototype can be demonstrated in a relevant environment (i.e. either ground or space).

The current design of the thermionic LaB_6 cathodes is able to achieve an emission current of 64 mA with an input power of 56 Watts. This makes it a promising technology that should be further developed and optimised in order to increase the efficiency of the system. Furthermore, the price of the thermionic LaB_6 cathodes is interesting. With a unit price of around 1500 EUR, the thermionic LaB_6 cathodes are competitive compared to other thermionic LaB_6 cathodes. In addition to that, it is important to mention that this price is able to be lowered considerably as the material prices will decrease when material is purchased in bulk. Next to that, if more and more thermionic LaB_6 cathodes will be produced per year, then the learning effect will cause the production time to decrease. This is beneficial for the total price of a thermionic LaB_6 cathode. Products such as this one are required for many space missions and therefore it is viable to be able to produce many different configurations according to the client's requirements in a short time period.

8

CONCLUSION AND RECOMMENDATIONS

This chapter discusses the thesis report by giving conclusions and recommendations. These are given in Sections 8.1 and 8.2 respectively.

8.1. CONCLUSION

In order to reflect on the research questions that are posed in Chapter 2, they are discussed in this part. Furthermore, conclusions are given.

1. What criteria are relevant in order to assess the performance of various types of cathodes for micro electric propulsion systems?
    - The main criteria for describing the performance of cathodes for micro electric thruster systems are input power in terms of watts and operating temperature in terms of Kelvins, where the latter depends on the first. In addition to that, emission current is an important aspect which is also dependent on the first two terms, since it is directly described by the Richardson Equation (3.1) as a function of temperature. In addition to those, non quantitative parameters are of secondary importance for cathodes such as material selection, poisoning and lifetime aspects. The latter can be described in terms of degradation rate however. LaB_6 thermionic cathodes can be operated for 1000 of hours according to literature [3], however they strongly degrade if they are operated at very high temperatures (higher than nominal) at 2000 K. Finally, parameters such as affordability and complexity play an important role in the design of the cathode system.
2. What is the value and quality of the different types of cathodes in view of the assessment criteria?
    - As has been discussed in Section 3.3, the LaB_6 thermionic cathode proves to be the most suitable option for an efficient, highly affordable and high performance cathode for micro electric thruster systems. This is because of the fact that it has a good performance in terms of electron emission and hence theoretically requires a low input power. Next to that, procurement of the required materials and the manufacturing process is of such a low complexity that not only the system as a whole holds a low complexity, but is in addition to that also highly affordable. The goal of this cathode is to be operated with the high efficiency multistage plasma thruster that is being developed at Airbus. This system has a low complexity, needs only little propellant and can be operated without the need for large power supplies. The thruster system can be miniaturised in order to fit into a tuna can shape cylinder extension that is installed at the far end of a 3U CubeSat with a diameter of 64 mm and a height of 36 mm.
3. What do we learn from comparing results from the analyses and the results of the different types of cathodes in order to establish recommendations on how to develop an efficient cathode for micro propulsion systems?
    - According to the posed requirements in Section 4.1, the cathode shall be able to achieve an emission current of 10 mA at an operating power in the range of 1 - 15 Watts. This is a typical input power operating range according to the market survey that has been performed in the literature study phase of the MSc Thesis. Whereas the emission current requirement has been met, the input power remains rather high with 56 Watts and requires further design iterations and improvements. Hence, the power requirement is not yet met.

8.2. RECOMMENDATIONS

When the vacuum chamber tests are performed, it is important to take radiation losses into account. These are especially important for emitter materials that are operated at high temperatures such as Lanthanum Hexaboride (T > 1300 K), as radiation heat losses scale with T^4. Radiation heat losses inside the vacuum chamber are possible due to the temperature differences between the test setup and the walls of the chamber. In order to take these into account, one can make an assessment of them using initial estimations from the heat radiation equation or by making a model in a thermal modelling suite such as ESATAN. Furthermore, radiation losses can be minimised by covering the test setup with a aluminium foil house or a multi-layer insulation blanket. Nevertheless, it is important to keep in mind that emitted electrons should not be able to travel towards such an equipment if it is used in the test setup.

In terms of design of the cathode, it is recommended to proceed with a direct heated thermionic LaB_6 cathode, but with the heating graphite elements insulated in a molybdenum guard shield in order to reduce heat radiation losses. In addition to that, the LaB_6 emitter pellet can be made smaller while still meeting the emission current requirement of 10 mA. This results in the a configuration similar to the COTS Kimball Physics cathode, using direct graphite heating elements and a molybdenum guard ring that also acts as a heat shield.

Considering the storage of the cathode parts, it is recommended to use nitrogen purged bags or environments. Here, oxygen levels and low and in this manner, oxidation and contamination risks are minimised and the quality and performance of the cathode can be ensured. Furthermore, it is important to use organic cleansing solvents such as isopropyl alcohol on components that are in direct proximity to the emitter material in order to prevent contamination by outgassing. In this manner degradation in performance of the emitter material is reduced.

Finally, it is recommended to perform qualification and acceptance tests on the cathode system in the near future. In this manner, the current technology readiness level (TRL) can be increased from 4 to 6. The current TRL is 4. This means that the cathode has been tested on a component level in a laboratory environment (i.e. vacuum chamber). After the commercialisation and qualification the TRL can be increased to 6. At that level, the cathode prototype can be demonstrated in a relevant environment (i.e. either ground or space).

REFERENCES

[1] L. Guerra and P. Graf, *Cost Estimating Module* (National Aeronautics and Space Administration, 2008).

[2] M. Advadhanulu and P. Kshirsagar, *A Textbook of Engineering Physics* (S. Chand, 2014).

[3] G. Sutto, *Extended Life LaB_6 Cathode User Information* (Kimball Physics Inc., 1991).

[4] European Space Agency, *LISA Unveiling a hidden Universe - Assessment Study Report* (ESA/SRE, 2011).

[5] F. G. Hey, *Development and Test of a Micro-Newton Thruster Test Facility and Micro-Newton HEMP Thruster* (Technische Universität Dresden, 2016).

[6] S. Frosch, *Development of a LaB6 Cathode for Micro Electric Thrusters* (Duale Hochschule Baden-Württemberg Ravensburg, 2017).

[7] E. Buchen and D. DePasquale, *Nano / Microsatellite Market Assessment* (SpaceWorks Enterprises, 2014).

[8] G. P. Sutton and O. Biblarz, *Rocket Propulsion Elements*, 9th ed. (Wiley, 2016).

[9] D. Goebel and I. Katz, *Fundamentals of Electric Propulsion: Ion and Hall Thrusters* (Wiley, 2008).

[10] P. Verschuren and H. Doorewaard, *Designing a Research Project*, 2nd ed. (Eleven International Publishing, 2010).

[11] N. E. Jensen and J. A. Gonzalez del Amo, *Present and Future of Space Electric Propulsion in Europe* (European Space Agency, 2015).

[12] F. G. Hey, M. Vaupel, I. G. Moneva, D. Papendorf, C. Braxmaier, and M. Tajmar, *The Next Generation milli-Newton μHEMPT as Potential Main Thruster for Small Satellites*, 35th ed. (International Electric Propulsion Conference, 2017).

[13] C. Kittel, *Introduction to Solid State Physics*, 8th ed. (John Wiley and Sons Ltd., 2004).

[14] L. P. Rand, *A Calcium Aluminate Electricde Hollow Cathode* (Colorado State University, 2014).

[15] R. Eisberg and R. Resnick, *Quantum Physics of Atoms, Molecules, Solids, Nuclei and Particles*, 2nd ed. (John Wiley & Sons Inc., 1985).

[16] S. Dushman, *Electron Emission from Metals as a Function of Temperature*, Vol. 21 (Physical Review Journals Archive, 1923).

[17] K. L. Jensen, *Advances in Imaging and Electron Physics*, Vol. 149 (Electron Emission Physics, 2007).

[18] O. W. Richardson, *The Emission of Electricity from Hot Bodies* (Longmans, Green and Company, 1921).

[19] C. D. Child, *Discharge from Hot CaO*, Vol. 32 (Physical Review Journals Archive, 1911).

[20] I. Langmuir, *The Effect of Space Charge and Residual Gases on Thermionic Currents in High Vacuum*, Vol. 2 (Physical Review Journals Archive, 1913).

[21] D. Martin, *Top Hat Cathodes Product Information* (Applied Physics Technologies, 2011).

[22] K. Gunter, *Handling and Operation Notes* (Heat Wave Labs Inc., 2002).

[23] T. Schuldt, *An Optical Readout for the LISA Gravitational Reference Sensor* (Humboldt Universität Berlin, 2010).

[24] M. Whalen, *DAWN - A journey to the beginning of the solar system* (National Aeronautics and Space Administration, 2015).

[25] T.G.E. van 't Klooster, *Micro Propulsion Systems - Development of a LaB6 Cathode for Micro Electric Thrusters - Literature Study Report* (Delft University of Technology, 2018).

[26] J. H. Henninger, *Solar Absorptance and Thermal Emittance of Some Common Spacecraft Thermal-Control Coatings* (National Aeronautics and Space Administration, 1984).

[27] S. Cesare and G. Sechi, *Next Generation Gravity Mission*, Vol. 31 (Distributed Space Mission for Earth System Monitoring, 2013).

[28] M. McCullar and R. Howard, *Thermal Vacuum Testing: Test Preparation* (NASA Johnson Space Center, 2013).

[29] L. Tebyani, *Thermal Vacuum Chamber Operation and Testing* (California Polytechnic State University, 2013).

[30] ECSS Secretariat, *Thermal control general requirements* (European Cooperation for Space Standardization, 2008).

[31] ECSS Secretariat, *Space Engineering, Testing* (European Cooperation for Space Standardization, 2002).

[32] A. Keller, *Feasibility of a down-scaled HEMP Thruster* (University of Giessen, 2013).

[33] A. Keller, P. Köhler, W. Gärtner, B. Lotz, D. Feili, P. Dold, M. Berger, C. Braxmaier, D. Weise, and U. Johann, *Feasibility of a down-scaled HEMP Thruster*, 32nd ed. (Internation Electric Propulsion Conference, 2011).

[34] H. Leiter, D. Block, B. Lotz, D. Feili, and C. Edwards, *Qualification of the miniaturized Ion Thruster RIT µX - Perspectives, Program, Results and Outlook*, 32nd ed. (International Electric Propulsion Conference, 2011).

[35] T. Randolph, V. Kim, H. Kaufman, K. Kozubsky, V. Zhurin, and M. Day, *Facility Effects in Stationary Plasma Thruster Testing*, 23rd ed. (International Electric Propulsion Conference, 1993).

[36] A. Sengupta, J. A. Anderson, C. Garner, J. R. Brophy, K. L. deGroh, B. A. Banks, and T. A. K. Thomas, *Deep Space 1 Flight Spare Ion Thruster 30,000 hours Life Test*, Vol. 25 (The Journal of Propulsion and Power, 2009).

[37] R. Nadalini, Private conversation, Sonaca Space GmbH (May 2017).

[38] J. R. Bertucci and G. R. Beecher, *Introduction to Bayard-Alpert Ionization Gauges* (Granville-Phillips Helix Technology Corporation, 2009).

[39] F. G. Hey, *Development, Integration and Test of a Micro Newton Thrust Balance* (Technische Universität Dresden, 2012).

[40] J. W. Dankanich, M. W. Swiatek, and J. T. Yim, *A Step Towrards Electric Propulsion Testing Standards: Pressure Measurement and Effective Pumping Speeds*, Vol. 50 (American Institute of Aeronautics and Astronautics, 2012).

[41] R. Blott, S. Gabriel, and D. Robinson, *Draft Handbook for Electric Propulsion (EP) Verification by Test* (ESA/ESTEC, 2012).

[42] F. G. Hey, A. Keller, U. Johann, C. Braxmaier, M. Tajmar, E. Fitzsimons, and D. Weise, *Development of a Micro Thruster Test Facility which fulfils the LISA requirements*, 610th ed. (Journal of Physics: Conference Series, 2015).

[43] F. G. Hey, C. Altmann, U. Johann, C. Braxmaier, M. Tajmar, E. Fitzsimons, and D. Weise, *Development of a Highly Sensitive Micro-Newton Thrust Balance: current status and latest results*, 34th ed. (International Electric Propulsion Conference, 2015).

[44] F. G. Hey, M. Vaupel, and C. Braxmaier, *Development of a Highly Sensitive, Highly Stable Micro-Newton Thrust Balance*, 35th ed. (International Electric Propulsion Conference, 2017).

[45] W. Lahmadi, *VSS Stepper Motor - For Applications up to Ultra-high-vacuum* (Phytron, Inc., 2017).

[46] H. P. Harmann, *Untersuchung und Modellierung der Ionenstrahl formung grossflaechiger Ionenquellen mit Hilfe einer beweglichen Faradaysondenzeile* (University of Giessen, 2003).

[47] W. Gaertner, *Design, Konstruction und Test eines praezisen Gegenfeldanalysators zur energetischen Strahlvermessung eines µN RIT Triebwerkes* (University of Giessen, 2010).

[48] A. Keller, P. E. Köhler, F. G. Hey, M. Berger, C. Braxmaier, D. Feili, D. Weise, and U. Johann, *Parametric Study of HEMP-Thruster Downscaling to µN Thrust Levels*, Vol. 43 (IEEE Transactions on Plasma Science, 2015).

[49] P. E. Koehler and B. K. Meyer, *Beam Diagnostics for Mini Ion Engines*, 33rd ed. (International Electric Propulsion Conference, 2013).

[50] F. G. Hey, M. Vaupel, and C. Groll, *Development of a Gridless Retarding Potential Analyser*, 35th ed. (International Electric Propulsion Conference, 2017).

[51] C. Böhm and J. Perrin, *Retarding-field analyzer for measurements of ion energy distributions and secondary electron emission coefficients in low-pressure radio frequency discharges*, Vol. 64 (Review of Scientific Instruments, 1993).

[52] M. Schramm, *Development of Thruster Plume Diagnostic Tools for Micro High Efficiency Multistage Plasma Thruster Characterization* (University of Stuttgart, 2014).

[53] A. H. Quintero, J. W. Welch, and H. Wolf, *Perceptiveness of Thermal Vacuum Testing*, 18th ed. (Aerospace Testing Seminar, Manhattan Beach, California, 1999).

[54] G. van Zuyl and R. Heckman, *Managing Arcs in RF Powered Plasma Processes* (Advanced Energy Industries, 2006).

[55] J. Hanson and D. Koenig, *Fault arc effects under vacuum conditions on cable bundles for space applications*, 13th ed. (International Symposium on Discharges and Electrical Insulation in Vacuum, 1996).

[56] F. G. Hey, Private conversation, Airbus (November 2017).

[57] E. Ambrosetto and D. Pedersen, *Properties and Characteristics of Graphite* (POCO Graphite an Entegris Company, 2015).

[58] B. Benthem and A. Maas, *AE4S20 Satellite Thermal Control Lecture Slides* (Airbus Defence and Space, 2016).

[59] P. Wellmann, *Materialien der Elektronik und Energietechnik: Halbleiter, Graphen, funktionale Materialien* (Springer Vieweg, 2016).

[60] D. M. Goebel and R. M. Watkins, *Compact lanthanum hexaboride hollow cathode*, Vol. 81 (Review of Scientific Instruments, 2010).

[61] M. S. McDonald, A. D. Gallimore, and D. M. Goebel, *Note: Improved heater design for high-temperature hollow cathodes*, Vol. 88 (Review of Scientific Instruments, 2017).

[62] S. Keevil, T. Gilk, and T. O. Woods, *Safety Guidelines for Magnetic Resonance Imaging Equipment in Clinical Use*, 3rd ed. (Medicines and Healthcare Products Regulatory Agency, 2014).

[63] T. C. Cosmus and M. Parizh, *Advances in Whole-Body MRI Magnets*, Vol. 21 (IEEE Transactions on Applied Superconductivity, 2011).

[64] M. Vaupel, Private conversation, Airbus (February 2018).

[65] K. Guadagni, Private conversation, Kimball Physics Inc. (February 2018).

[66] F. Hey, Private conversation, Airbus (April 2018).

[67] Y. Goueffon, D. Herbin, and L. Gessler, *MetOp-SG Cleanliness Requirement Specification*, 3rd ed. (Airbus Defence and Space, 2014).

[68] ECSS Secretariat, *Space product assurance: Ultracleaning of flight hardware* (European Cooperation for Space Standardization, 2017).

[69] J. D. Anderson, *Fundamentals of Aerodynamics*, 5th ed. (McGrawHill, 2011).

[70] K. Lemmer, *Propulsion for CubeSats*, Vol. 134 (ACTA Astronautica, 2017).

[71] R. Zeledon and M. Peck, *Electrolysis Propulsion for CubeSat-Scale Spacecraft* (AIAA Space Conference & Exposition, 2011).

[72] D. Schmuland, R. Masse, and C. Sota, *Hydrazine Propulsion Module for CubeSats* (Small Satellite Conference, 2011).

A

TECHNICAL DRAWINGS

This appendix contains the technical drawings of the components that are used in order to test the cathodes. First, the technical drawing of the graphite heater is given in Appendix A.1. Next, the boron nitride spacer is described in Appendix A.2. Subsequently, Appendices A.3 and A.4 describe the top and bottom macor insulator disc respectively. Furthermore, the LaB_6 insert is illustrated in Appendix A.5. Finally, an overview of the cathode assembly can be seen in Appendix A.6.

A.1. GRAPHITE HEATER

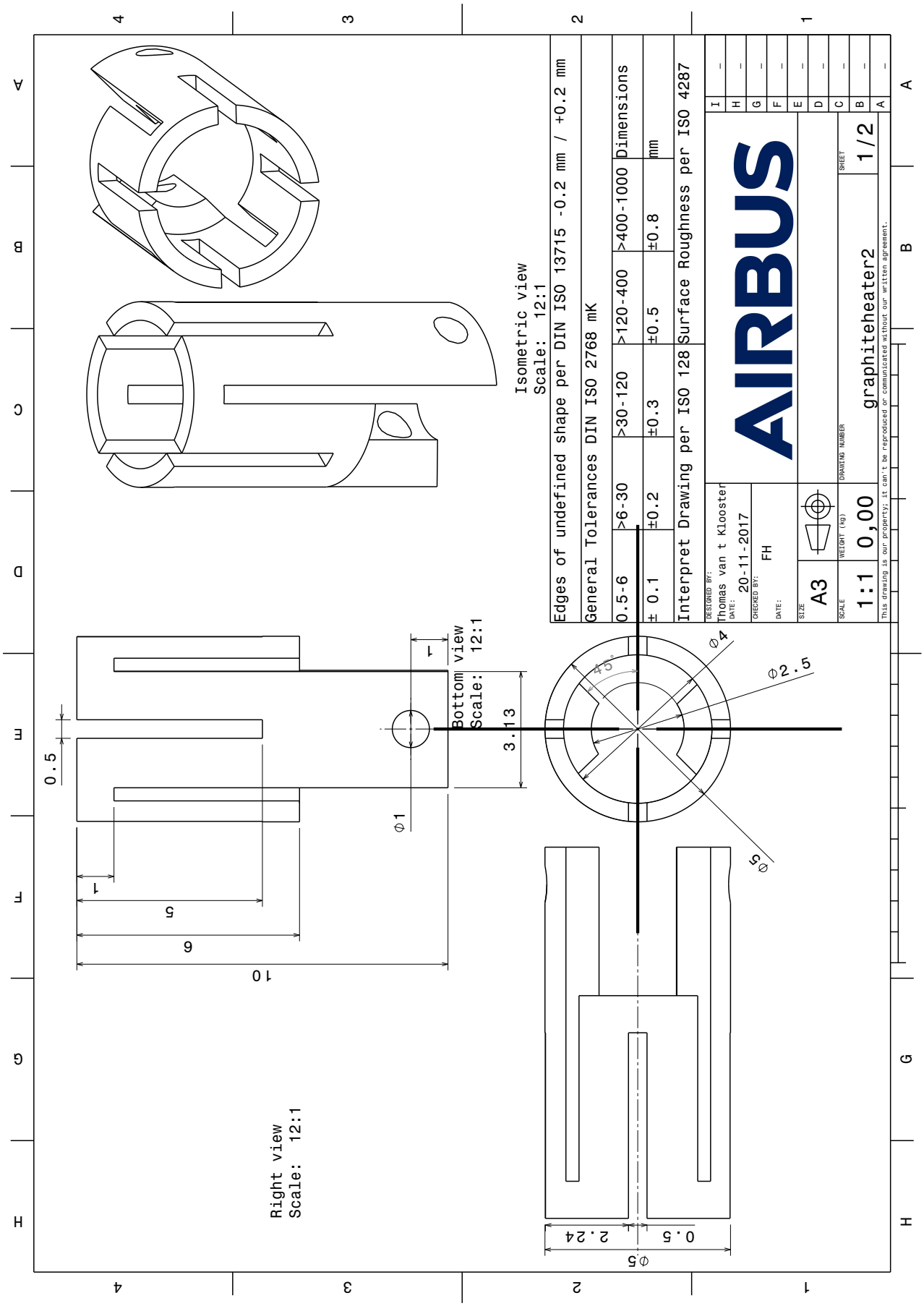

A.2. BORON NITRIDE SPACER

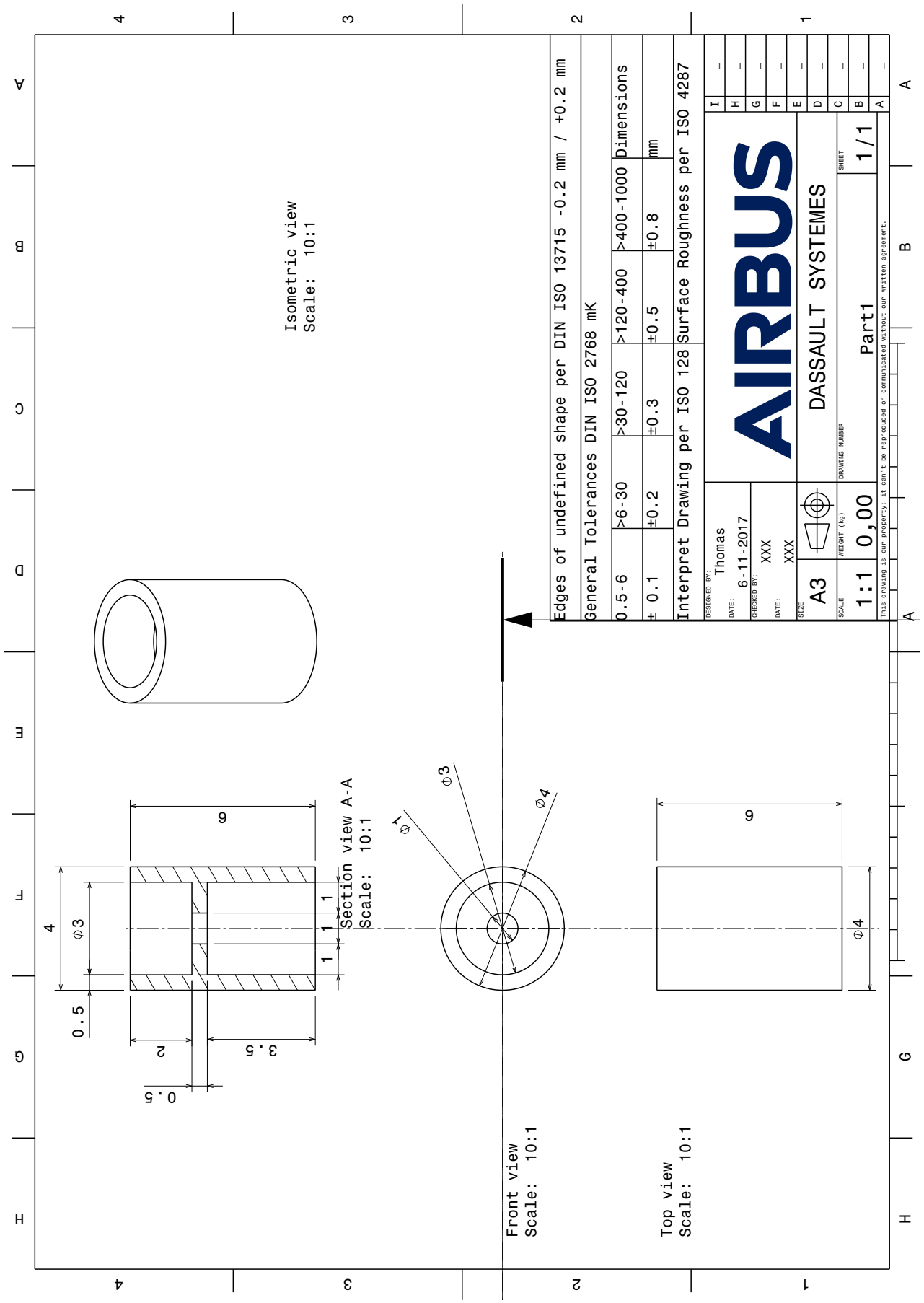

A.3. MACOR TOP INSULATOR DISC

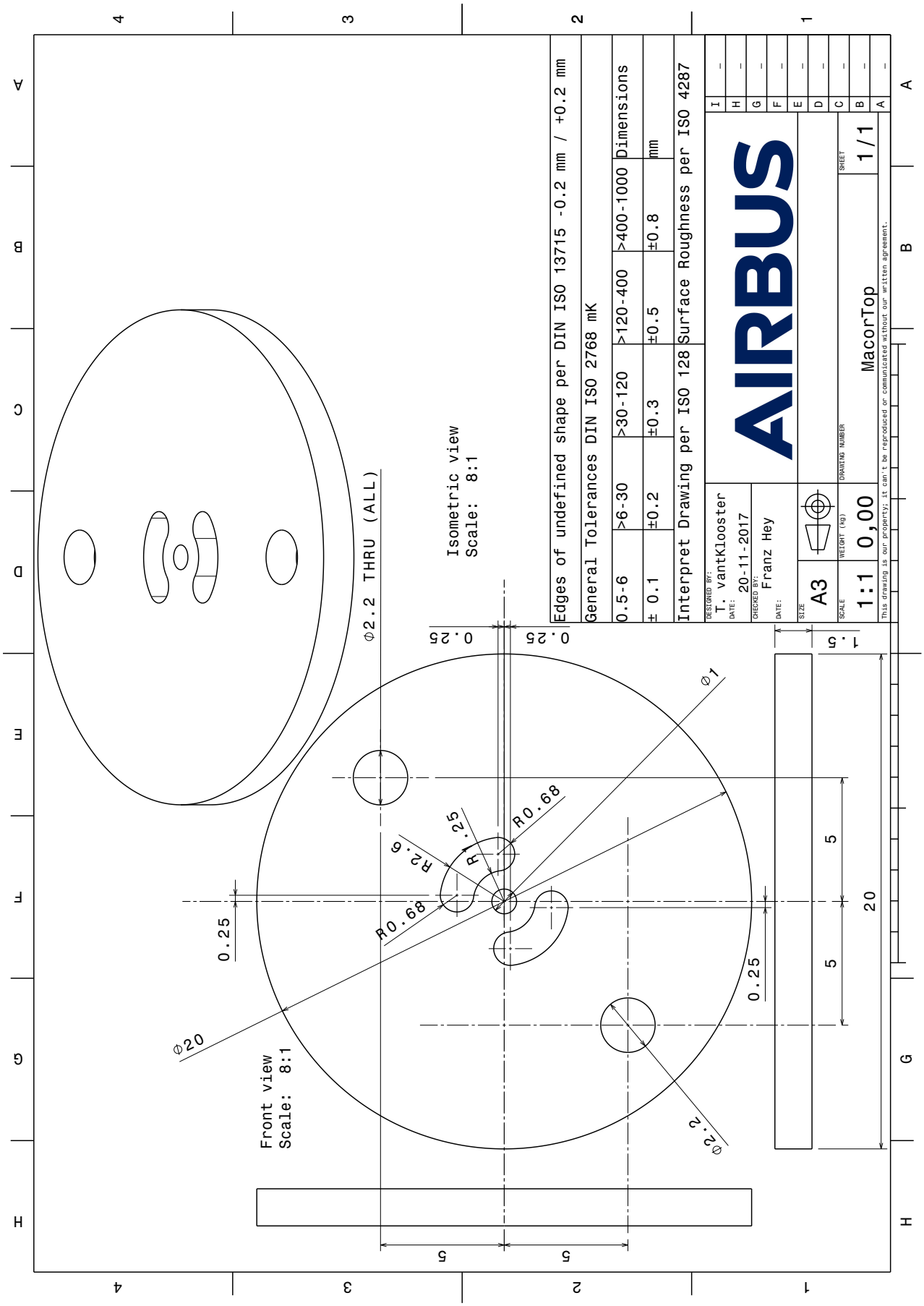

A.4. MACOR BOTTOM INSULATOR DISC

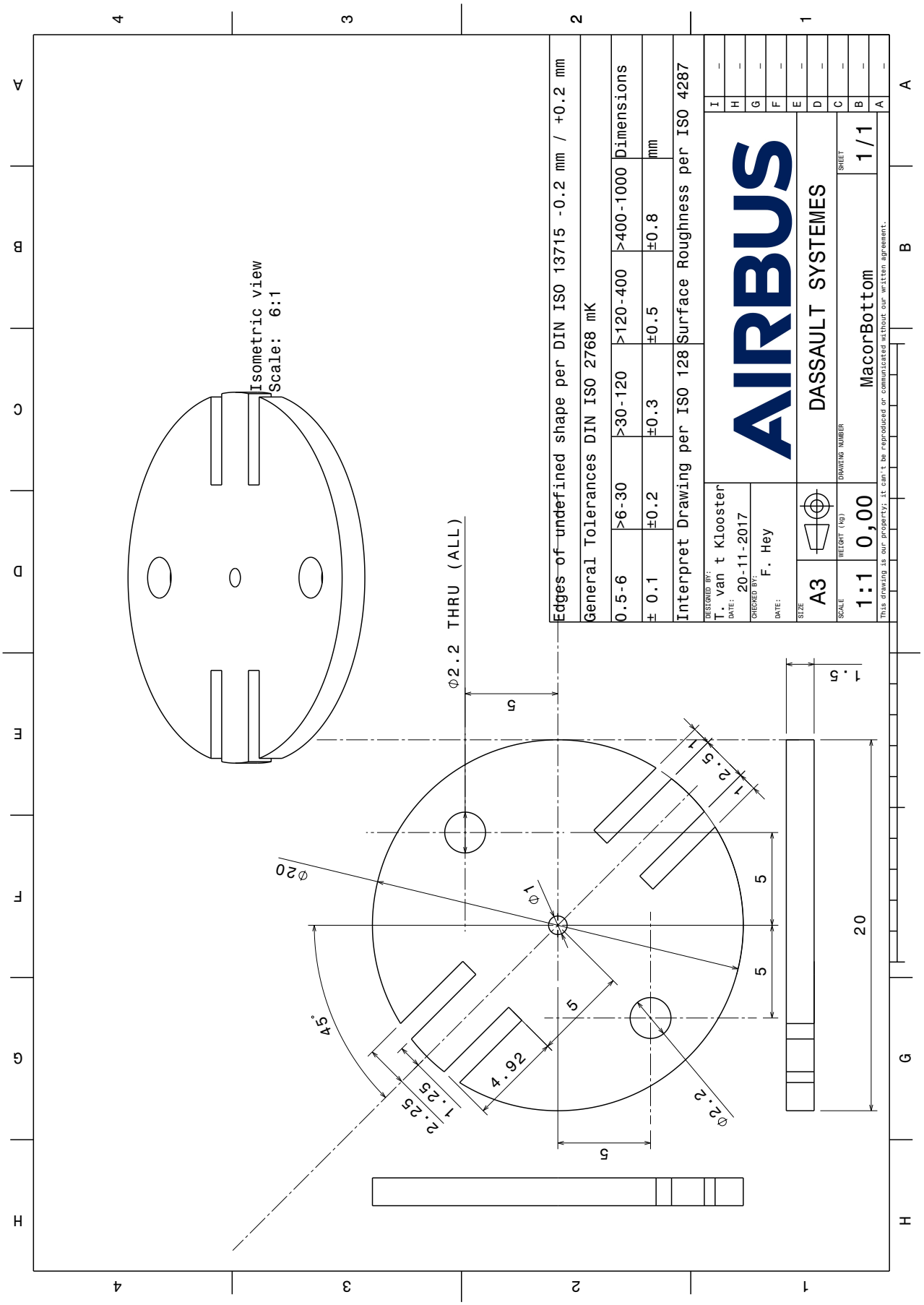

A.5. LaB_6 INSERT

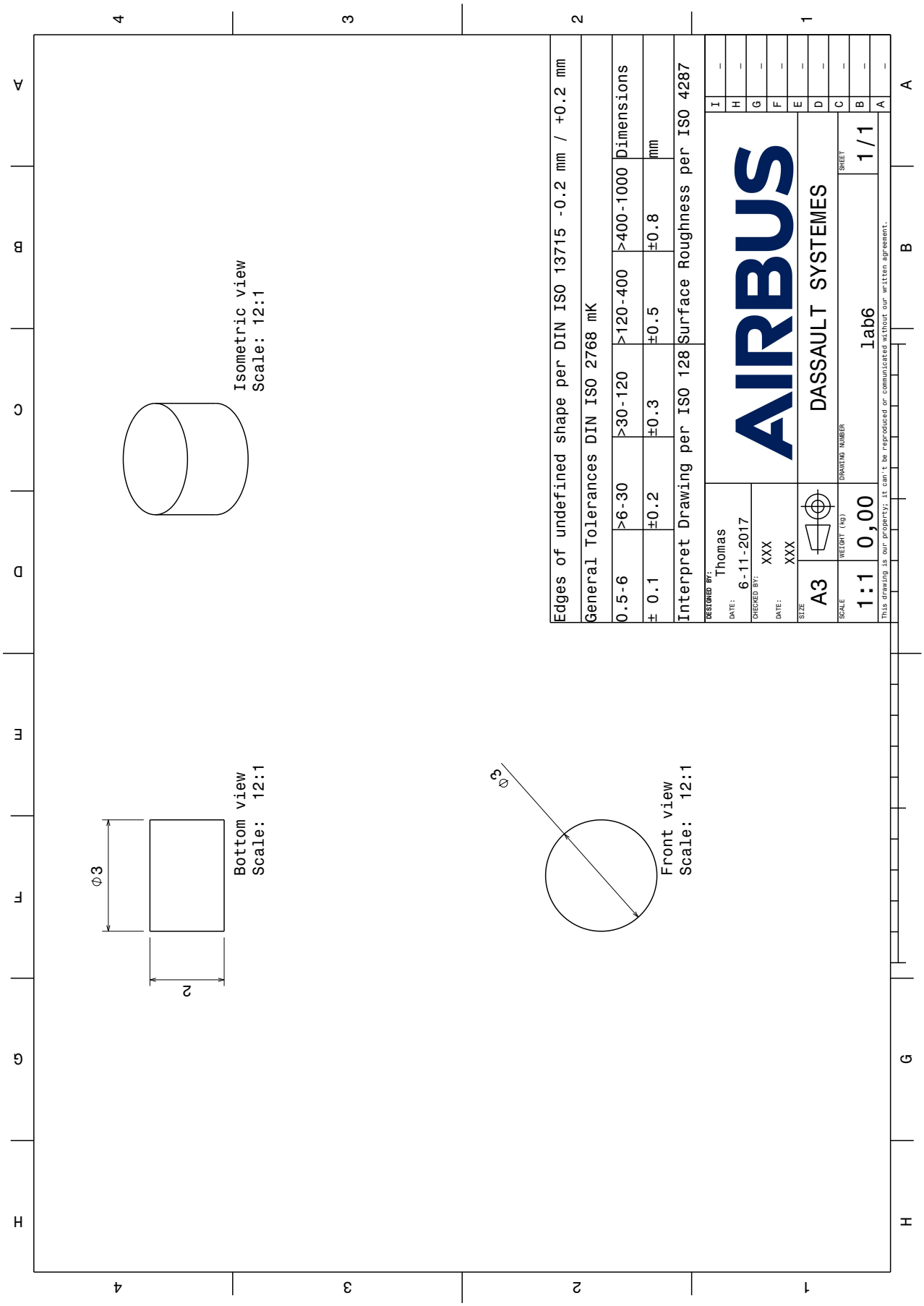

A.6. CATHODE ASSEMBLY

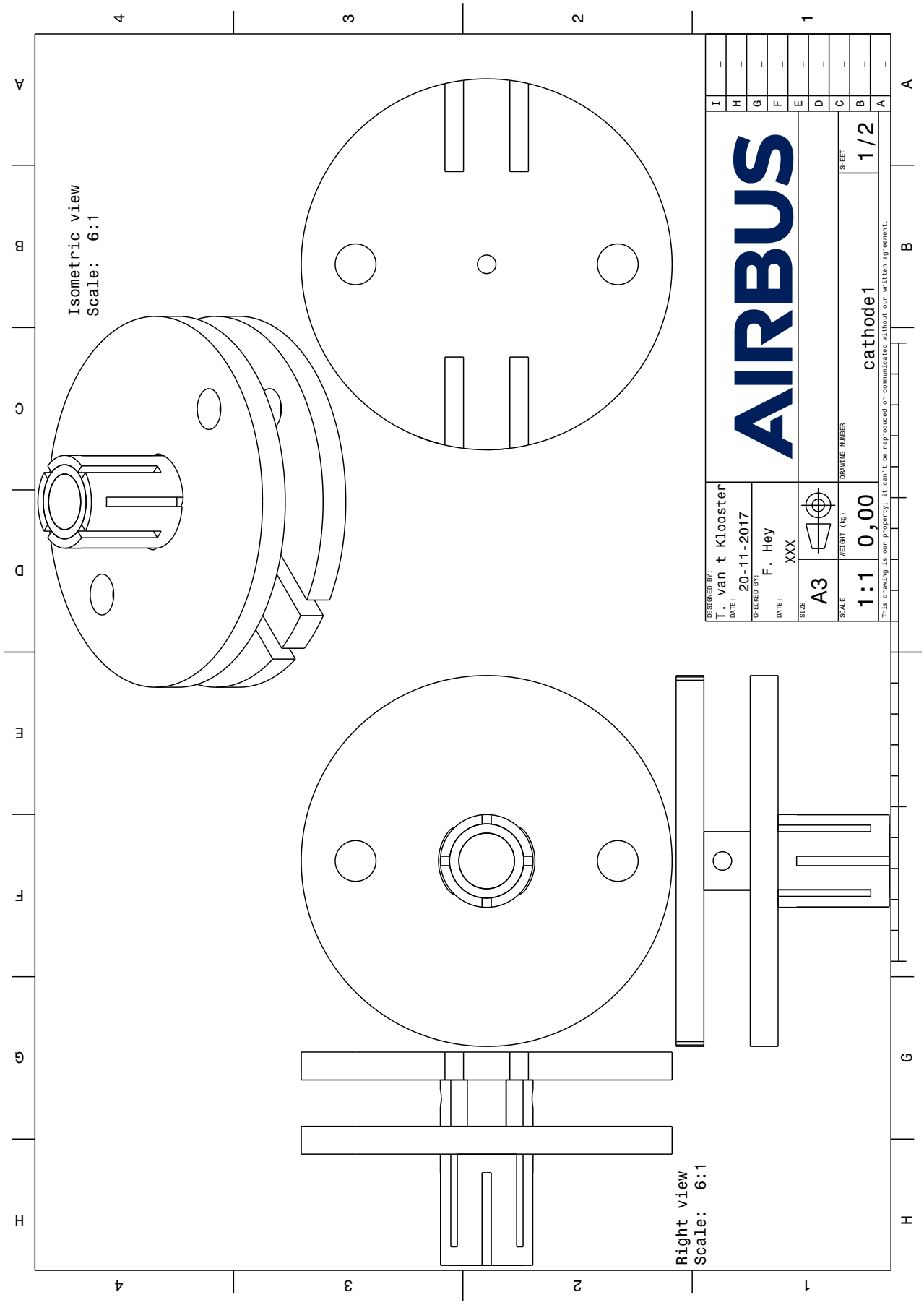

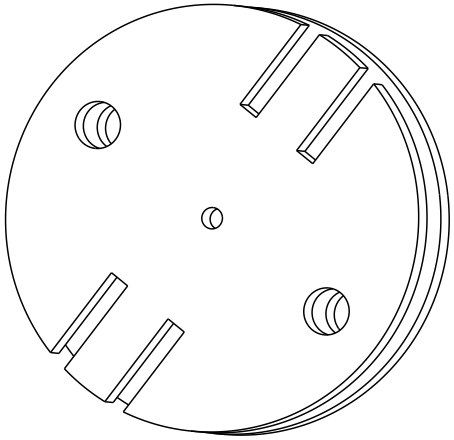

Isometric view
Scale: 5:1

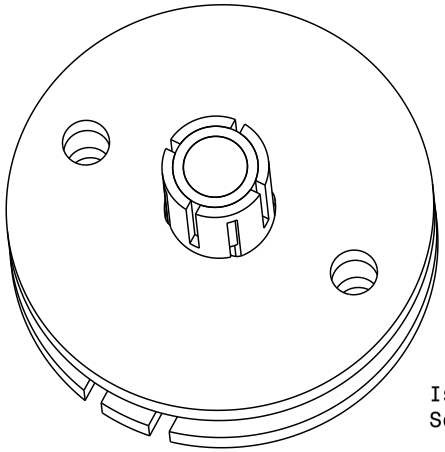

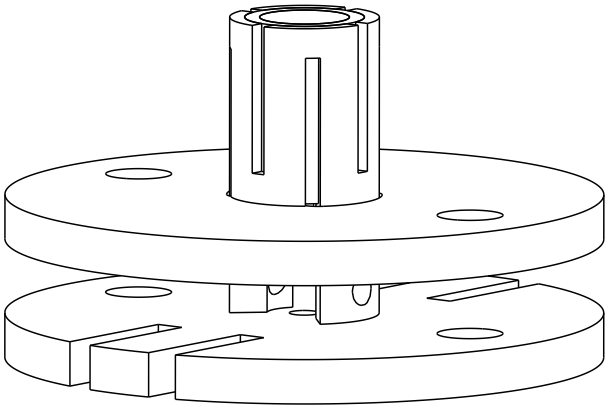

With bottom macor plate, excl. silver wires

Isometric view
Scale: 5:1

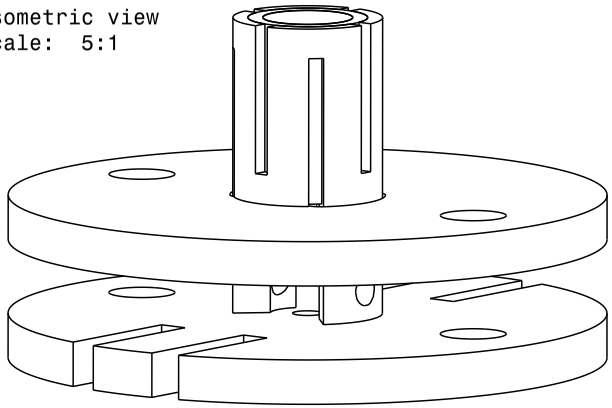

DESIGNED BY: T. van t Klooster		AIRBUS	
DATE: 20-11-2017			
CHECKED BY: F. Hey			
DATE: XXX			
SIZE A3			
SCALE 1:1	WEIGHT (kg) 0,00	DRAWING NUMBER cathode1	SHEET 2/2